Reactions of Protected Alanine and Glycine Dimers

Daniel Richard Coghlan

Thesis submitted for the degree of

Doctor of Philosophy

in

The University of Adelaide

(Faculty of Science)

Awarded 1995

Contents

Acknowledgements

I wish to thank my supervisor, A/Prof. Chris Easton, not only for the financial support, but for his guidance, time and friendship over the last few years. It has been my privilege to have had the chance to work with Chris.

I would like to thank Bruce May for his friendship and expertise in all the areas of Chemistry that you would wish to think of.

I would also like to thank Caroline and the other fellow lab members for their help and friendship.

I would like to acknowledge the continual help provided by the professional officers and the technical staff to me and all the other students. Without their support research is not possible.

I am grateful to Drs. P. Steel and E. Tiekink for providing crystallographic analyses

I wish finally to thank my mum for her support and friendship over the many years. Everybody loves their mum and I'm no exception.

Statement

This work contains no material which has been accepted for the award of any other degree or diploma in any university or other tertiary institution and, to the best of my knowledge and belief, contains no material previously published or written by another person, except where due reference has been made in the text.

I give consent to this copy of my thesis, when deposited in the University Library, being available for loan and photocopying.

18/11/94

Abstract

With the aim of delineating factors that influence the rates of formation of α-centred radicals of protected amino acids, reactions of dimethyl 2,3-dibenzamido-2,3-dimethylbutanedioate and dimethyl 2,3-dibenzamidobutanedioate have been investigated.

Reactions of the racemic and *meso*-isomers of dimethyl 2,3-dibenzamido-2,3-dimethylbutanedioate in 1,2,4-trichlorobenzene at 214°C involved decomposition through homolysis of the central carbon-carbon bond. The rate constants for decomposition were found to be 2.22×10^{-5} sec^{-1} and 6.29×10^{-5} sec^{-1} for the racemic and *meso*-isomers, respectively. The rate constants for decomposition of the diastereomers in DMF at 150°C were found to be at least 200 times greater than for the reactions in 1,2,4-trichlorobenzene at the same temperature. The rate constants for reaction in DMF at 150°C were found to be 7.13×10^{-5} sec^{-1} and 8.37×10^{-5} sec^{-1} for the racemic and *meso*-isomers, respectively, while the rate constants for reaction in 1,2,4-trichlorobenzene at 150°C were found to be less than 4×10^{-7} sec^{-1}. The greater reactivity in the polar solvent can be attributed to the disruption of intramolecular hydrogen bonds.

Reactions of the diastereomers of dimethyl 2,3-dibenzamido-butanedioate in 1,2,4-trichlorobenzene at 214°C involved their interconversion without decomposition. The rate constants for equilibration of the diastereomers were found to be 4.41×10^{-4} sec^{-1} and 6.58×10^{-4} sec^{-1} for the racemic and *meso*-isomers, respectively. The rate constants for equilibration of the diastereomers in DMF at 150°C were found to be approximately 100 times greater than for the reactions in 1,2,4-trichlorobenzene at the same temperature. The rate constants for

equilibration in DMF at 150°C were found to be 6.86×10^{-4} sec^{-1} and 6.31×10^{-4} sec^{-1} for the racemic and *meso*-isomers, respectively. The mechanism for equilibration was shown, through a deuterium incorporation experiment, to involve exchange of the hydrogens on the α,α′-carbons and not homolysis of the central dimer bond followed by recombination of the product radicals.

The rates of interconversion of the diastereomers of dimethyl 2,3-dibenzamidobutanedioate were found to be far greater than the rates of racemisation of *N*-benzoyl-(2*S*)-alanine methyl ester and *N*-benzoyl-(2*S*)-valine methyl ester, determined under the same conditions, and this observation prompted an investigation into the mechanism of equilibration.

The rates of interconversion of the α-deuteriated analogues of the diastereomers of dimethyl 2,3-dibenzamidobutanedioate were investigated for possible deuterium isotope effects. The rate of equilibration of the *meso*-isomer of dimethyl 2,3-dibenzamido-2,3-dideuteriobutanedioate in 1,2,4-trichlorobenzene at 214°C exhibited a primary deuterium isotope effect of 2.35, which indicated that the mechanism for equilibration involved base-induced deprotonation from the α-carbons. The racemic isomer exhibited a smaller deuterium isotope effect of 1.48. The rates of interconversion of the diastereomers of dimethyl 2,3-dipentafluorobenzamidobutanedioate in 1,2,4-trichlorobenzene at 214°C were investigated to determine whether the reduced base strength of the amide carbonyls affected the equilibration rates. The racemic fluorinated isomer was found to react 5.0 times slower and the *meso*-isomer 17.7 times slower than for the corresponding diastereomers of dimethyl 2,3-dibenzamidobutanedioate. These results show that the reactions of the diastereomers of dimethyl 2,3-dibenzamidobutanedioate in 1,2,4-trichlorobenzene at 214°C involve tautomerisation facilitated by the amide carbonyls through a six-membered ring transition state.

Free radicals generated during the irradiation of proteins, at room temperature, were observed through the application of ESR spectroscopy, by Gordy and Shields[1,2] in the late 1950's. Two main types of signals were identified, the first very broad and anisotropic and the second, a doublet[3]. The broad pattern was similar to that generated when a single crystal of cystine dihydrochloride was irradiated, which led Kurita and Gordy[4] to conclude that the broad pattern was indicative of sulphur centred radicals. The doublet pattern was thought to be due to an unpaired electron on carbon adjacent to only one hydrogen, the simplest case being that of radicals formed by hydrogen abstraction from glycine residues. Irradiation of single crystals of *N*-acetylglycine[5] and glycylglycine[6] produced the expected doublet pattern in the ESR spectra, due to specific hydrogen abstraction to produce the radicals **1** and **2**, respectively.

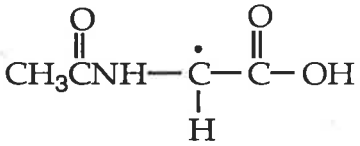

1

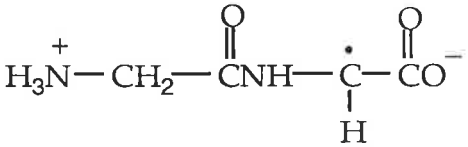

2

The ESR doublet pattern is not restricted to radicals formed on glycine residues as some side chains of other amino acids contain methylene groups, which may be susceptible to hydrogen transfer[7]. ESR evidence for the preferential formation of α-centred glycyl radicals over other carbon radicals in a protein was that the ratio of the doublet resonance to the sulphur resonance was dependent on the ratio of glycine to cysteine and cystine residues in the protein[8].

Chemical selectivity for reaction of glycine residues was shown by Elad *et al.*,[9-13] through photoalkylation experiments on protected dipeptides and

proteins. The dipeptide derivatives **3 - 6** containing glycine and either alanine, valine, phenylalanine or modified tyrosine residues, were modified only at the glycine residues, when exposed to visible light, an α-diketone as a photoinitiator, di-*t*-butyl peroxide and toluene (Scheme 1)[10]. The glycine

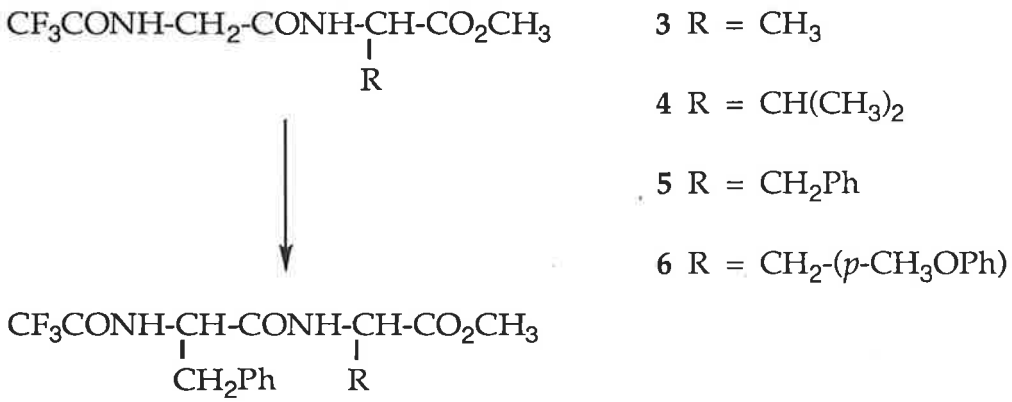

3 R = CH_3

4 R = $CH(CH_3)_2$

5 R = CH_2Ph

6 R = CH_2-(*p*-CH_3OPh)

Scheme 1

residues were converted to phenylalanine residues in yields of 25 - 60%.

Modification of glycine residues also occurred on photoalkylation of proteins with ultraviolet light, acetone and either but-1-ene **10** or toluene **15**. A free radical mechanism was proposed for the modifications (Scheme 2)[11]. Photosensitised (λ > 290 nm) acetone **7** removes an α-hydrogen from a glycine residue **8**. The resultant glycyl radical **9** then adds to but-1-ene **10** or couples with benzyl radical **16** formed by hydrogen abstraction from toluene **15**. The

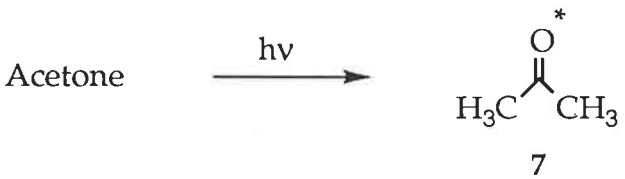

7

Scheme 2

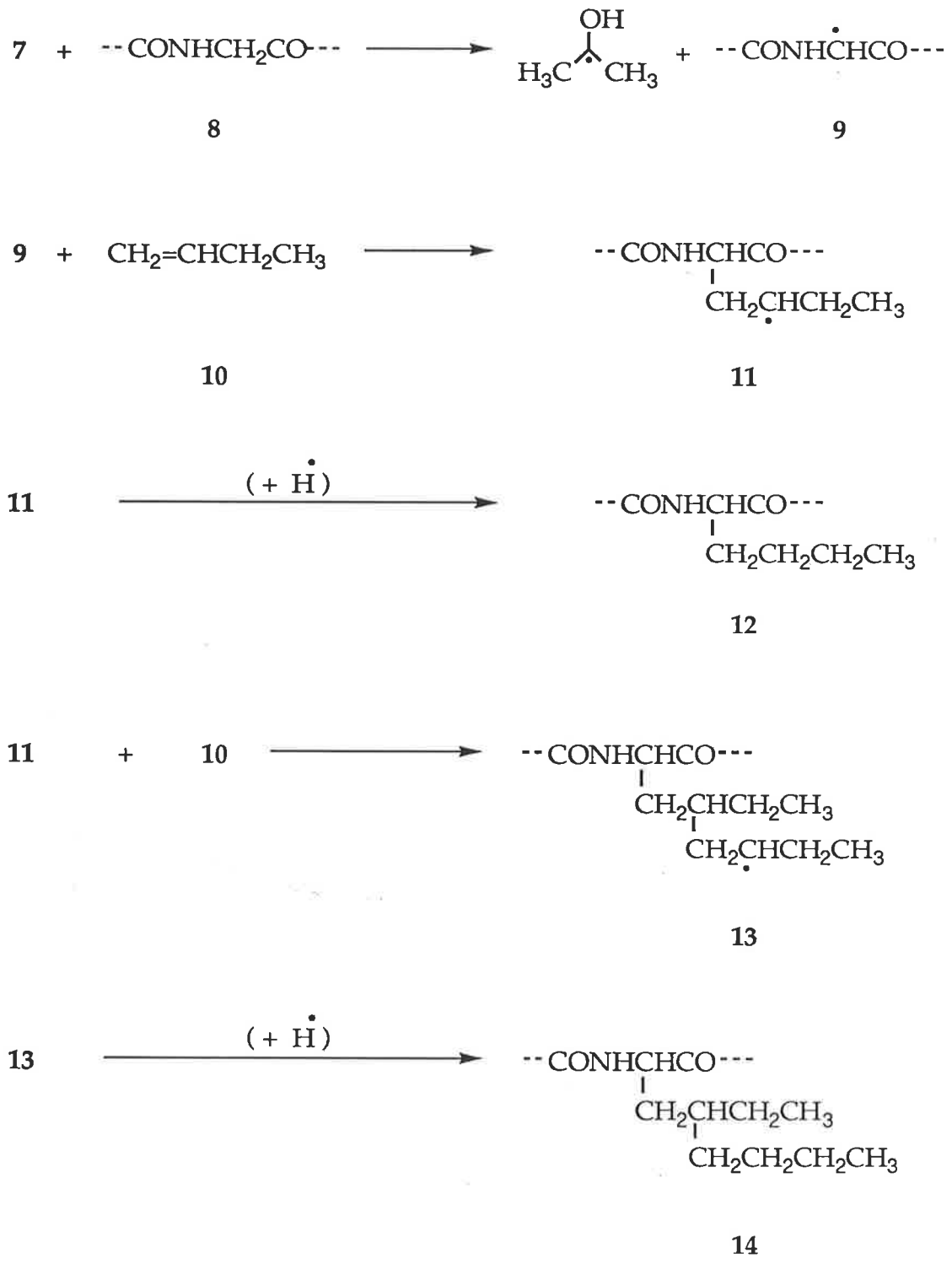

Scheme 2 cont.

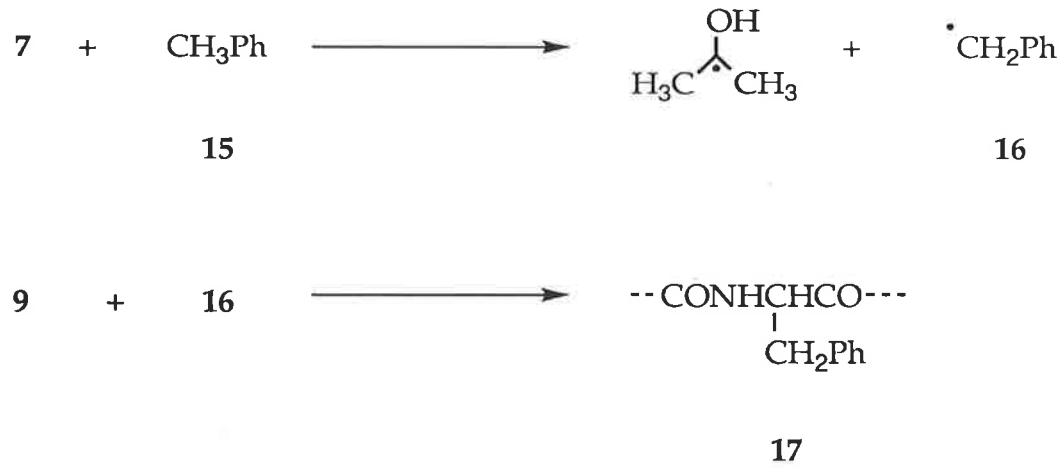

Scheme 2 cont.

product **11** formed by the addition of the glycyl radical **9** to but-1-ene **10**, either abstracts hydrogen to form a norleucine derivative **12**, or undergoes a second addition with but-1-ene **10** to produce the radical **13**, which then abstracts hydrogen to give the amino acid derivative **14**. The reaction of the glycyl radical **9** with benzyl radical **16** produces the phenylalanine derivative **17**. The identification of other products formed through radical coupling helped verify that the reaction involved a free radical mechanism. For the reactions involving toluene **15**, bibenzyl, produced from the coupling of two benzyl radicals **16**, was found.

When the protected glycylalanine dipeptide **3** was irradiated in the presence of acetone only, the products after acid hydrolysis were 1,2-diaminosuccinic acid **20** and alanine[9]. This was the result of coupling

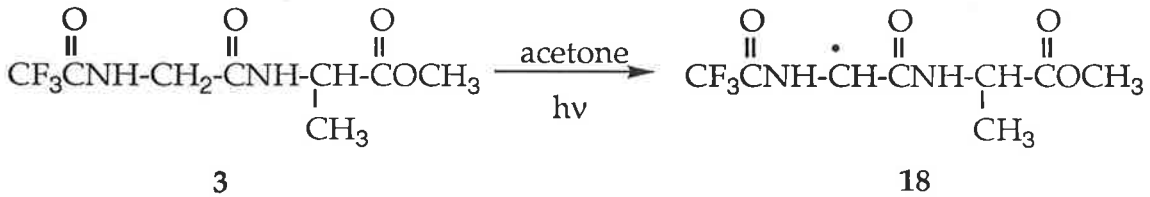

3 **18**

Scheme 3

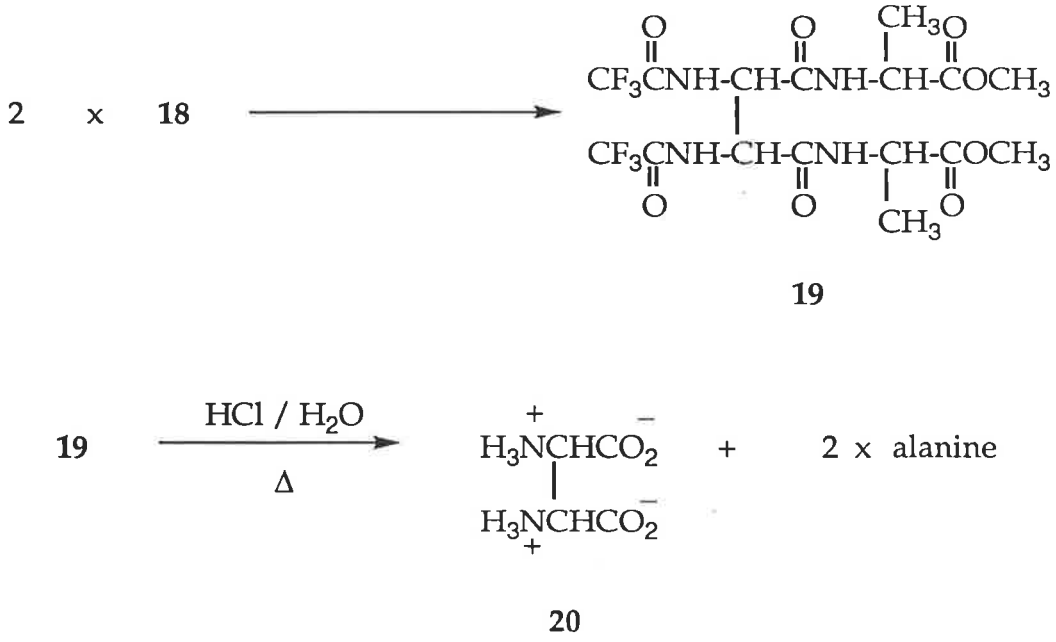

Scheme 3 cont.

between two of the glycyl radicals **18** (Scheme 3).

Hydrogen abstraction from the α-centre of an amino acid derivative, produces a secondary radical **9** in the case of a glycine residue and a tertiary radical for each of the other amino acid residues. The preferential formation of α-carbon centred secondary radicals **9** over tertiary radicals, by hydrogen abstraction from amino acid derivatives, was investigated further by Elad *et al.*[11] Photoalkylation experiments were carried out on various types of polypeptides (MWt > 3100) containing only glycine and alanine residues, as well as *N*-trifluoroacetyl (Tfa) methyl ester (OMe) protected amino acids and dipeptides of glycine and alanine, in the presence of either toluene **15** or but-1-ene **10**. Some of the results are shown in Table 1. The glycine residues in the polypeptides shown in Table 1 were modified by 7 - 25%. Elad *et al.*,[11] observed a different degree of selectivity for reaction at glycine between the

Table 1 - Results of photochemical reactions of glycine and alanine derivatives.

Amino acid derivative	Gly : Ala[a]	Phe : MePhe[b]	Nle : MeNle[c]
(*S*-Ala-Gly-Ala)$_n$	1 : 2	30 : 1	—
(Gly)$_m$(Ala)$_n$	1 : 9	30 : 1	9 : 1
Tfa-Gly-Ala-OMe (3)	1 : 1	7 : 1	10 : 1
Tfa-Ala-Gly-OMe	1 : 1	20 : 1	7 : 1
Tfa-Gly-OMe/Tfa-Ala-OMe	1 : 9	2 : 1	4 : 1

a. Initial ratio. b. Ratio of phenylalanine (Phe) to 2-methylphenylalanine (MePhe); produced through coupling of benzyl radical **16** with glycyl radicals **9** and alanyl radicals, respectively. c. Ratio of norleucine (Nle) to 2-methyl-norleucine (MeNle); produced through addition of glycyl **9** and alanyl radicals, respectively, to but-1-ene **10**, followed by hydrogen atom abstraction.

peptides and the single amino acid derivatives. To examine whether hydrogen abstraction from an amino acid residue was reversible, polypeptides containing only *S*-alanine residues were used to check whether any racemisation of those residues occurred, but this was found to be negligible. The product ratios therefore reflect preferential hydrogen abstraction from glycine derivatives.

Hydrogen abstraction from proteins has been suggested to occur more readily from glycine residues, as the smaller side chain can rearrange more easily to produce a planar intermediate, required for delocalisation of the α-centred radical through the amido and carboxyl π-orbitals[7]. The delocalisation of the unpaired spin density by electron withdrawing (carboxyl) and electron donating (amido) groups, has been termed captodative stabilisation by Viehe *et al.*,[14] who proposed the idea that cooperative stabilisation of a captodative radical led to enhanced stabilisation. The idea

had been reported earlier by Dewar[15], Balaban[16], as push-pull stabilisation and Katritzky[17], as merostabilisation. Much research has been done to determine whether there is a synergistic effect resulting from cooperative stabilisation, but only a few examples offer evidence that this is so[18-21].

To better understand the selectivity for hydrogen abstraction from glycine derivatives, Easton *et al.*,[22] examined the rates of radical brominations of amino acid derivatives with *N*-bromosuccinimide (NBS) and of reactions of amino acid derivatives with di-*t*-butyl peroxide (DTBP) **21**.

The mechanism of bromination of most organic compounds with NBS is as outlined in Scheme 4[23]. Bromination involves abstraction of a

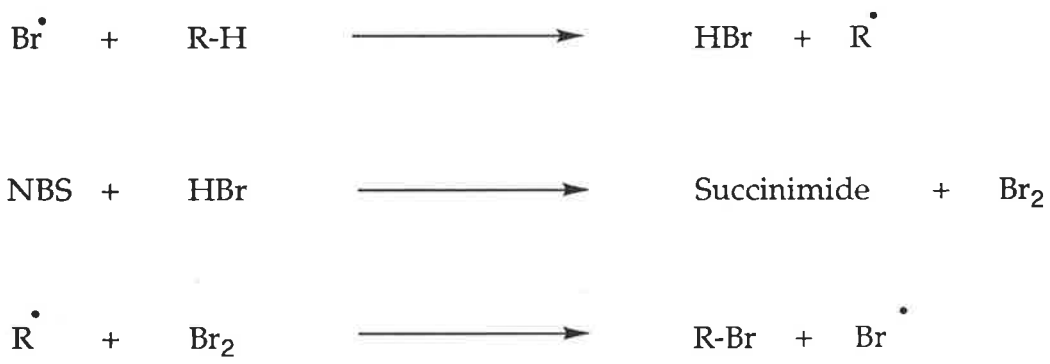

Scheme 4

hydrogen from a substrate by a bromine atom to produce hydrogen bromide and a carbon-centred radical. The hydrogen bromide reacts with *N*-bromo-succinimide to give succinimide and molecular bromine. The carbon-centred radical abstracts a bromine atom from molecular bromine, to produce a brominated product and atomic bromine. The atomic bromine goes on to continue the bromination cycle. Bromination reactions using molecular bromine instead of NBS show the same characteristics, providing evidence

for the formation of molecular bromine during the bromination cycle[24,25]. In the hydrogen transfer step of a radical reaction with NBS, there is a high degree of development of the carbon-centred radical[26]. Relative rates of hydrogen abstraction reactions therefore reflect the relative stabilisation of the radicals being formed.

The mechanism of photochemically induced reactions of DTBP **21** with organic compounds is outlined in Scheme 5[27]. Irradiation of DTBP **21** cleaves

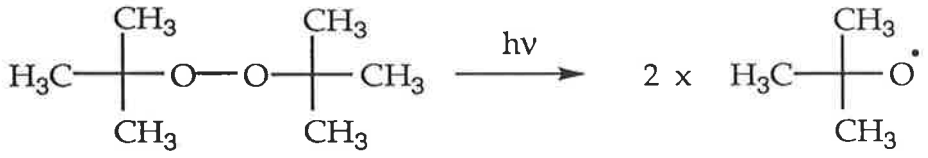

21 **22**

23

24

Scheme 5

the peroxide bond to give *t*-butoxy radical **22**. *t*-Butoxy radical **22** can undergo several reactions: firstly, β-scission to generate methyl radical **23** and acetone and secondly, hydrogen abstraction from a substrate to give *t*-butanol **24** and a carbon-centred radical species. The carbon-centred radical species can either couple with methyl radical **23**, or undergo dimerisation. Hydrogen transfer reactions involving *t*-butoxy radical **22** are less sensitive than those involving bromine atom, to factors affecting stabilisation of the incipient radicals, as the carbon-centred radicals are less developed in the transition states of the former reactions[26].

The relative rates of reaction of the *N*-benzoyl methyl ester derivatives **25 - 28** of the amino acids: glycine, alanine, valine and sarcosine, as well as the methyl ester **29** of pyroglutamic acid, with NBS and DTBP were determined through a series of competitive experiments and these are shown in Table 2[22]. Deuterium isotope effects and product studies showed that the reactions

Table 2 - Relative rates of reaction of the amino acid derivatives **25 - 29** with NBS and DTBP **21**.

Amino Acid Derivative	Relative Reaction Rates	
	NBS	DTBP **21**
25	1.0[a]	1.0[b]
26	0.33 ± 0.05	0.24 ± 0.02
27	0.04 ± 0.01	0.19 ± 0.03
28	0.37 ± 0.05	0.40 ± 0.03
29	3.1 ± 0.7	2.4 ± 0.2

a. Rate of bromination of the glycine derivative **25** assigned as unity. b. Rate of consumption of the glycine derivative **25** by reaction with DTBP **21** assigned as unity; the rates with NBS and DTBP **21** are not compared.

of the amino acid derivatives **25 - 29** with NBS involved formation of the corresponding radicals **30 - 34**. Similar studies of the reactions of DTBP **21** with the amino acid derivatives **25 - 29** showed that only the glycine, alanine and pyroglutamic acid derivatives **25, 26** and **29** reacted by regiospecific hydrogen abstraction at the α-carbon, to produced the radicals **30, 31** and **34**, respectively. Hydrogen abstraction from the valine derivative **27** occurred at both the α- and β-carbons, while *t*-butoxy radical **22** abstracted hydrogen from the α-carbon and the *N*-methyl group of the sarcosine derivative **28**. The relative rates of reaction of the amino acid derivatives **27** and **28** with DTBP **21**, shown in Table 2, are therefore greater than the rates of formation of the radicals **32** and **33**, respectively.

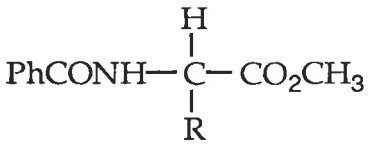

25 R = H

26 R = CH_3

27 R = $CH(CH_3)_2$

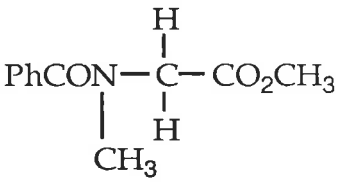

28

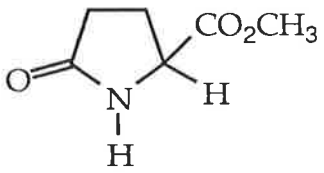

29

Non-bonding interactions in the α-centred amino acid radical derivatives **30 - 34** of glycine, alanine, valine, sarcosine and pyroglutamic acid, respectively, are shown in Figure 1. From the relative reaction rates, the ease of hydrogen abstraction at the α-carbon during bromination is greater for the glycine derivative **25** than for the derivatives of either alanine **26**, valine **27** or

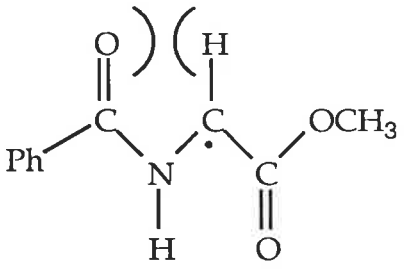

30

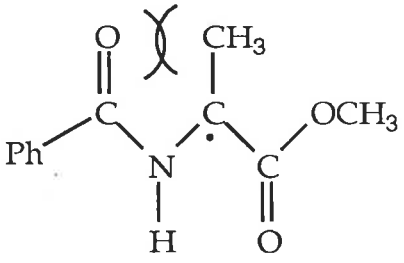

31

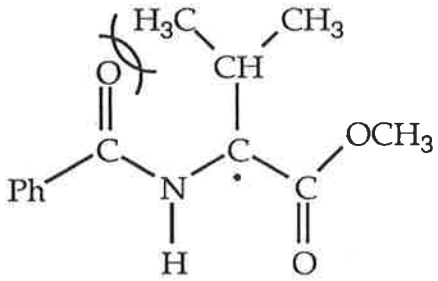

32

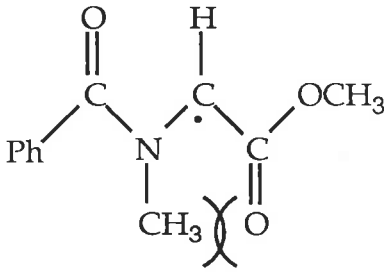

33

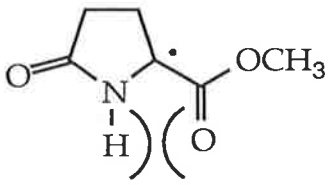

34

Figure 1 - Non-bonding interactions in planar conformations of the radicals **30** - **34**.

sarcosine **28**. Easton *et al.*,[22] proposed that the different rates reflect differences in the stabilisation of the radicals **30** - **33** in the reaction transition states, arising from non-bonding interactions in planar conformation of the radicals required for delocalisation of their unpaired electrons. Planar orientations of the radicals **31** and **33** will be of approximately equal energy, but greater than those of the radical **30** due to increased non-bonding

interactions. Greater non-bonding interactions in planar conformations of the radical **32** result in a slower rate of bromination of the valine derivative **27** than either the derivatives of glycine **25**, alanine **26** or sarcosine **28**. Bromination of the pyroglutamic acid derivative **29** occurred faster than for the glycine derivative **25**. The radical **34** can adopt planar conformations that are relatively free of non-bonding interactions. Hydrogen abstraction from the amino acid derivative **29** also results in some relief of gauche interactions in the ring, which helps lower the activation energy required for radical generation. The relative rates of abstraction of the α-hydrogen from the amino acid derivatives **25 - 29** in reactions with DTBP **21**, showed similar trends to those for the reactions with NBS.

Radical stability is not the only factor that determines the reactivity of an amino acid derivative in a radical reaction, as polar and steric effects also need to be considered. The difference in electronegativity of an attacking radical and a substrate led to the idea of radicals possessing electrophilic or nucleophilic character, though not to the same degree as for ionic species[26]. Polar effects arise during radical brominations where the electronegative bromine atom abstracts a hydrogen and induces a partial positive charge in the transition state on the carbon from which the hydrogen is being abstracted[26]. Hydrogen abstraction by bromine atom may be retarded unless the partial positive charge build-up can be delocalised.

Polar effects helped explain the relative rates of bromination of *N*-benzoylglycine methyl ester **25**, *N*-benzoyl-β-alanine methyl ester **35**, *N*-phthaloylglycine methyl ester **36** and *N*-phthaloyl-β-alanine methyl ester **37**[28]. The glycine derivative **25** reacted at least ten times faster than the β-alanine derivative **35**, which in turn was at least ten times as reactive as the β-alanine derivative **37**, which was at least ten times as reactive as the glycine

derivative **36**. The products of bromination of the compounds **25** and **35 - 37** indicated that reaction, in each case, involved hydrogen abstraction from the methylene group adjacent to the nitrogen.

$PhCONH\text{-}CH_2CH_2\text{-}CO_2CH_3$

35

$Phth\text{-}CH_2\text{-}CO_2CH_3$

36

$Phth\text{-}CH_2CH_2\text{-}CO_2CH_3$

37

The greater rate of reaction of the *N*-benzoyl-β-alanine derivative **35** over the phthaloyl-β-alanine derivative **37** indicated that resonance stabilisation of the unpaired spin density and the induced charge in the transition state for hydrogen abstraction is greater with the benzamido group than with the phthaloyl group. Preferential bromination of the *N*-benzoyl-glycine derivative **25** over the *N*-benzoyl-β-alanine derivative **35** is the result of a proactive combination of the effects of the carboxyl and amido groups in the amino acid derivative **25**, whereas the slower rate of bromination of the phthaloylglycine derivative **36** compared with the phthaloyl-β-alanine derivative **37** results from a counteractive combination of the effects of the carboxyl and phthalimido groups in the amino acid derivative **36**. The proactive effect of the benzamido and carboxyl groups results from the benzamido group's ability to delocalise positive charge build-up, that would otherwise retard hydrogen abstraction by bromine at a site adjacent to a carboxyl, and the benzamido and carboxyl groups abilities to delocalise the unpaired spin density in the transition state for hydrogen abstraction by bromine atom. The reduced ability of the phthaloyl group to delocalise the

radical character and charge, coupled with the reduced delocalisation of the radical **38** through the carboxyl π-orbitals due to steric interactions in planar conformations (Figure 2), lead to a counteractive effect of the carboxyl group with the phthalimido group in the glycine derivative **36**.

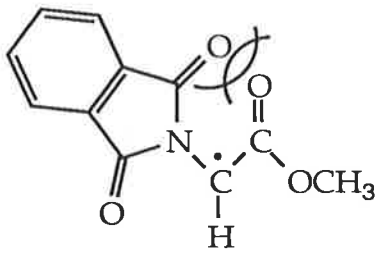

38

Figure 2 - Non-bonding interactions associated with planar conformations of the radical **38**.

The relative rates of bromination of the protected amino acids **25 - 29** (Table 2) may reflect polar effects as well as radical stability during development of the corresponding radicals **30 - 34**. The rates of bromination of the amino acid derivatives **25 -29** could be influenced by the degree of coplanarity of the benzamido and carboxyl groups as increased non-bonding interactions of planar conformations in the transition states for hydrogen abstraction by bromine atom would reduce the ability of the captodative substituents to delocalise developing charge and unpaired spin density simultaneously. The faster rate for bromination of the glycine derivative **25** over the valine derivative **27**, for example, may reflect a greater extent of charge delocalisation in the former amino acid derivative (Figure 3).

Steric interactions also need to be considered as another factor which may influence the rates of radical bromination of amino acid derivatives. Steric effects in radical reactions generally refer to the effect on reactivity of a

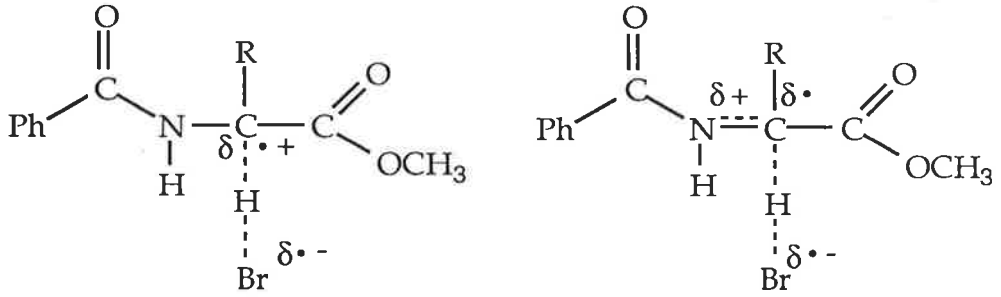

Figure 3 - Delocalisation of induced partial charge during hydrogen abstraction by bromine atom from an amino acid derivative.

hindered radical and not the attack of a radical at a hindered site[26], though there are examples of the regioselectivity of radical reactions being determined by steric interactions of the substrate[29]. In most cases, steric interactions only partially affect the preferential formation of tertiary over secondary radicals, which in turn are formed in preference to primary radicals[26]. The preferential formation of the secondary glycyl radical **30**, over the tertiary radicals **31** and **32**, may reflect greater accessibility of the relatively unhindered α-hydrogens on the glycine derivative **25** to an attacking radical species, than the α-hydrogens of the amino acid derivatives **26** and **27**. Photoalkylations on proteins show that the tertiary structure of a peptide protects some sensitive residues from attack as they are sterically inaccessible (Table 1). Conformational effects in protected amino acids or steric interactions between the side chain of an amino acid derivative with an attacking radical species may be a contributing factor in the rate of hydrogen abstraction from the amino acid derivatives **25 - 29**, and in the more general selectivity for reaction of glycine derivatives in radical reactions.

To separate the various factors that could explain selectivity for hydrogen abstraction from glycine derivatives, it was decided to study the

rates of formation of protected amino acid radicals by carbon-carbon bond homolysis of the corresponding amino acid dimers (Scheme 6). Generating

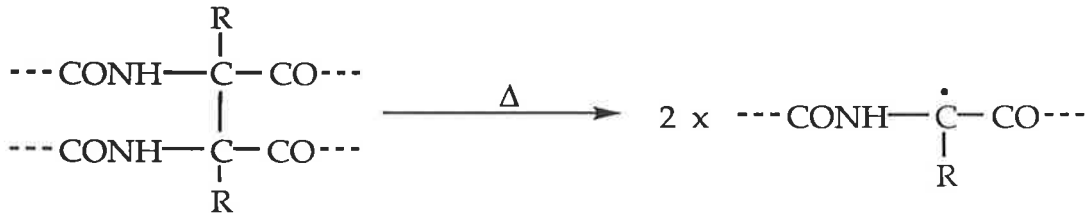

Scheme 6

radicals by homolysis eliminates polar effects in the transition state[20]. Homolysis of the central dimer bond excludes partial charge build-up in the transition state, as both groups around the dimer bond have the same electronegativity. There is no longer an external influence from an electrophilic or nucleophilic atom abstracting species. Steric restrictions on the external radical no longer apply, as radical generation does not rely on intermolecular interactions. Steric effects, if any, favour homolysis of the protected amino acids dimers with α,α'-substituents, due to increased bulk around the dimer bond, thus favouring formation of tertiary over secondary radicals. A sterically more crowded quaternary-quaternary carbon dimer bond has greater strain than a tertiary-tertiary carbon dimer bond and this results in bond elongation of the dimer bond to relieve the strain (Figure 4)[30,31].

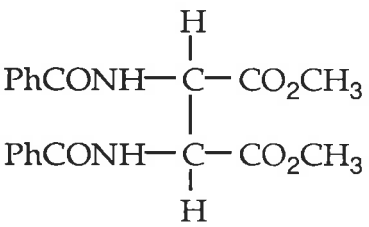

39

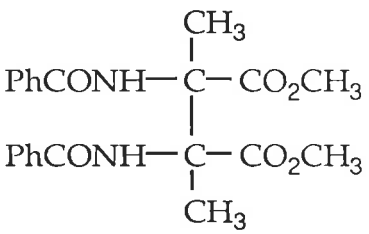

40

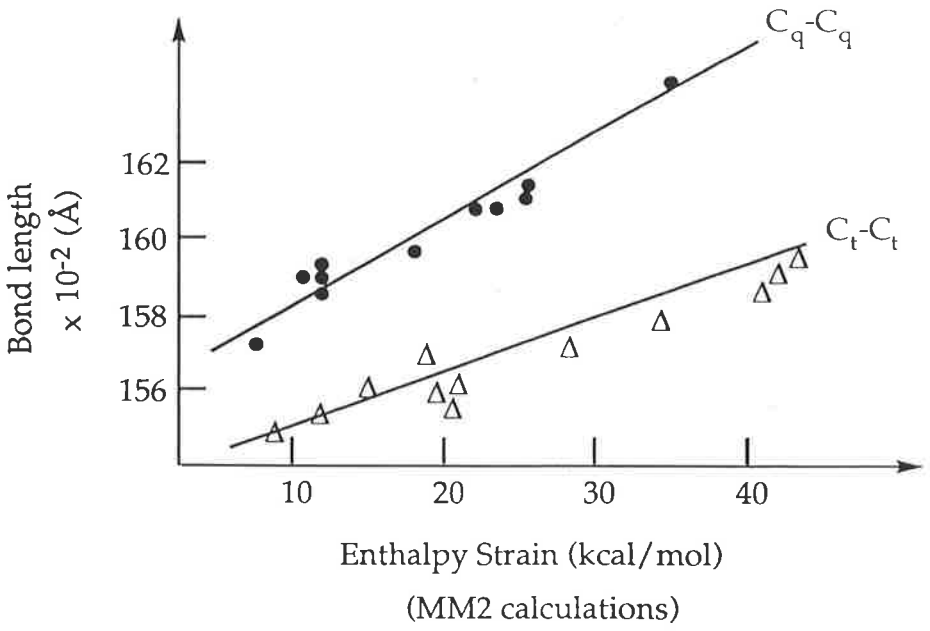

Δ Various alkanes $R^1R^2CH\text{-}CHR^1R^2$

• Various alkanes $R^1R^2R^3C\text{-}CR^1R^2R^3$

Figure 4 - Effect of steric interactions in a dimer on the dimer bond length.

Relative rates of radical generation through homolysis of protected amino acid dimers should reflect the relative stabilities of the protected amino acid radicals. If the protected glycyl radical **30** forms faster than the protected alanyl radical **31**, by homolysis of the protected amino acid dimers **39** and **40**, respectively, even though steric effects favour homolysis of the dimer **40**, the determining factor of the rate of radical production must be the extent of non-bonding interactions in planar conformations of the protected amino acid radicals **30** and **31**, and the consequent extent of delocalisation of the unpaired spin density in those species.

Related experiments have shown the formation of radicals through dimer homolysis. Koch *et al.*,[32] found that solutions of the photoreductive dimer **41** were in equilibrium with the stabilised radical **42** (Scheme 7). ESR

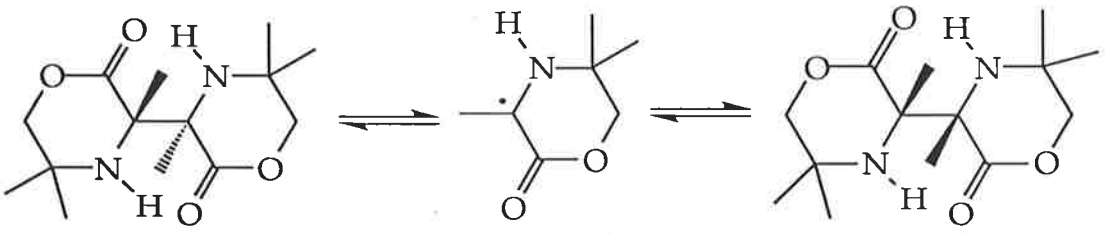

meso - **41** **42** *dl* - **41**

Scheme 7

evidence and spin trapping experiments with 2,2'-azobis-(2-methyl-propionitrile) confirmed the formation of radical **42** when the dimer **41** was dissolved in solution. Koch *et al.*,[32] found that the enthalpy of dissociation of the dimer **41** was solvent dependent and could be calculated from a plot of log hT vs. 1/T, where h was the ESR signal intensity and T the absolute temperature. In chloroform, the enthalpy of dissociation, calculated using a mixture of diastereomers, was 22.0 ± 1.1 kcal/mol, and in ethanol, 10.6 ± 0.3 kcal/mol (*c.f.* the carbon-carbon bond strength in ethane is 88.2 kcal/mol)[33]. Steric interactions around the central bond of the dimer **41** and stabilisation of the radical **42** were given as the main reasons for the low enthalpy of dissociation of the dimer **41**. The faster rate of homolysis of the dimer **41** in ethanol than in chloroform was reasoned to be due to greater stabilisation of the radical **42** in the polar solvent[32,34]. Protic solvents are important in the stabilisation of polar resonance structures of radicals of this type (Figure 5). The unusually weak central bond of the dimer **41** was apparent in the crystal structure of the *dl*-diastereomer from the elongation of that bond to a length of 1.591(4) Å[35]. Also present in the crystal structure were intermolecular hydrogen bonds with lengths of 2.13, 2.18, 2.21 and 2.22 Å, formed between

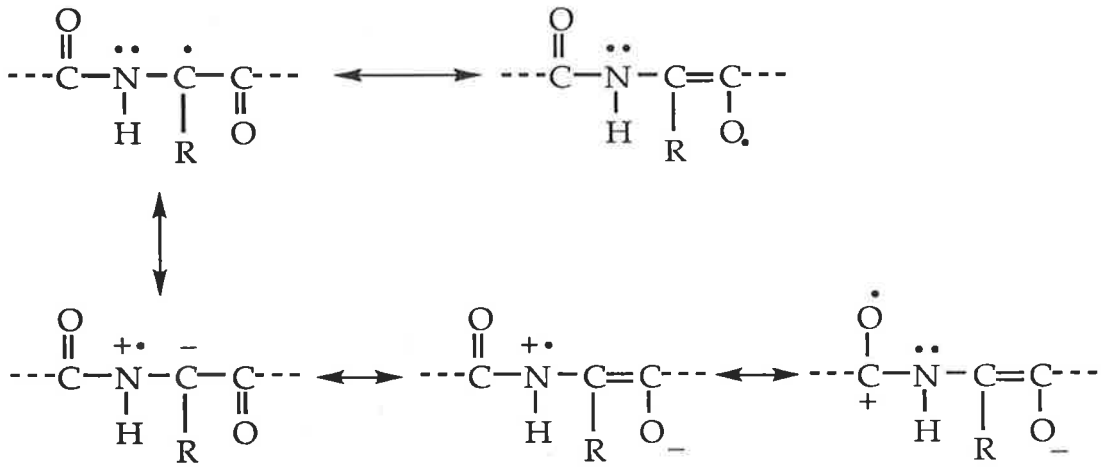

Figure 5 - Resonance delocalisation of an unpaired electron by adjacent amido and carboxyl substituents.

two independent molecules of the *dl*-isomer of the dimer **41** in the asymmetric unit, between the carboxyl oxygens and amino hydrogens.

The rate of dimer homolysis can be determined in several ways. The most common methods have been to measure the rate of equilibration of one diastereomer of a dimer in solution by NMR[36,37], to measure the ESR signal intensity of the radicals produced by dimer homolysis, or by product analysis of homolysis reaction mixtures of dimers with radical scavengers, using NMR or GC[36-38]. Koch *et al.*,[37] used the radicals generated by homolysis of the dimer **41** as one electron reducing agents and showed that homolysis was the rate determining step in the reduction reactions. The production rate of the radical **42** was calculated, using NMR spectroscopy, from the rate of dimer consumption in the reduction reactions. The rate constant for reduction by the *meso*-isomer of the dimer **41** was found to be three times greater than the rate constant for reduction by the *dl*-isomer, though the reason for this difference was not discussed.

The radical **44**, produced by homolysis of the dimer **43** (Scheme 8), is stabilised by amido and amino substituents. From kinetic studies, similar to

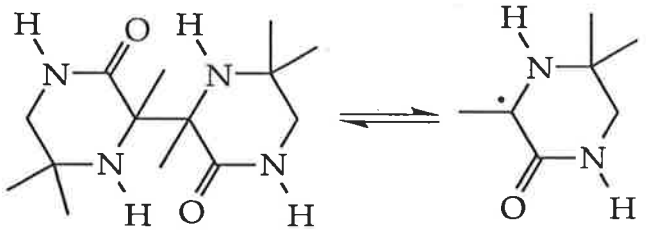

43 **44**

Scheme 8

those carried out on the dimer **41**, homolysis of the dimer **43** was shown to occur less readily[39]. The calculated activation enthalpies for homolysis in methanol of the *dl*- and *meso*-diastereomers of the dimer **43** were 28.0 ± 0.3 and 27.7 ± 0.2 kcal/mol, respectively. The activation enthalpy for the *dl*-diastereomer of the dimer **41** in methanol was 22.6 ± 0.4 kcal/mol. The difference in the rates of formation of the radicals **42** and **44**, by homolysis of the respective dimers **41** and **43**, was said to be due to different conformational effects in the dimers **41** and **43** and greater stability of the radical **42** over the radical **44**. The crystal structure of the *dl*-diastereomer of the dimer **43** showed less strain around the dimer bond than in the dimer **41**, by the reduced elongation of the dimer bond which measured 1.581(5) Å in length[39]. The ESR β-proton hyperfine coupling constant for the methyl group adjacent to the radical centre in the radicals **42** and **44** was smaller for the radical **42** than the radical **44**, implying greater delocalisation, hence stabilisation, of the radical **42**.

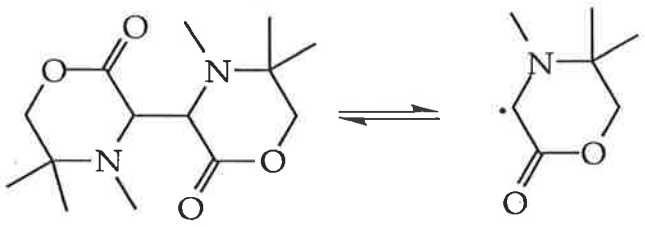

45 **46**

Scheme 9

Homolysis of the dimer **45** produces the secondary radical **46** (Scheme 9). ^{1}H NMR kinetic studies on the rate of reduction of diphenylpicrylhydrazyl (DPPH) by the radical **46** showed that the activation enthalpy for the production of the radical **46** from the dimer **45** (the diastereomer was not indicated) was 26.4 ± 0.1 kcal/mol in 95% ethanol, compared with 20.4 ± 2.0 kcal/mol for the formation of the radical **42** from the *dl*-diastereomer of the dimer **41** in absolute ethanol[40]. The rate constants for the formation of the radicals **46** and **42**, from the respective dimers **45** and **41**, at 25°C, were 1.9×10^{-6} sec^{-1} and 1.2×10^{-3} sec^{-1}, respectively. The slower rate of homolysis of the dimer **45**, compared with the dimer **41**, reflects reduced steric crowding about the central bond of the dimer **45** and lower stability of the radical **46** formed. The crystal structure of the *dl*-diastereomer of the dimer **45** showed a central bond of 1.563(3) Å[40]. As can be seen from the rates of homolysis of the dimers **41**, **43** and **45**, steric crowding around a dimer bond may be an important factor in determining the rate of radical production.

The effect of steric strain on the rate of homolysis of a dimer can be taken into account in the determination of a radical's stability from the rate of radical production. Rüchardt *et al.*,[41] have studied the steric factors that affect

bond strength and determined a linear relationship between bond dissociation energies (BDEs) and strain energies. The stability of a radical can be calculated from the difference between the BDE of a dimer and the BDE of the corresponding hydrocarbon dimer in which the substituents have been exchanged to give equal strain. Calculation of radical stabilities from the BDEs of dimers enabled Beckhaus and Rüchardt, as reported by Sustmann and Korth[18], to examine captodative stabilisation of the radicals **48**. The BDE of the dimers **47**, as well as the BDEs of analogous dimers containing only one radical stabilising substituent and the BDEs of suitably strained hydrocarbon dimers, enabled the captodative stabilisation of the radicals **48** to be calculated. This stabilisation was found to be about 4 kcal/mol greater than the additive stabilisation of the substituents.

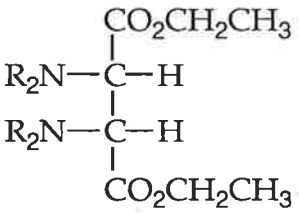

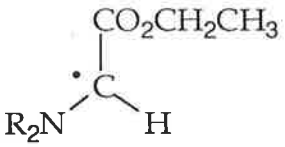

R = CH_3, C_2H_5, *i*-C_3H_7

47 **48**

The synthesis of the dimers **39**, **40** and **49** of *N*-benzoylglycine methyl ester **25**[22,42], *N*-benzoylalanine methyl ester **26**[22] and methyl pyroglutamate **29**[43], respectively, has been reported. Irradiation of a benzene solution containing methyl pyroglutamate **29** and DTBP **21** (1 mole equiv.) produced a 1 : 1 diastereomeric mixture of the dimer **49** in 64% yield. Similarly, irradiation using 3500 Å lamps of a solution of benzene, *N*-benzoylglycine methyl ester **25** and DTBP **21** (4.6 mole equivalents) gave a 1 : 1 mixture of the

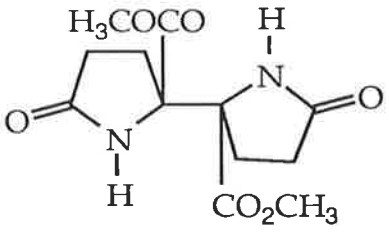

49

diastereomers of the dimer **39**, in 37% yield, and *N*-benzoylalanine methyl ester **26**, in 34% yield. The mechanism of the reaction has already been outlined in Scheme 5. The glycyl radical **30**, produced by hydrogen abstraction with *t*-butoxy radical **22**, either couples with another glycyl radical **30** to give the dimer **39**, or couples with methyl radical **23** to produce the alanine derivative **26**. Irradiation of a mixture of *N*-benzoylalanine methyl ester **26** and DTBP **21** (12.7 mole equivalents) in *t*-butanol produced the dimer **40** in 20% yield and methyl 2-benzamido-2-methylpropanoate **50** in 10% yield.

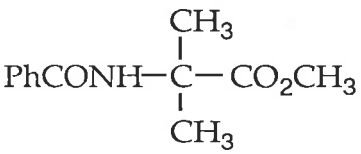

50

To assess the viability of producing protected amino acid radicals by homolysis of the corresponding dimers, the initial study described in this thesis focussed on the relative rates of homolysis of the protected glycine and alanine dimers, **39** and **40**, respectively. It was expected that the relative rates of homolysis would help delineate factors affecting formation of the corresponding radicals **30** and **31**. This thesis therefore begins with a

description of the synthesis of the dimers **39**, **40** and **49**. The crystal structures of the *meso*-diastereomer of the dimer **39**, both diastereomers of the dimer **40** and both diastereomers of the dimer **49** were also examined, to determine whether there is a relationship between dimer bond elongation and radical stability, as indicated by Koch *et al.*,[32] or whether bond elongation is a consequence of the steric interactions in a dimer. Later chapters examine the reactions of the dimers **39** and **40** under homolytic conditions and the effect of solvent on the rates of reaction.

Results and Discussion Chapter One

Synthesis and Crystal Structures of Protected Amino Acid Dimers

The dimers **39**, **40** and **49** of protected glycine **25**, alanine **26** and pyroglutamic acid **29**, respectively, were required for the examination of their relative rates of homolysis and the study of their crystal structures to determine the degree of central bond elongation. Synthesis of the dimers **39**, **40** and **49** followed reported procedures, involving the irradiation of benzene or *t*-butanol **24** solutions containing DTBP **21** and the amino acid derivatives **25**, **26** and **29**, respectively[22,42,43].

The product mixture from the photochemical reaction of *N*-benzoyl-glycine methyl ester **25** and DTBP **21** in benzene was shown by TLC and HPLC analysis to contain the diastereomers of the dimer **39**, *N*-benzoylalanine methyl ester **26** and an unknown compound. The mechanism of formation of the amino acid derivative products **26** and **39** is as outlined for the general case in Scheme 5. One diastereomer of the dimer **39** precipitated from the reaction mixture and was obtained in 21% yield after filtration. The other diastereomer was isolated in 11% yield, from the evaporated filtrate of the reaction mixture, by crystallisation from ethyl acetate-hexane. These yields represent the first crop of each diastereomer isolated. Subsequent crops contained mixtures of the diastereomers and these could not be efficiently separated by crystallisation. The unknown material in the reaction mixture of the glycine derivative **25** and DTBP **21** was isolated by chromatography and identified as biphenyl **51** from its physical and spectroscopic properties, which were identical to those of an authentic sample. Formation of biphenyl **51** most likely involves the production of phenyl radical by hydrogen abstraction

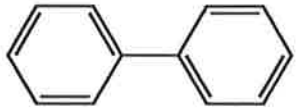

51

from the solvent, followed by addition to benzene then loss of a hydrogen atom[44].

Chiral phase HPLC analysis of the diastereomer of the dimer **39** that precipitated from the reaction mixture of the glycine derivative **25** and DTBP **21** showed that it resolved into two components and was therefore the *dl*-isomer. Reverse phase HPLC analysis showed that this isomer of the dimer **39** was pure. The infrared spectrum of the *dl*-isomer of the dimer **39** indicated the presence of hydrogen bonding between the amide hydrogens and the ester carbonyls by the broadening of the absorbances for these groups at 3250 cm^{-1} and at 1750 and 1740 cm^{-1}, respectively. The ^{1}H NMR spectrum of the *dl*-isomer of the dimer **39** showed a distinct doublet for the α,α'-hydrogens at δ 5.32 (*J* 5Hz), which differs from the signal for the α-hydrogens of the starting material **25** at δ 4.26, while the α,α'-carbons in the ^{13}C NMR spectrum resonated at δ 54.5, distinct from the starting material **25** α-carbon resonance which occurred at δ 41.7. Hydrogen bonding is also evident from the ^{1}H NMR spectrum of the *dl*-isomer of the dimer **39** by the downfield shift of the signal for the amide hydrogens to δ 7.2, from δ 6.8 for the amide hydrogen of the starting material **25**. As the ^{1}H NMR sample of the *dl*-isomer of the dimer **39** was a dilute and relatively non-polar solution ($CDCl_3$) the hydrogen bonding is most probably intramolecular (Figure 6). The *dl*-isomer of the dimer **39** was found to have a molecular ion at m/z 384 in its mass spectrum. The appearance of a peak at m/z 193 corresponded to the cation radical of the

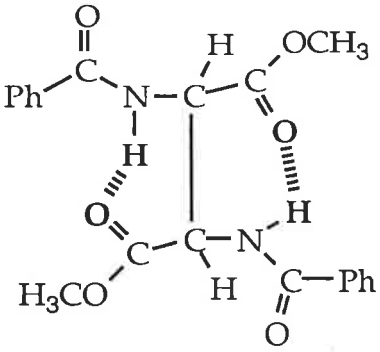

Figure 6 - Intramolecular hydrogen bonding in the dimer **39**.

monomer **25**. A possible mechanism for the formation of the species at m/z 193 is shown in Scheme 10. It involves the molecular ion undergoing dimer bond cleavage when an amide hydrogen on one half of the molecule is removed by an amide carbonyl on the other half. The radical cation thus

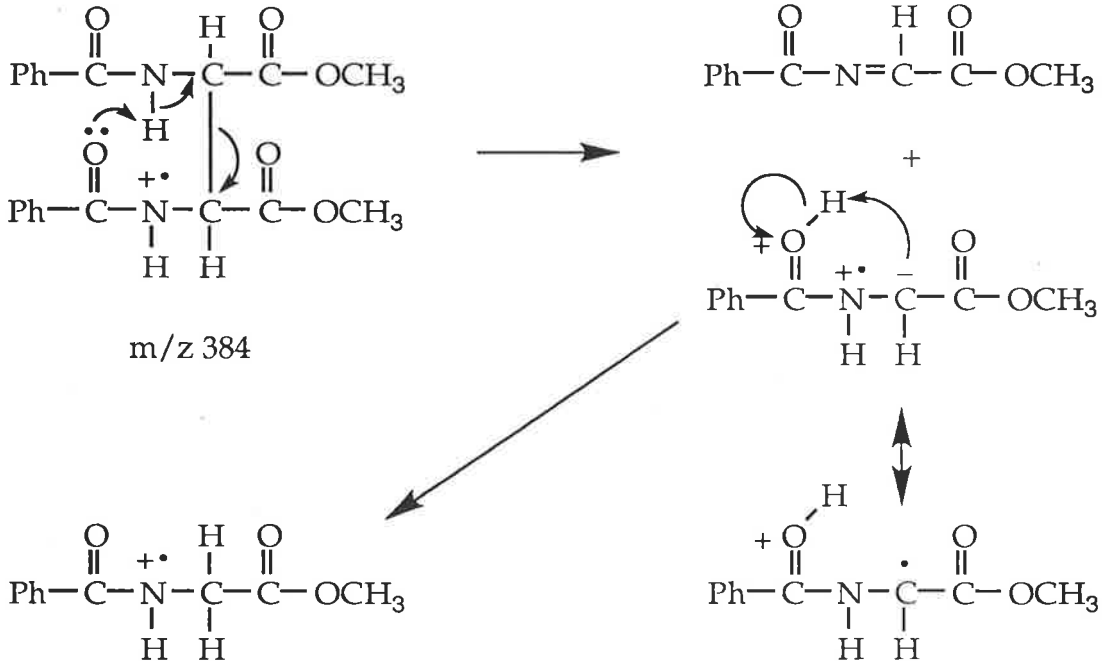

Scheme 10

formed is resonance stabilised and is a tautomer of the radical cation of *N*-benzoylglycine methyl ester **25**. A similar mechanism involving the ester carbonyl acting as the base is also possible, but less likely as amides are generally much more basic than esters[45].

Chiral phase HPLC analysis of the other diastereomer of the dimer **39**, isolated from the reaction mixture of the amino acid derivative **25** and DTBP **21**, confirmed that it was the *meso*-isomer, as it was found to consist of only one major component. Reverse phase HPLC analysis showed that the *meso*-isomer of the dimer **39** contained 3% of the *dl*-isomer. The greater solubility of the *meso*-isomer of the dimer **39** over the *dl*-isomer in organic solvents resulted in the *meso*-isomer always containing some (up to 5%) of the other diastereomer after recrystallisation. The spectral properties of the *meso*-isomer of the dimer **39** were similar to those of the *dl*-isomer. The infrared spectrum of the *meso*-isomer of the dimer **39** showed broadening of the amide hydrogen and ester carbonyl absorbances, at 3300 and 1735 cm^{-1}, respectively. The signal due to the α,α'-hydrogens of the *meso*-isomer of the dimer **39** appeared as a doublet at δ 5.34 (*J* 6Hz) in the ^{1}H NMR spectrum while the signal for the α,α'-carbons appeared at δ 56.3 in the ^{13}C NMR spectrum. Hydrogen bonding as indicated by the infrared spectrum of the *meso*-isomer of the dimer **39** was also seen in the ^{1}H NMR spectrum, by the downfield shift of the signal for the amide hydrogens to δ 8.0, from δ 6.8 in the starting material **25**. The mass spectrum of the *meso*-isomer of the dimer **39** showed a molecular ion at m/z 384 and a fragment ion at m/z 193.

The structure of the *meso*-isomer of the dimer **39**, determined by X-ray crystallographic analysis of a crystal grown in ethanol-water, is shown in Figure 7 and the relative orientation of the substituents is represented using a Newman projection in Figure 8. Bond distances and bond angles in the

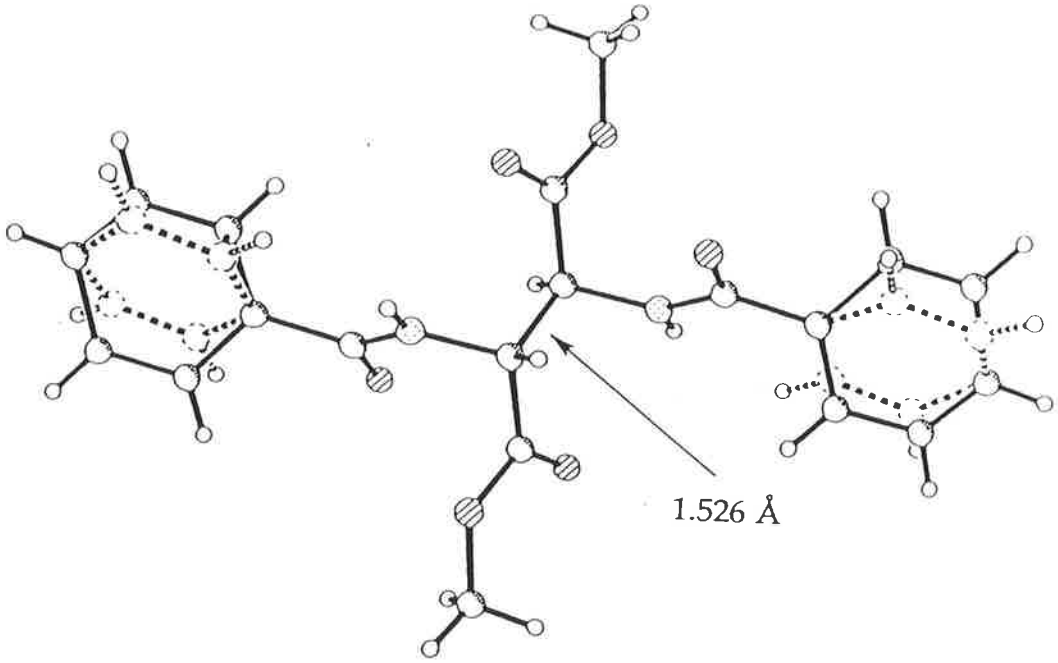

Figure 7 - Crystal structure of the *meso*-isomer of the dimer 39.

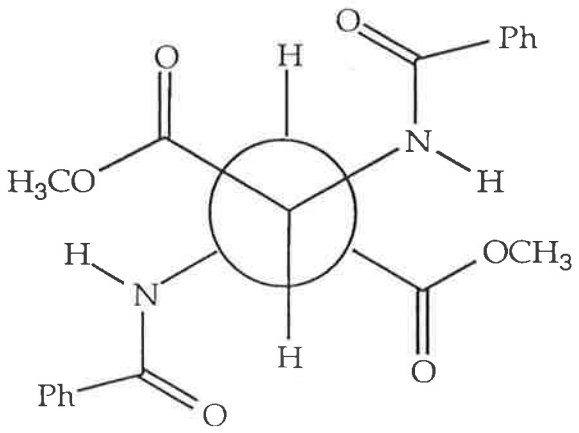

Figure 8 - Newman projection of the *meso*-isomer of the dimer 39, based on crystal structure data.

crystal structure can be found in the Appendix. The crystal structure confirmed the *meso* configuration and showed two conformational orientations of the phenyl groups. Intramolecular hydrogen bonding was not found in the crystal structure of the *meso*-isomer of the dimer 39. There

were, however, intermolecular hydrogen bonds, each with lengths of 2.01(5) Å, between amide hydrogens and neighbouring amide carbonyls. The lack of intramolecular hydrogen bonds may reflect their disruption in the polar solvent from which the crystal was obtained. The length of the central bond in the *meso*-isomer of the dimer **39**, of 1.526(6) Å, did not show the elongation found for the central bonds of the dimers **41**, **43** and **45**, which were shown to have lengths of 1.591, 1.581 and 1.563 Å, respectively[35,39,40]. The central bond of the *meso*-isomer of the dimer **39** is of similar length to the carbon-carbon bond of ethane, which measured 1.534 Å[46], indicating that there is very little steric crowding around the central bond of the *meso*-isomer of the dimer **39**. Factors affecting stabilisation of the protected glycyl radical **30** do not appear to affect the length of the central bond of the *meso*-isomer of the dimer **39**, even though these factors were indicated by Koch *et al.*,[35] as being partially responsible for the weakening of the central bond of the dimer **41**.

The physical and spectroscopic properties of the *dl*- and *meso*-isomers of the dimer **39** did not correspond with the properties reported in the literature[42]. Further investigations revealed that the data in the literature had been assigned to the wrong stereoisomers.

The photoinduced reaction of *N*-benzoylalanine methyl ester **26** and DTBP **21** in *t*-butanol **24**, to give the protected alanine dimer **40**, has been reported[22]. The literature procedure was followed except for a reduction in the amount of DTBP **21** (previously 12.7 mole equivalents), to make isolation of the products easier. Chromatography of the crude reaction mixture, followed by fractional crystallisation of the fractions obtained, yielded the *dl*- and *meso*-isomers of dimethyl 2,3-dibenzamido-2,3-dimethylbutanedioate **40**, methyl 2-benzamido-2-methylpropanoate **50**, 2-benzamido-2,4-dimethyl-4-

hydroxypentanoic acid γ-lactone **52** and 2,5-dimethylhexane-2,5-diol **53**. The products were identified from their physical and spectroscopic properties.

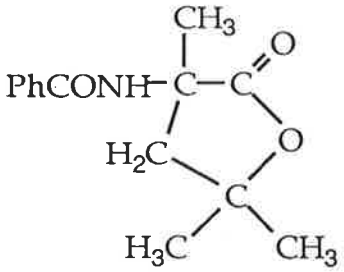

52

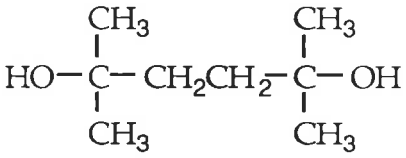

53

Assignment of the configurations of the diastereomers of the dimer **40** was on the basis of their crystal structures.

The structure of the *dl*-isomer of the dimer **40**, determined by X-ray crystallographic analysis of a crystal grown in ethyl acetate-hexane, is shown in Figure 9. Bond distances and bond angles in the crystal structure can be

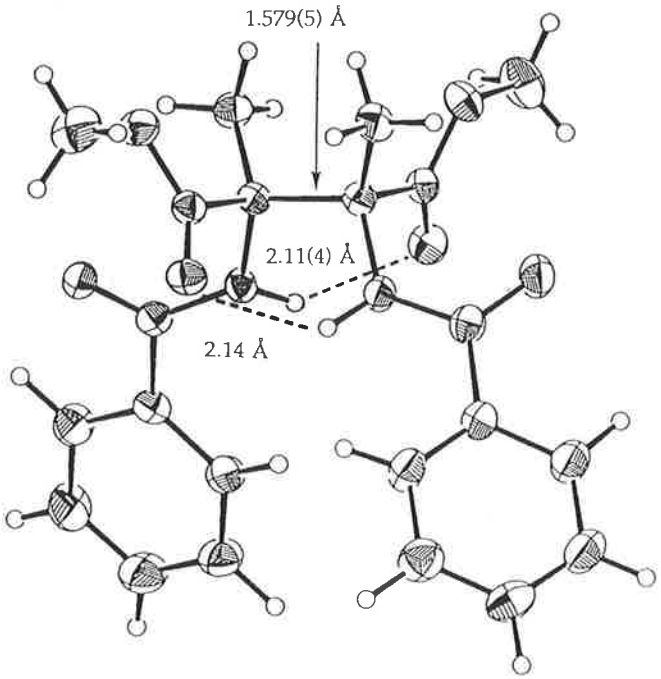

Figure 9 - Crystal structure of the *dl*-isomer of the dimer **40**.

found in the Appendix. Intramolecular hydrogen bonding was found between the two halves of the dimer, with two hydrogen bonds per molecule, between the amide hydrogens and the ester carbonyls. The hydrogen bonds were 2.11 and 2.14 Å in length. A Newman projection of the *dl*-isomer of the dimer **40**, illustrating the hydrogen bonds, is shown in Figure 10. Greater

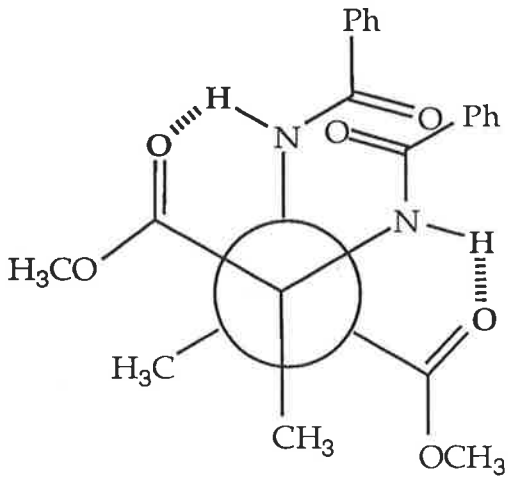

Figure 10 - Newman projection of the *dl*-isomer of the dimer **40**, based on crystal structure data.

steric strain around the central bond of the *dl*-isomer of the dimer **40** (Figure 10), compared with the *meso*-isomer of the dimer **39** (Figure 8), is evident from the elongation of the central bond which has a length of 1.579(5) Å.

The structure of the *meso*-isomer of the dimer **40**, determined by X-ray crystallographic analysis of a crystal grown in ethyl acetate-hexane, is shown in Figure 11. Bond distances and bond angles in the crystal structure can be found in the Appendix. Two intramolecular hydrogen bonds were found, each measuring 2.34 Å in length. The relative orientation of the substituents in the *meso*-isomer of the dimer **40**, shown in the crystal structure, is represented using a Newman projection in Figure 12. The relative

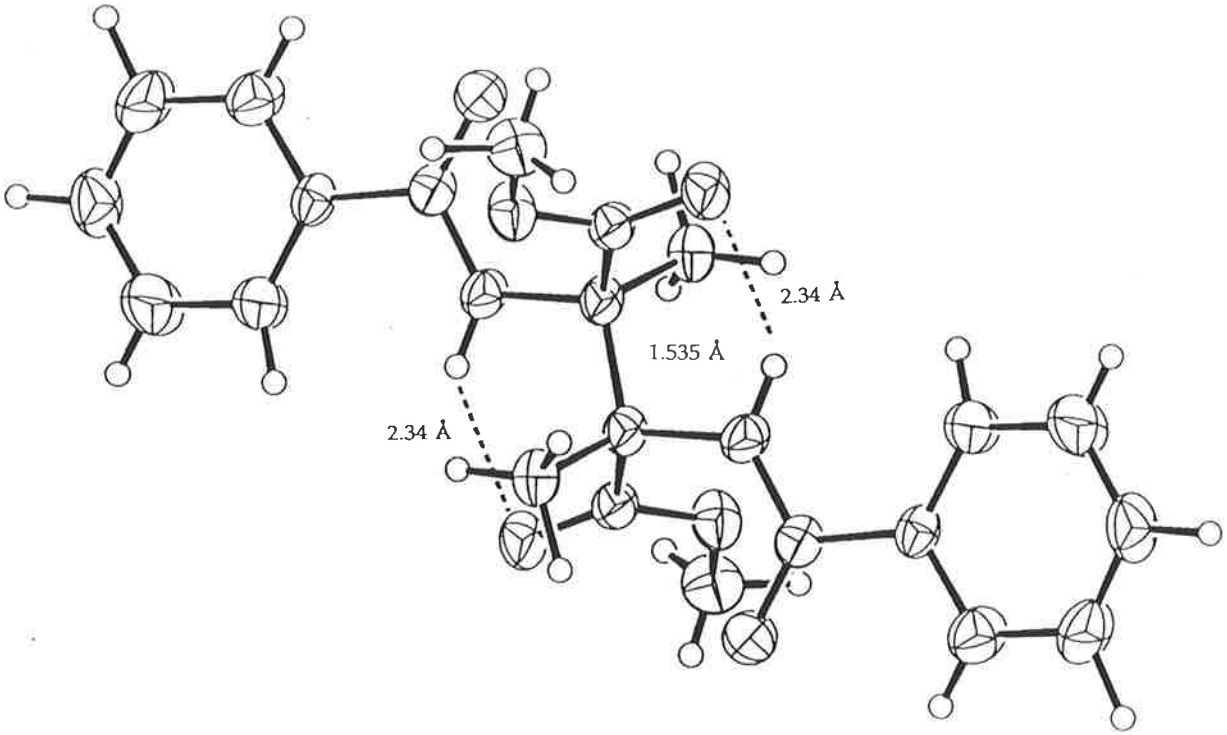

Figure 11 - Crystal structure of the *meso*-isomer of the dimer **40**.

orientation of the substituents is similar to that for the *meso*-isomer of the protected glycine dimer **39**, with the exception that the orientation of the methoxycarbonyl substituents is redirected by intramolecular hydrogen

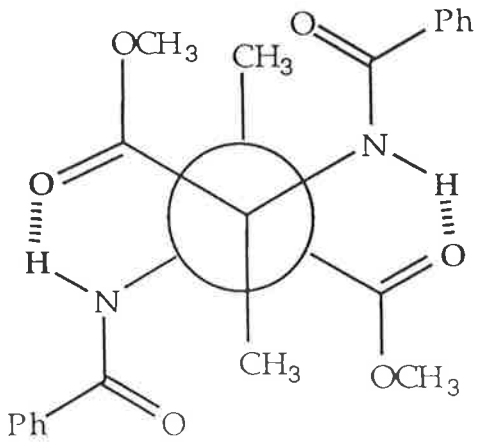

Figure 12 - Newman projection of the *meso*-isomer of the dimer **40**, based on crystal structure data.

bonding in the alanine derivative **40**. This difference can be attributed to the fact that the crystal of the *meso*-isomer of the alanine derivative **40** was produced in a relatively non-polar solvent mixture, facilitating intramolecular hydrogen bonding. The length of the central bond of the *meso*-isomer of the dimer **40**, of 1.535(7) Å, may be attributed to steric crowding around the dimer bond being less than for the *dl*-isomer of the dimer **40**, but greater than for the *meso*-isomer of the dimer **39**, as shown in the Newman projections (Figures 8, 10 and 12). It is interesting to note that the *dl*-isomer of the dimer **40** with the longer central bond has the shorter and stronger hydrogen bonds, compared with those of the *meso*-isomer of the dimer **40**. Elongation of the central bond of the *dl*-isomer of the dimer **40**, compared with that of the *meso*-isomer, may be a consequence of intramolecular hydrogen bonding, as for hydrogen bonding to occur in the *dl*-isomer a sterically unfavourable conformation is required.

Reverse phase HPLC analysis revealed that the *dl*-isomer of the dimer **40** contained 0.2% of the *meso*-diastereomer. The infrared spectrum of the *dl*-isomer of the dimer **40** showed two amide hydrogen absorbances at 3440 and 3420 cm^{-1} and two ester carbonyl absorbances at 1740 and 1735 cm^{-1}. The duplication can be attributed to two different hydrogen bonds involving these groups, as shown in the crystal structure. The ^{1}H NMR spectrum of the *dl*-isomer of the dimer **40** showed no α-hydrogen signal of the starting material **26** and the collapse of the doublet signal for the α-methyl group to a singlet which occurred at δ 1.64. ^{13}C NMR spectroscopy confirmed dimerisation by the downfield shift of the α-carbon signal from δ 48.5 for the starting material **26** to δ 62.7. Analysis of the ^{1}H NMR spectrum also confirmed the presence of hydrogen bonding by the downfield chemical shift of the signal of the amide hydrogens from δ 6.8 for the starting material **26** to δ 8.5. The mass spectrum

displayed a protonated molecular ion at m/z 413 and a fragment ion at m/z 207, probably arising from dimer bond cleavage of the molecular ion (Scheme 11).

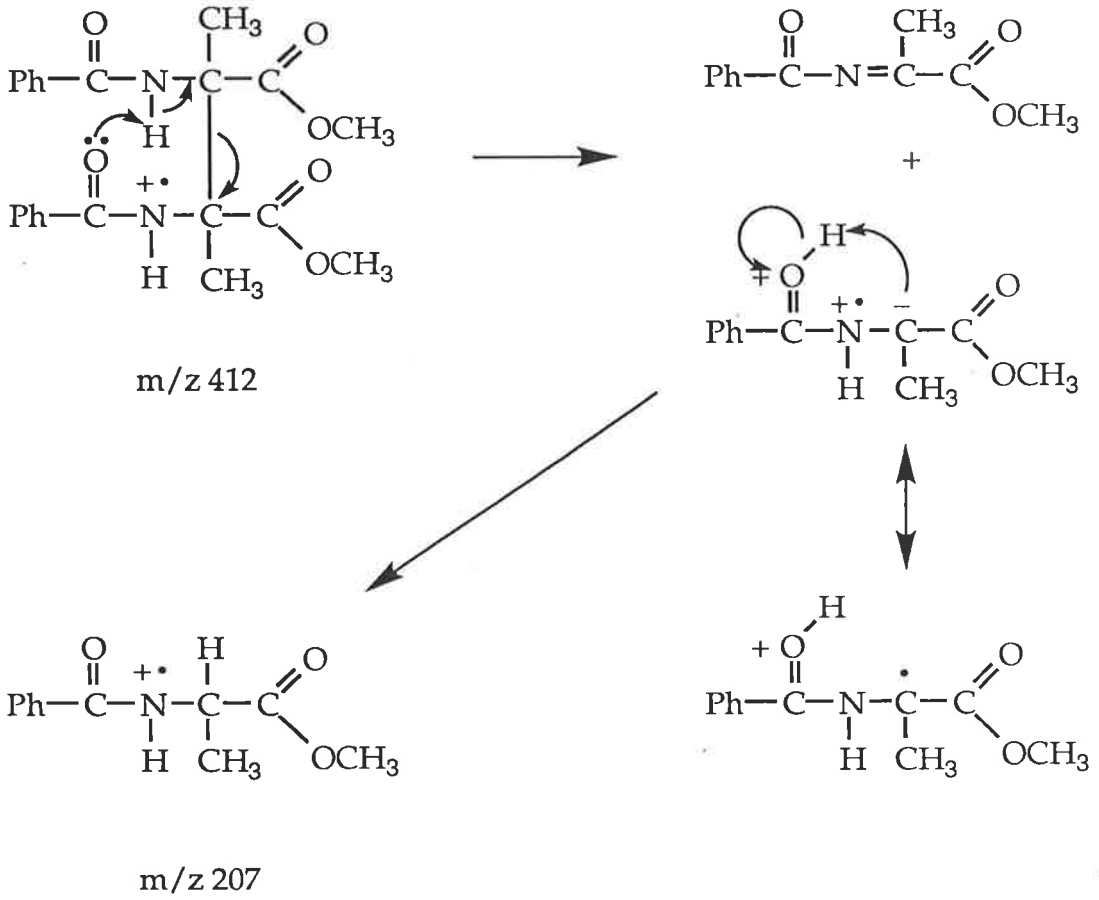

Scheme 11

Reverse phase HPLC analysis showed that the *meso*-isomer of the dimer **40** contained 3% of the *dl*-diastereomer. The ester carbonyl and amide hydrogen absorbances at 3450 and 1725 cm^{-1}, respectively, in the infrared spectrum of the *meso*-isomer of the dimer **40** did not show broadening characteristic of hydrogen bonding, but this was indicated by the shift of

25 cm^{-1} to a lower wavenumber for the ester carbonyl absorbance compared with the infrared absorbance of the ester carbonyl of the protected alanine **26**. ^1H NMR spectroscopy showed the α,α'-methyl resonance of the *meso*-isomer of the dimer **40** to be a singlet at δ 1.98 and the α,α'-carbons gave rise to a resonance at δ 65.9 in the ^{13}C NMR spectrum. The signal due to the hydrogen bonded amide hydrogens was found at δ 8.2 in the ^1H NMR spectrum. The mass spectrum of the *meso*-isomer of the dimer **40** showed a protonated molecular ion of m/z 413 and a fragment ion at m/z 207.

The chemical shifts of the signals due to the amide hydrogens of the *dl*- and *meso*-isomers of the dimer **40**, of δ 8.5 and δ 8.2, respectively, reflect the relative lengths and strengths of the intramolecular hydrogen bonds in the crystal structures, with lengths of 2.11 and 2.14 Å for the *dl*-isomer and 2.34 Å for the *meso*-isomer. By analogy, it can be assumed that the *meso*-isomer of the dimer **39** has stronger intramolecular hydrogen bonds than the corresponding *dl*-isomer, based on the relative chemical shifts of the signals of the amide protons, of δ 8.0 and δ 7.2, respectively.

The other expected product from the reaction was the α-methylalanine derivative **50**. The amino acid derivative **50** was shown to be pure by reverse phase HPLC analysis and its physical and spectroscopic properties matched those reported[47]. The first of the previously unreported products from the reaction between the alanine derivative **26** and DTBP **21**, 2-benzamido-2,4-dimethyl-4-hydroxypentanoic acid γ-lactone **52**, was identified from its crystal structure which is shown in Figure 13. Bond distances and bond angles in the crystal structure can be found in the Appendix. The lactone **52** was shown to be pure by reverse phase HPLC analysis. The ^1H NMR spectrum of the lactone **52** showed singlets for the methyl groups at δ 1.52, 1.62 and 1.69 and doublets for the diastereotopic methylene hydrogens at δ 2.33 (*J* 13Hz) and

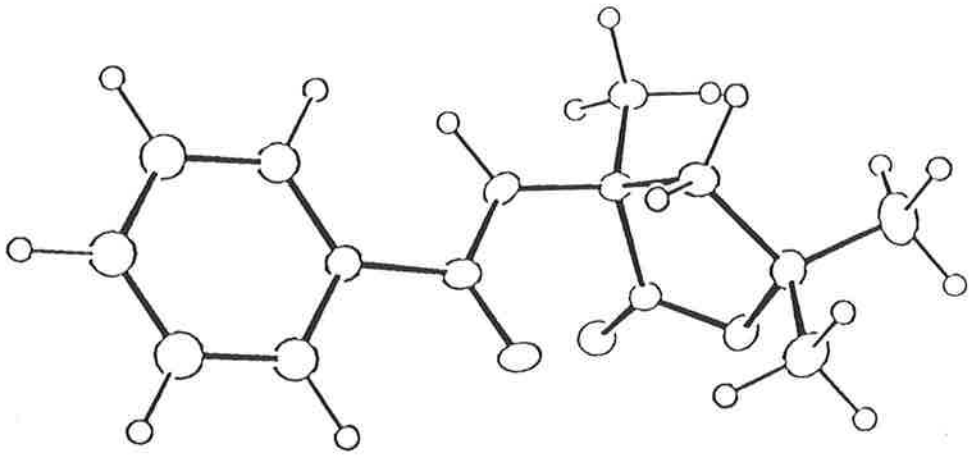

Figure 13 - Crystal structure of the lactone **52**.

δ 2.75 (*J* 13Hz). The infrared spectrum of the lactone **52** showed an absorbance at 1745 cm^{-1} for the lactone carbonyl, which had a carbon resonance at δ 176.8 in the ^{13}C NMR spectrum. The mass spectrum showed a protonated molecular ion at m/z 248, and a fragment ion at m/z 188 corresponding to the loss of the isopropyloxy group from the molecular ion. The other unreported product from the reaction, 2,5-dimethylhexane-2,5-diol **53**, had identical physical and spectroscopic characteristics to those of an authentic sample.

The mechanism of formation of the lactone **52** and the diol **53** from the reaction between DTBP **21** and *N*-benzoylalanine methyl ester **26** is outlined in Schemes 5 and 12. The photolysis of the peroxide bond in DTBP **21** generates *t*-butoxy radical **22**, which can undergo β-scission to form acetone and methyl radical **23** or abstract hydrogen from the α-position of *N*-benzoyl-alanine methyl ester **26** to form *t*-butanol **24** and the stabilised radical **31**.

Coupling of the *N*-benzoylalanine methyl ester radical **31** produces the diastereomers of the dimer **40**, while reaction of the radical **31** with methyl radical **23** forms the α-methylalanine derivative **50**. *t*-Butoxy radical **22** can also abstract a hydrogen from the solvent, *t*-butanol **24** to give *t*-butanol **24** and the carbon-centred radical **54**. This radical then either couples with the *N*-benzoylalanine methyl ester radical **31** to produce the hydroxy ester **55**,

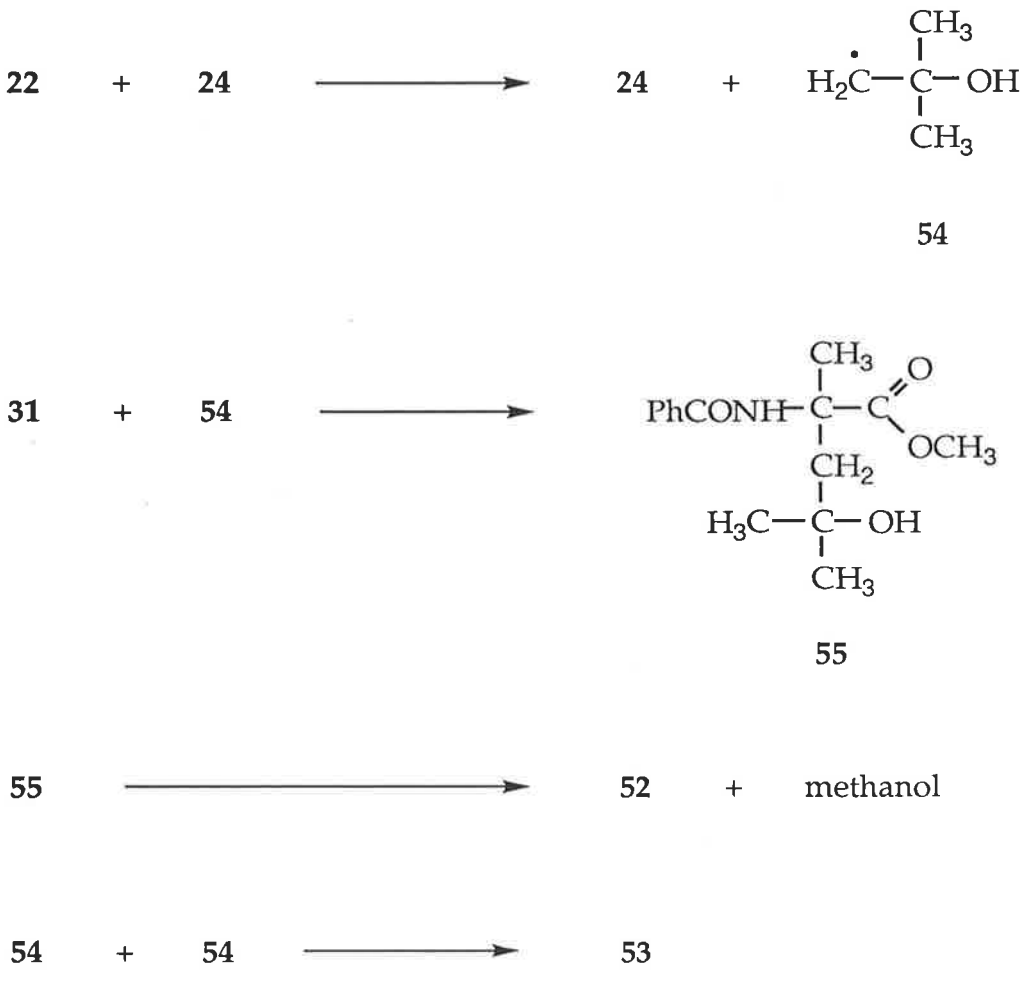

Scheme 12

which undergoes cyclisation to produce the lactone **52**, or it dimerises to give the diol **53**.

The literature procedure[43] was followed for the synthesis and isolation of the diastereomers of the dimer **49** of methyl pyroglutamate **29**, with the exceptions of doubling the ratio of DTBP **21** (previously 1 mole equivalent) to methyl pyroglutamate **29** and using 16 x 3500 Å lamps in a Rayonet photochemical reactor instead of a low pressure mercury lamp. After photolysis, concentration of the reaction mixture gave a solid which was shown by TLC analysis to contain many components including biphenyl **51**. The diastereomers of the dimer **49**, isolated by chromatography and fractional crystallisation of the fractions, had physical and spectroscopic properties in agreement with those reported in the literature[43]. The infrared and ^{1}H NMR spectra of the diastereomers of the dimer **49** indicated that hydrogen bonding exists, with stronger intramolecular hydrogen bonds for the *meso*-isomer. The infrared spectrum of the *dl*-isomer of the dimer **49** showed broad amide hydrogen and lactam carbonyl absorbances, at 3250 and 1705 cm^{-1}, respectively, and duplicate absorbances for the ester carbonyl group, at 1750 and 1735 cm^{-1}, indicating the presence of two different hydrogen bonds. The infrared spectrum of the *meso*-isomer of the dimer **49** showed broad absorbances for the amide hydrogen, lactam carbonyl and ester carbonyl groups at 3200, 1690 and 1730 cm^{-1}, respectively. The ^{1}H NMR chemical shifts of the signals for the amide hydrogens, of samples dissolved in deuteriochloroform, were δ 6.4, δ 6.6 and δ 6.9, for methyl pyroglutamate **29**, the *dl*-isomer of the dimer **49** and the *meso*-isomer of the dimer **49**, respectively. The mass spectrum of each diastereomer of the dimer **49** showed a molecular ion at m/z 284 and a fragment ion at m/z 142.

The structure of the *dl*-isomer of the dimer **49**, determined by X-ray

crystallographic analysis of a crystal grown in methanol, is shown in Figure 14. Bond distances and bond angles in the crystal structure can be found in

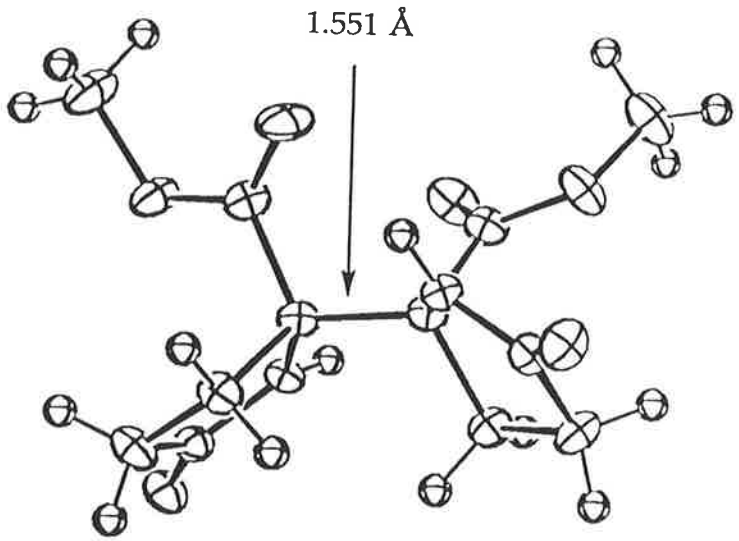

Figure 14 - Crystal structure of the *dl*-isomer of the dimer **49**.

the Appendix. The crystal structure showed that there were no close hydrogen bond contacts and that the length of the central bond was 1.551(6) Å. The relative orientation of the groups in the *dl*-isomer of the dimer **49** is shown in Figure 15.

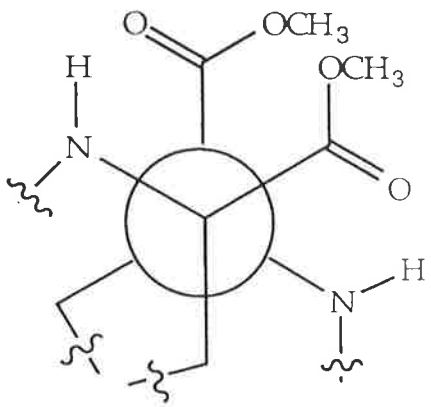

Figure 15 - Newman projection of the *dl*-isomer of the dimer **49**, based on the crystal structure.

The structure of the *meso*-isomer of the dimer **49**, determined by X-ray crystallographic analysis of a crystal grown in methanol-acetone, is shown in Figure 16. Bond distances and bond angles in the crystal structure can be found in the Appendix. The crystal structure showed that the relative

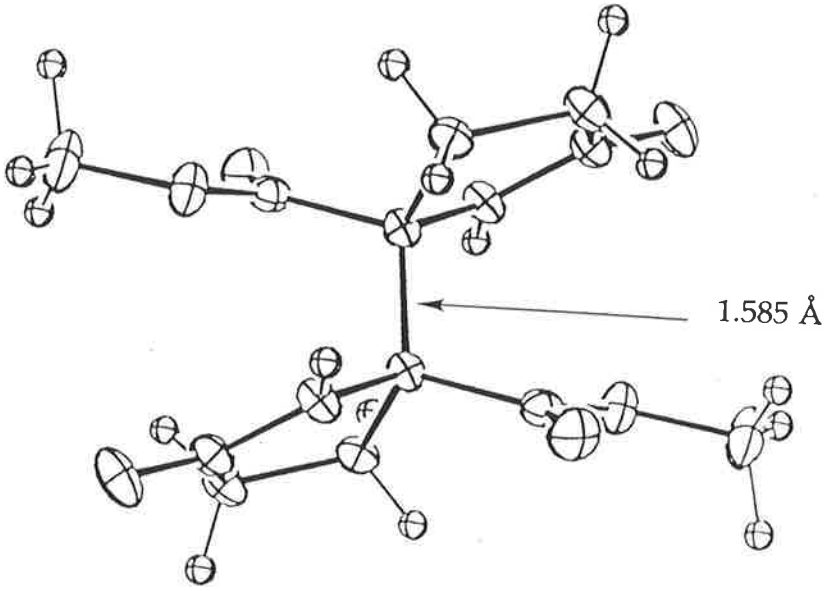

Figure 16 - Crystal structure of the *meso*-isomer of the dimer **49**.

orientation of the substituents (Figure 17) is similar to that found for the *meso*-isomer of the dimer **40** (Figure 12). Intermolecular hydrogen bonds were found, each with lengths of 2.102 Å, between amide hydrogen and amide carbonyl groups. The central bond of the *meso*-isomer of the dimer **49** was 1.585(4) Å in length, which is longer than the central bonds of the *dl*-isomer of the dimer **49** and the diastereomers of the dimer **40**. There is no obvious reason for the elongated central bond, as steric interactions around the central bonds of the *dl*- and *meso*-isomers of the dimer **49** appear to be similar (Figures 15 and 17). Intermolecular hydrogen bonding in the *meso*-

isomer of the dimer **49** may cause the substituents to adopt conformations that increase the steric strain in that compound.

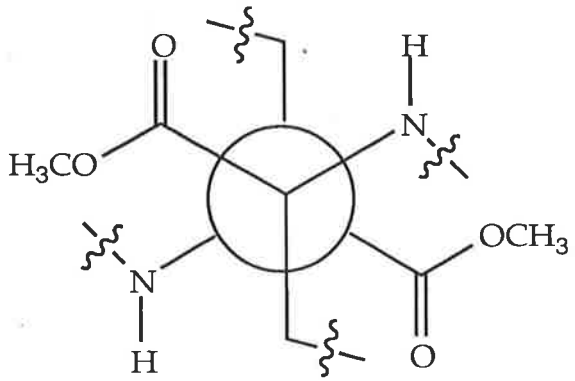

Figure 17 - Newman projection of the *meso*-isomer of the dimer **49**, based on the crystal structure.

Another compound that was synthesised was the dimer **57** of *N*-*t*-butoxycarbonylglycine methyl ester **56**. The change of the nitrogen protecting group from an amide to a carbamate was expected to enhanced dative stabilisation of the radical **58** by the carbamate group, relative to the amide, leading to a weaker central bond in the dimer **57**.

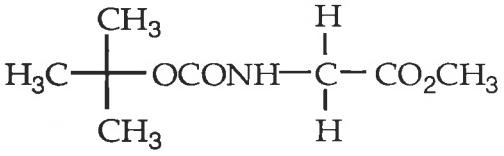

56

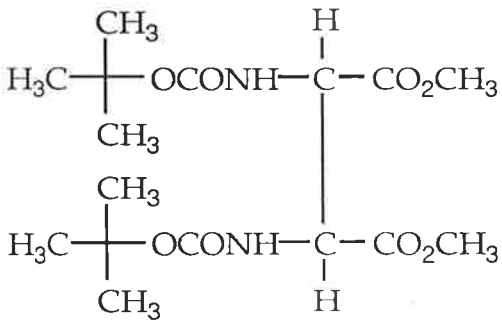

57

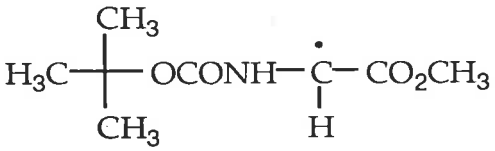

58

Irradiation of a solution containing DTBP **21** and *N*-*t*-butoxycarbonyl-glycine methyl ester **56** in benzene produced the diastereomers of the dimer **57**, which were isolated from the reaction mixture by chromatography followed by fractional crystallisation of the concentrated fractions. It was not possible to determine the stereochemistry of the diastereomers of the dimer **57** as they could not be resolved by chiral phase HPLC and the crystals obtained from several different solutions were not of a quality suitable for X-ray analysis. The ^{1}H NMR spectrum of the first diastereomer of the dimer **57** to elute off the column, **57a**, showed resonances for the α,α'-hydrogens at δ 4.80, and for the α,α'-carbons at δ 55.3 in the ^{13}C NMR spectrum, which differ from the NMR signals for the α-hydrogens and α-carbon of the starting material **56**, which resonate at δ 3.87 and δ 42.2, respectively. The mass spectrum of the dimer **57a** showed a protonated molecular ion at m/z 377 and a fragment ion corresponding to the radical cation of the monomer **56** at m/z 189. The second diastereomer of the dimer **57** to elute off the column, **57b**, showed the resonance for the α,α'-hydrogens at δ 4.86 in the ^{1}H NMR spectrum and the resonance for the α,α'-carbons at δ 55.9 in the ^{13}C NMR spectrum. Hydrogen bonding in the diastereomers of the dimer **57** appeared to be weaker than in the diastereomers of the dimer **39**, as determined by ^{1}H NMR spectroscopy, based on the relative chemical shifts of the resonances of the amide and carbamate hydrogens of the dimers **39** and **57** and the

starting amino acid derivatives **56** and **25**. The ^{1}H NMR spectra showed signals for the carbamate hydrogens at δ 5.3 and δ 5.5 for the dimers **57a** and **57b**, respectively, slightly downfield from the signal for the carbamate hydrogen of the glycine derivative **56**, at δ 5.1. The infrared spectrum of the dimer **57a** showed absorbances at 3350, 1745, 1720, 1710 and 1675 cm^{-1}, while the infrared spectrum of the dimer **57b** showed absorbances at 3425, 3350, 1760, 1730, 1705 and 1690 cm^{-1}. The infrared spectra of the diastereomers of the dimer **57** are very complicated with broad carbamate hydrogen absorbances and duplicate absorbances for the carbamate and ester carbonyls, indicating the existence of several different hydrogen bonds.

The presence of intramolecular hydrogen bonds in the dimers **39, 40, 49** and **57** was shown by ^{1}H NMR and infrared spectroscopic analysis. Intramolecular hydrogen bonding was also seen in the crystal structures of the dimers if the crystals were grown in non-polar solvent, otherwise intermolecular hydrogen bonds were often found. The central bond lengths of the dimers **39, 40** and **49** indicate that elongation of the central bond is due to steric strain and not the stability of the radical of the monomer. By analogy, the central bond elongation of the dimers **41, 43** and **45**, reported by Koch *et al.*,[35,39,40] is probably determined by steric factors alone.

Various conditions for the photolysis of DTBP **21** in the presence of either the glycine derivative **25** or the alanine derivative **26** were studied to examine the effect on product ratios. The photoinduced reactions involving DTBP **21** and the derivatives **29** and **56** of pyroglutamic acid and *N*-*t*-butoxycarbonylglycine, respectively, were not further examined as it proved difficult to develop procedures for the HPLC analysis of those product mixtures.

The various conditions that were studied for the photolysis of DTBP **21** in the presence of the glycine derivative **25** involved examination of the

effects of changing the polarity of the solvent, the photolysis lamps and the ratio of DTBP **21** to the amino acid derivative **25** (Table 3). Each reaction mixture was analysed by reverse phase HPLC and the components identified by their retention times and through co-injections with authentic samples. The ratio of *N*-benzoylglycine methyl ester **25**, *N*-benzoylalanine methyl ester **26** and both diastereomers of the dimer **39** was calculated from the peak integrations and is given as a percentage of the total in Table 4. The mole responses of the derivatives **25** and **26** of glycine and alanine, respectively, and the mole responses of each diastereomer of the dimer **39**, for ultraviolet absorption at 254 nm, were measured using a ultraviolet spectrophotometer and then compared. The diastereomers of the dimer **39** absorbed twice as much as the amino acid derivatives **25** and **26**, as would be expected on the basis of the number of benzamido substituents per molecule.

Irradiation of a solution containing *N*-benzoylglycine methyl ester **25** (0.13M) and 4.6 mole equivalents of DTBP **21** in benzene for 23 hours produced the diastereomers of the dimer **39** in approximately equal amounts

Table 3 - Variation of reaction conditions for the photolysis of DTBP **21** with *N*-benzoylglycine methyl ester **25**.

Reaction [a]	Conc. of **25** (M)	Molar ratio of **25** : **21**	solvent
1	0.13	1.0 : 4.6	PhH
2	0.12	1.0 : 4.6	*t*-BuOH
3	0.13	1.0 : 1.0	PhH
4	0.05	1.0 : 6.2	PhH
5 [b]	0.05	1.0 : 6.3	PhH

a. Reaction time of 23 hours. b. 3000 Å lamps used instead of 3500 Å.

Table 4 - Components of the product mixtures, from reactions described in Table 3, as a percentage of the total.

Reaction	**25**	**26**	*dl*-**39**	*meso*-**39**
1	30.5	7	30.5	32
2	44	19	30	7
3	62	— [a]	20	18
4	47	6	27	20
5	40	14	27	19

a. not detected.

and a small amount of *N*-benzoylalanine methyl ester **26** (Reaction 1). The change of solvent from benzene to *t*-butanol **24** led to a more complex reaction mixture. The *dl*- and *meso*-isomers of the dimer **39** were no longer formed in a ratio of 1 : 1, but 4 : 1 favouring the *dl*-diastereomer (Reaction 2). The increased ratio is likely to be a consequence of the polar solvent disrupting the hydrogen bonding that may aid formation of the *meso*-diastereomer. This is consistent with the greater hydrogen bond strength of the *meso*-isomer of the dimer **39** compared with the *dl*-isomer, as shown by ^{1}H NMR spectroscopy and discussed above. The change to a polar solvent increased the relative extent of production of *N*-benzoylalanine methyl ester **26** over the diastereomers of the dimer **39**. This may be attributed to an increased rate of β-scission of *t*-butoxy radical **22** in polar solvent, to give methyl radical **23**. Studies on the reaction of *t*-butoxy radical **22**, generated by photolysis of *t*-butylhypochlorite, found the relative rate of hydrogen abstraction from cyclohexane (0.1 M) over the rate of β-scission at 40°C was 2.62 in benzene and 0.70 in acetic acid[48]. More recently the solvent effect on the rates of hydrogen abstraction and β-scission of cumyloxy radical **59** was

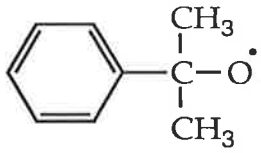

59

reported[49]. The rate constants for β-scission at 30°C were (3.75 ± 0.53) x 10^5 sec^{-1} in benzene and (5.84 ± 1.06) x 10^5 sec^{-1} in *t*-butanol. The rate for hydrogen abstraction from cyclohexane by the radical **59** in each solvent was found to be (1.24 ± 0.12) x 10^6 $M^{-1}sec^{-1}$. The increased rate of production of methyl radical **23** should increase the formation of *N*-benzoylalanine methyl ester **26** relative to the diastereomers of the dimer **39**. The extent of reaction of the protected glycine **25** with 1 mole equivalent of DTBP **21** (Reaction 3) was less than that in the reaction containing 4.6 mole equivalents of DTBP **21** (Reaction 1). Though the increased ratio of DTBP **21** to the glycine derivative **25** increased the extent of reaction, isolation of the products became more difficult due to the increased amounts of byproducts that were shown to be present by ^1H NMR spectroscopy of the crude reaction mixture. Changing the wavelength of the lamps used for photolysis from 3500 Å (Reaction 4) to 3000 Å (Reaction 5) increased the amount of *N*-benzoylalanine methyl ester **26** produced. The higher energy lamps may have increased the reaction temperature, which would have then increased the rate of β-scission of the *t*-butoxy radical **22** over hydrogen abstraction[50].

The photochemical reactions of DTBP **21** and the alanine derivative **26**, outlined in Table 5, were carried out to examine the product ratios. The five main components: the starting material **26**, the α-methylalanine derivative **50**, the lactone **52** and the diastereomers of the dimer **40**, were resolved using

reverse phase HPLC. The results are shown in Table 6 with the ratio of the major products given as a percentage of their total peak areas. The mole responses of the diastereomers of the dimer **40** to ultraviolet absorption were twice that of the other amino acid derivatives **26, 50** and **52** in the product mixture. The product ratios were confirmed by ^{1}H NMR spectroscopy of the product mixtures.

The conditions for Reaction 6 were analogous to those for Reaction 1. From the relative extents of these reactions it is clear that hydrogen abstraction from the alanine derivative **26** occurs at a significantly slower rate

Table 5 - Variation of reaction conditions for the photolysis of DTBP **21** with *N*-benzoylalanine methyl ester **26**.

Reaction	Conc. of **26** (M)	Molar ratio of **26** : **21**	solvent	time (hr)
6	0.13	1.0 : 4.6	PhH	23
7	0.20	1.0 : 5.5	*t*-BuOH	65
8	0.05	1.0 : 12.4	*t*-BuOH	108

Table 6 - Components of the product mixtures, from reactions described in Table 5, as a percentage of the total.

Reaction	**26**	*dl*-**40**	*meso*- **40**	**50**	**52**
6	92	4	4	— [a]	— [a]
7	32	10	10	21	27
8	— [a]	11	11	16	62

a. not detected.

than that for the glycine derivative **25**, and this reflects the relative rates of reaction of the derivatives **25** and **26** of glycine and alanine, respectively, with DTBP **21** shown in Table 2. The diastereomers of the dimer **40** were produced in equal amounts. The conditions shown for Reaction 7 were those used for the preparative synthesis of the diastereomers of the alanine dimer **40**. The photochemical reaction of DTBP **21** and the alanine derivative **26** in *t*-butanol **24** (Reaction 7) gave an increased number of products over the reaction in benzene (Reaction 6). The greater extent of formation of the methylated product **50** over the diastereomers of the dimer **40** may reflect an increased rate of β-scission of the *t*-butoxy radical **22** in polar solvent. The extent of formation of the dimer **40** was also reduced due to the scavenging of the alanyl radical **31** by the primary *t*-butanol derived radical **54**. The conditions used in Reaction 8 were analogous to the conditions reported in the literature for the reaction between DTBP **21** and the alanine derivative **26**[22]. The larger ratio of DTBP **21** to the amino acid derivative **26** ensured that all of the starting material **26** was consumed. The negative side of having a higher concentration of DTBP **21** was the high proportion of the product **52** from the reaction of the protected alanyl radical **26** with the radical **54** derived from the *t*-butanol **24**, though this could lead to synthetically useful preparations of lactones derived from amino acid derivatives.

Results and Discussion Chapter Two

Reactions of Protected Alanine Dimers

The diastereomers of the protected alanine dimer **40**, synthesised as reported in Chapter 1, were examined to determine their rates of homolysis in non-polar solvent. The solvent chosen for the study was 1,2,4-trichloro-benzene as it is inert, non-polar and has a boiling point of 214°C, the temperature at which measurable reaction rates were obtained. The study of each diastereomer of the dimer **40** started with the pure material and continued until 90% of the material had reacted. HPLC analysis of the reaction mixtures showed that during the reaction of the *dl*-isomer of the dimer **40** up to 2% of the *meso*-isomer formed and during the reaction of the *meso*-isomer of the dimer **40** up to 8% of the *dl*-isomer formed, though the main reaction was decomposition for each isomer. The extent of decomposition of each diastereomer of the dimer **40** was measured with respect to an external standard, benzanilide, that was added prior to HPLC analysis. The results were plotted as the log of the percentage of each diastereomer remaining over time and are shown in Graph 1. From the equations of the lines of best fit, the half lives and rate constants of reactions of the diastereomers were calculated. The errors were calculated from the correlation values given for each set of data. The raw data from the integration of the HPLC traces can be found in the Experimental section. The rate constants calculated from the half lives were:

$$(2.22 \pm 0.03) \times 10^{-5}\ \text{sec}^{-1}$$

and $(6.29 \pm 0.01) \times 10^{-5}\ \text{sec}^{-1}$,

for decomposition of the *dl*- and *meso*-isomers, respectively. The linearity of the data shown in Graph 1 shows that the reactions follow first order kinetics.

Graph 1 - Decomposition of the diastereomers of the dimer **40** in 1,2,4-trichlorobenzene at 214°C.

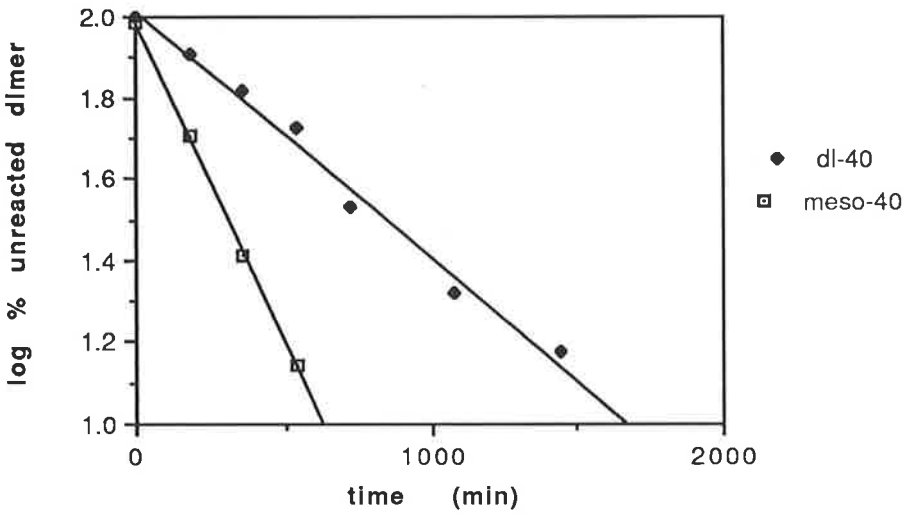

To determine whether decomposition of the diastereomers of the dimer **40** occurred by dimer bond homolysis, the reactions in 1,2,4-trichlorobenzene at 214°C were repeated in the presence of a hydrogen source. The hydrogen donors chosen were thiocresol **60** and 9,10-dihydroanthracene **61** as they have

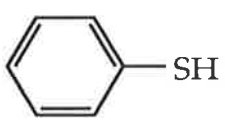

60

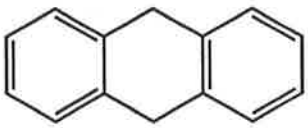

61

been shown to be efficient hydrogen atom sources, reducing compounds in yields of 65 to 93%[38]. Production of the alanyl radical **31** through reaction of

the protected alanine dimer **40**, in the presence of a hydrogen source, should produce the alanine derivative **26** (Scheme 13). The *meso*-isomer of the dimer **40** was heated in the presence of thiocresol **60** for 10 hours. HPLC analysis of the product mixture showed the presence of only a trace of *N*-benzoylalanine methyl ester **26**. The reaction was repeated with 9,10-dihydroanthracene **61** instead of thiocresol **60**. *N*-Benzoylalanine methyl ester **26** was formed in 41% corrected yield from the *meso*-isomer of the

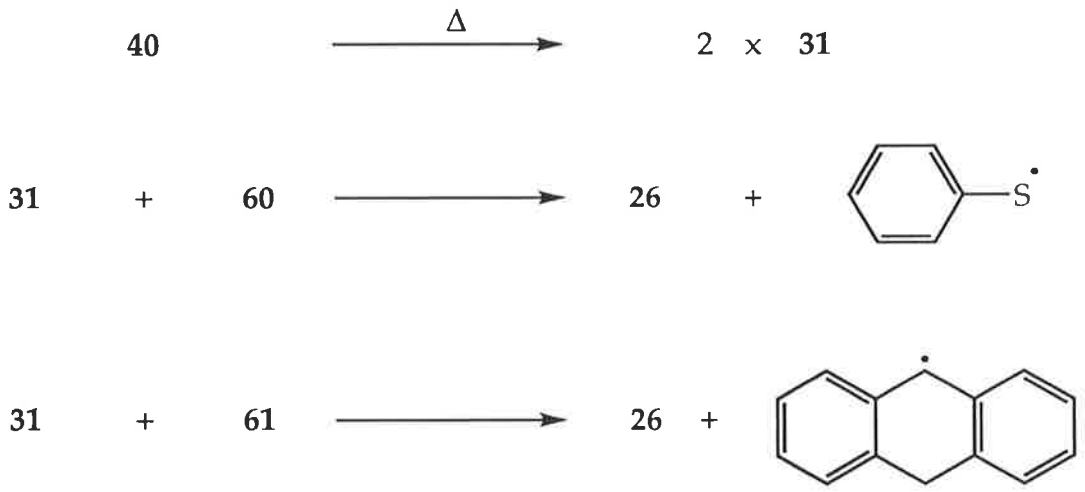

Scheme 13

dimer **40**. Similarly, 35% of the reacted *dl*-isomer of the dimer 40 formed the alanine derivative **26**, when heated for 24 hours with 9,10-dihydroanthracene **61**. The first order decay of each of the diastereomers of the dimer **40** in 1,2,4-trichlorobenzene at 214°C shows that the decomposition is unimolecular and this fact combined with the formation of *N*-benzoylalanine methyl ester **26**, when each of the diastereomers of the dimer **40** underwent reaction in the presence of a hydrogen source, indicates that homolysis of the central bond of the diastereomers of the dimer **40** is the major decomposition pathway.

The rate constants calculated for decomposition of the diastereomers of the dimer **40** at 214°C in 1,2,4-trichlorobenzene do not allow for the small percentage of the reaction that involves production, then recombination, of the alanyl radical **31**. However, this difference between the decomposition and homolysis rate constants is relatively small as little interconversion between the diastereomers of the dimer **40** was observed. The low tendency of recombination of the protected alanyl radical **31** probably results from its low concentration. In turn this results from the low concentrations of the diastereomers of the dimer **40** that were used, due to their poor solubility in 1,2,4-trichlorobenzene, and the slow rates of homolysis.

The rate constants for the decay of the diastereomers of the protected alanine dimer **40** show that the *dl*-isomer is three times less likely to undergo homolysis than the *meso*-isomer. The *dl*-isomer of the dimer **40**, with the longer central bond length of 1.579 Å, reacted more slowly than the *meso*-isomer, which has a central bond length of 1.535 Å. Thus it is clear that the length of the dimer bond does not correlate with homolytic activity. The greater stability of the *dl*-isomer of the dimer **40** at 214°C in non-polar solvent can be accounted for by that isomer's relatively stronger intramolecular hydrogen bonds. The shorter and stronger hydrogen bonds of the *dl*-isomer of the dimer **40**, with lengths of 2.11 and 2.14 Å in the crystal structure, retard the extent of homolysis more than for the *meso*-isomer, which has two weaker intramolecular hydrogen bonds, each 2.34 Å in length, as the hydrogen bonds must be broken along with the central bond for homolysis to occur.

The effect of solvent polarity on the rates of decomposition of the diastereomers of the dimer **40** was examined. The solvent chosen was *N*,*N*-dimethylformamide (DMF) as it is an inert polar solvent. Reactions of

the diastereomers of the dimer **40** in DMF at 214°C occurred too rapidly to be followed by HPLC analysis. The effect of DMF on the rates of reaction of the diastereomers of the dimer **40** was therefore examined at the lower temperature of 150°C, where measurable rates were obtained. HPLC analysis of the reaction mixtures showed that each diastereomer of the dimer **40** underwent decomposition. The results are shown in Graph 2, presented as

Graph 2 - Decomposition of the diastereomers of the dimer **40** in DMF at 150°C.

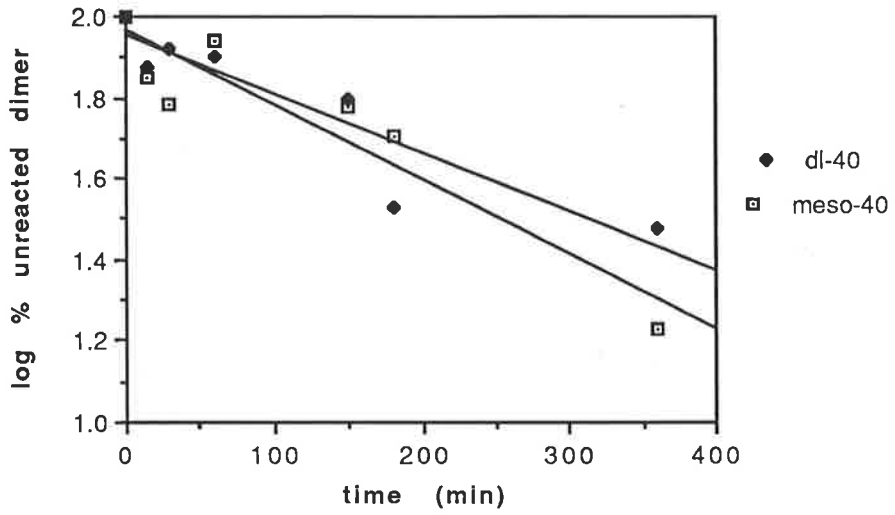

the log of the percentage of each isomer of the dimer **40** remaining over time. Reactions of the diastereomers of the dimer **40** were followed until 80% completion. The rate constants for the reactions of the diastereomers of the protected alanine dimer **40** in DMF at 150°C were:

$$(7.13 \pm 1.13) \times 10^{-5}\ \text{sec}^{-1}$$

and $(8.37 \pm 1.10) \times 10^{-5}\ \text{sec}^{-1}$,

for the *dl*- and *meso*-isomers, respectively.

Though there is not a high degree of correlation of the data shown in Graph 2 with the lines of best fit, it is clear that the efficiency of the reactions in DMF has been significantly enhanced compared to that in 1,2,4-trichlorobenzene. To show that the increased efficiency of the reactions of the diastereomers of the dimer **40** was due to the polarity of the solvent, the reactions in 1,2,4-trichlorobenzene at 150°C were examined. Heating of each diastereomer of the protected alanine dimer **40** at 150°C did not show any evidence of homolysis, neither interconversion nor decomposition being detected after 4 days by HPLC analysis. As HPLC analysis would conservatively detect changes of 10% in the dimer **40** concentrations, the rate constants for the reactions in 1,2,4-trichlorobenzene at 150°C were therefore less than 4×10^{-7} sec^{-1}, based on a half life of more than twenty days.

Homolysis of the central bond of each diastereomer of the protected alanine dimer **40** in DMF at 150°C could not be substantiated as the pathway for decomposition. HPLC and ^1H NMR spectroscopic analysis of the refluxed reaction mixture of the *meso*-isomer of the dimer **40** in DMF with a 20 fold molar excess of 9,10-dihydroanthracene **61** showed that only approximately 3% of the dimer remained after 10.5 hours, with no evidence for the formation of *N*-benzoylalanine methyl ester **26**. However, as the central bond of each diastereomer of the dimer **40** underwent homolysis in non-polar solvent, the mechanism for decomposition in polar solvent is likely to be the same.

The rate constants for decomposition of the diastereomers of the dimer **40** in DMF at 150°C are at least 200 times greater than for the reactions in 1,2,4-trichlorobenzene at the same temperature. The increased rates of decomposition in DMF most probably reflect the loss of intramolecular

hydrogen bonding in the diastereomers of the dimer **40** in the polar solvent. Homolysis of each diastereomer of the dimer **40** in polar solvent involves cleavage of the central dimer bond, whereas homolysis in non-polar solvent requires the simultaneous disruption of the hydrogen bonds and the central dimer bond. The similarity between the rate constants for decomposition of the diastereomers of the dimer **40** in DMF at 150°C also reflects the loss of the intramolecular hydrogen bonds, as the rates of decomposition are no longer being affected by the hydrogen bonds as seen in the ^{1}H NMR spectra and the crystal structures.

In summary, at 214°C in 1,2,4-trichlorobenzene the diastereomers of the dimer **40** decomposed. The relative rates of decomposition reflect the relative extents of intramolecular hydrogen bonding in the dimers, with the diastereomer with the shorter (stronger) central dimer bond and longer (weaker) hydrogen bonds reacting more rapidly than the other diastereomer. The rates of decomposition of the diastereomers of the dimer at 150°C are at least two hundred times faster than in 1,2,4-trichlorobenzene at the same temperature. The increased efficiency of homolysis of the diastereomers of the dimer **40** in polar solvent is probably due to the loss of the internal hydrogen bonds in the dimer. By analogy, it seems likely that the relative rate constants for reaction of the dimeric oxomorpholine derivative **41** in chloroform and ethanol, reported by Koch *et al.*,[32] reflect the difference in intramolecular hydrogen bonding in the dimer **41** in the two solvents.

Results and Discussion Chapter Three

Reactions of Protected Glycine Dimers

The rates of reaction of the diastereomers of the protected glycine dimer **39** in 1,2,4-trichlorobenzene at 214°C were examined to compare with the rates of homolysis of the diastereomers of the protected alanine dimer **40**, presented in Chapter 2. The reaction mixtures were analysed by reverse phase HPLC, and each diastereomer of the dimer **39** was found to undergo equilibration without decomposition, by comparing the HPLC trace integrations of the diastereomers of the dimer **39** to the external standard, benzanilide. The reactions of the diastereomers of the dimer **39** in 1,2,4-trichlorobenzene at 214°C were monitored until 90% had undergone equilibration and the data for the reactions, shown in Graph 3, is presented as the log of the percentage of each diastereomer in excess of the equilibrium

Graph 3 - Reactions of the diastereomers of the dimer **39** in 1,2,4-trichlorobenzene at 214°C.

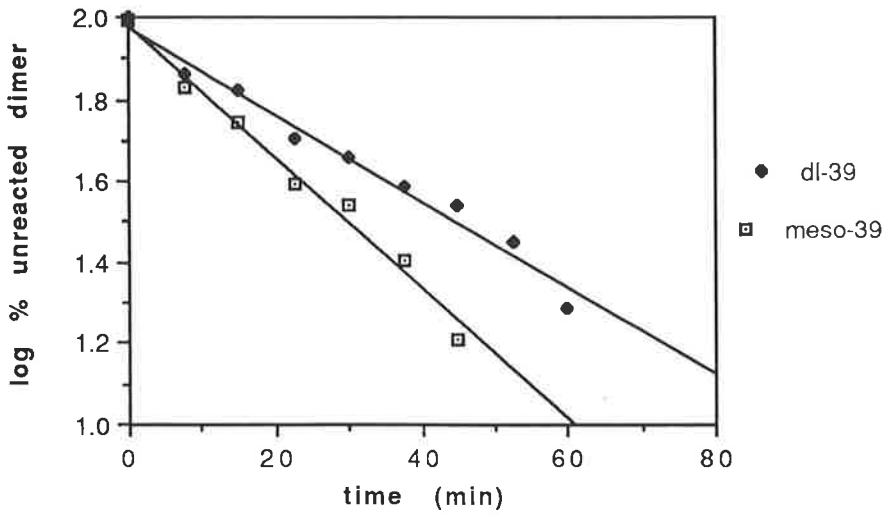

mixture remaining with time. The equilibrium position in non-polar solvent was ascertained by heating each of the diastereomers of the dimer **39** in 1,2,4-trichlorobenzene at 214°C for greater than three hours, which is more than seven half lives for reaction of each isomer. The *dl*-and *meso*-isomers of the dimer **39** equilibrated to a 43 to 57% mixture. The favoured formation of the *meso*-isomer in non-polar solvent is possibly due to the stronger intramolecular hydrogen bonding in that isomer, compared with that in the *dl*-isomer, as indicated by the relative chemical shifts of the ^{1}H NMR resonances for the amide hydrogens of the *meso*- and *dl*-isomers in deuteriochloroform of δ 8.0 and δ 7.2, respectively, as discussed in Chapter 1. From the equations for the lines of best fit, the calculated rate constants were:

$$(4.41 \pm 0.10) \times 10^{-4}\ \text{sec}^{-1}$$

and $$(6.58 \pm 0.11) \times 10^{-4}\ \text{sec}^{-1},$$

for equilibration of the *dl*- and *meso*-isomers of the dimer **39**, respectively.

The reactions of the diastereomers of the dimer **39** were examined in polar solvent to see whether the solvent increased the rates of reaction, as for the protected alanine dimer **40** case. The reaction of the *dl*-isomer of the dimer **39** was studied in DMF at 214°C to determine whether measurable reaction rates could be obtained. HPLC analysis revealed that a sample of the *dl*-isomer of the dimer **39** heated for 7.5 minutes had reached equilibrium, while samples heated for longer periods were found to have decomposed. The equilibrium position was 57 to 43% for the *dl*- and *meso*-isomers, the opposite of the equilibrium position in non-polar solvent. The difference of the equilibrium position in polar solvent, to that in non-polar solvent, can be attributed to the absence of intramolecular hydrogen bonding, and correlates

with the 4 : 1 preferential formation of the *dl*-isomer of the dimer **39** in the reaction of *N*-benzoylglycine methyl ester **25** with DTBP **21** in *t*-butanol compared with the 1 : 1 ratio of the diastereomers when the reaction was carried out in benzene.

The reactions of the diastereomers of the dimer **39** in DMF were repeated at the lower temperature of 150°C, so that measurable reaction rates could be obtained. The reactions were followed until 80% of each diastereomer of the dimer **39** had undergone equilibration. The equilibrium position was determined to be 60 to 40% for the *dl*- and *meso*-isomers, by heating each diastereomer for a period of eight half lives. The results were plotted as the log of the percentage of each diastereomer in excess of the equilibrium mixture remaining with time and are shown in Graph 4. The rate constants for equilibration of the diastereomers of the dimer **39**, calculated from the

Graph 4 - Reactions of the diastereomers of the dimer **39** in DMF at 150°C.

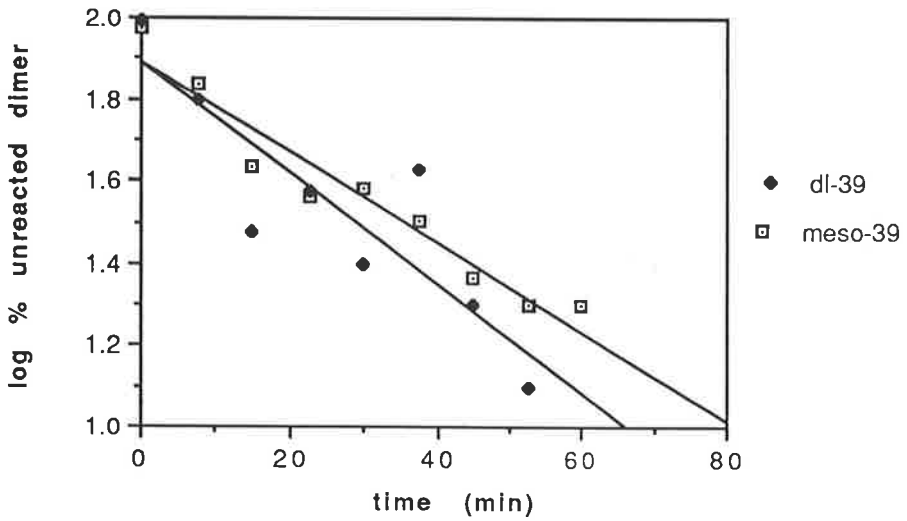

equations of the lines of best fit, were:

$$(6.86 \pm 1.59) \times 10^{-4}\ sec^{-1}$$

and $$(6.31 \pm 0.42) \times 10^{-4}\ sec^{-1},$$

for equilibration of the *dl*- and *meso*-isomers of the dimer **39**, respectively. Both diastereomers showed signs of decomposition after 2 hours of heating, with new signals appearing in the HPLC traces of the reaction mixtures. The largest of these had a peak area equal to 10% of the dimer peak area at the end of the study.

To verify that the greater efficiency of the reactions of the diastereomers of the dimer **39** in DMF at 150°C was due to the polarity of the solvent, the reactions at 150°C were repeated in 1,2,4-trichlorobenzene to measure the rates of equilibration, while the reaction of the *dl*-isomer of the dimer **39** in chlorobenzene at 214°C was examined for possible pressure effects.

Graph 5 - Reactions of the diastereomers of the dimer **39** in 1,2,4-trichlorobenzene at 150°C.

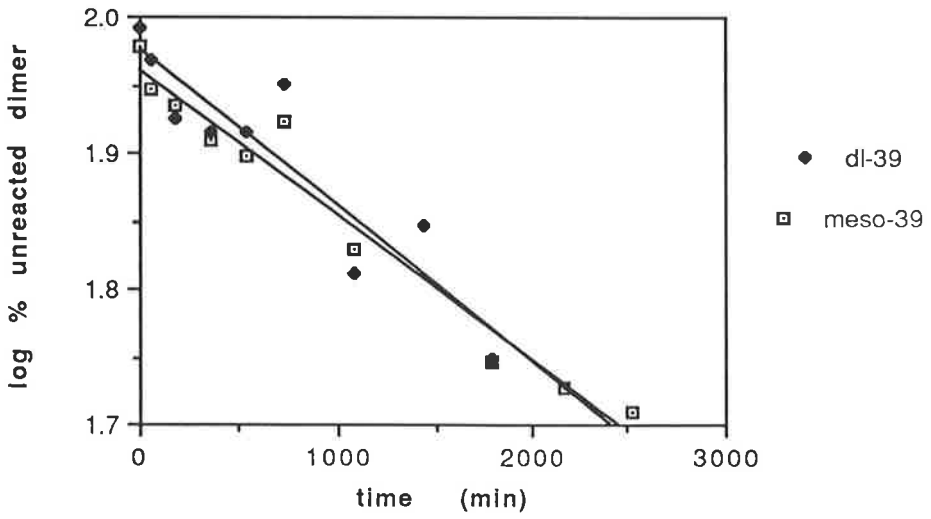

Reactions of the diastereomers of the dimer **39** in 1,2,4-trichlorobenzene at 150°C were monitored for 4 days. The results shown in Graph 5 represent the log of the percentage of each diastereomer in excess of the equilibrium mixture remaining with time, during the first 42 hours of reaction. The diastereomers of the dimer **39** in the reaction mixtures, heated for longer than 42 hours, underwent decomposition as well as equilibration. The rate constants for equilibration of the diastereomers of the dimer **39** in 1,2,4-trichlorobenzene at 150°C, calculated from the equations for the lines of best fit, were:

$$(5.40 \pm 0.87) \times 10^{-6}\ \text{sec}^{-1}$$

and $$(4.81 \pm 0.17) \times 10^{-6}\ \text{sec}^{-1},$$

for the *dl*- and *meso*-isomers of the dimer **39**, respectively.

The rates of reaction of the diastereomers of the dimer **39** were examined further to see whether pressure enhanced reactivity, as the reactions were conducted in sealed ampoules. The reaction of the *dl*-isomer of the dimer **39** in chlorobenzene (bp 132°C) at 214°C was examined. Chlorobenzene was chosen as it is similar in polarity to 1,2,4-trichlorobenzene but with a boiling point close to that of DMF. If pressure helped to accelerate the reactions of the diastereomers of the dimer **39** in DMF, then reaction of the *dl*-isomer in chlorobenzene at 214°C should have an enhanced rate relative to that for the reaction in 1,2,4-trichlorobenzene at 214°C. The results were plotted as the log of the percentage of the *dl*-isomer in excess of the equilibrium mixture remaining with time and are shown in Graph 6. The reaction was monitored until 90% of the *dl*-isomer had undergone equilibration. The rate constant for equilibration of the *dl*-isomer of the

Graph 6 - Reaction of the *dl*-isomer of the dimer **39** in monochlorobenzene at 214°C.

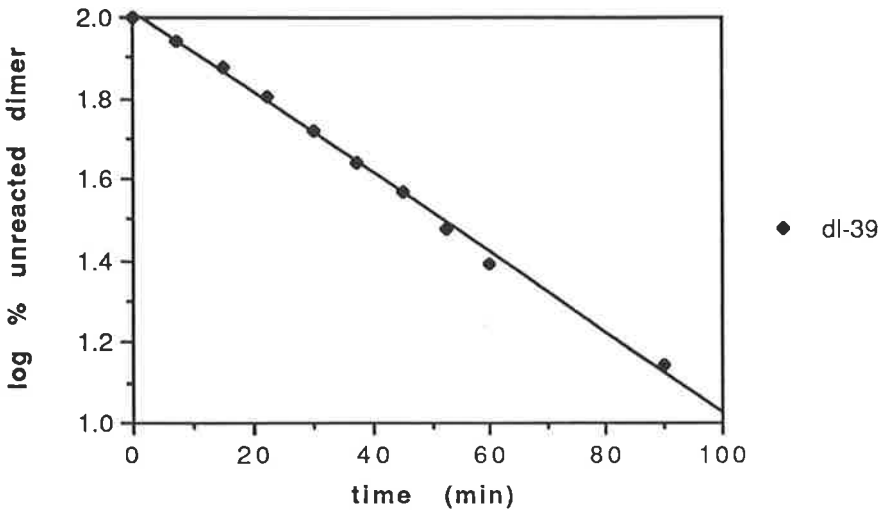

dimer **39**, calculated from the equation of the line of best fit, was:

$$(3.65 \pm 0.01) \times 10^{-4}\ sec^{-1}.$$

The rate of equilibration in chlorobenzene at 214°C is marginally slower than that in 1,2,4-trichlorobenzene at 214°C, indicating that pressure has little effect on the reactions of the diastereomers of the dimer **39**, and that this is unlikely to account for the one hundred fold increase in the reactivity at 150°C caused by changing the solvent from 1,2,4-trichlorobenzene to DMF.

To determine if equilibration of the diastereomers of the dimer **39** in 1,2,4-trichlorobenzene at 214°C involved dimer bond homolysis, the reactions were repeated in the presence of thiocresol **60** and 9,10-dihydroanthracene **61**. If equilibration of the protected glycine dimer **39** involved the production of the protected glycine radical **30**, then reaction in the presence of a hydrogen source should produce *N*-benzoylglycine methyl ester **25** (Scheme 14).

The *dl*-isomer of the dimer **39** and a twenty fold molar excess of

thiocresol **60** were refluxed in 1,2,4-trichlorobenzene for 4 hours, which is nine half lives for reaction of the glycine derivative **39**. HPLC and ^{1}H NMR spectroscopic analysis showed that the *dl*-isomer of the dimer **39** had reacted to give an equilibrium mixture of the diastereomers, with no evidence for the formation of *N*-benzoylglycine methyl ester **25**. The reaction was repeated

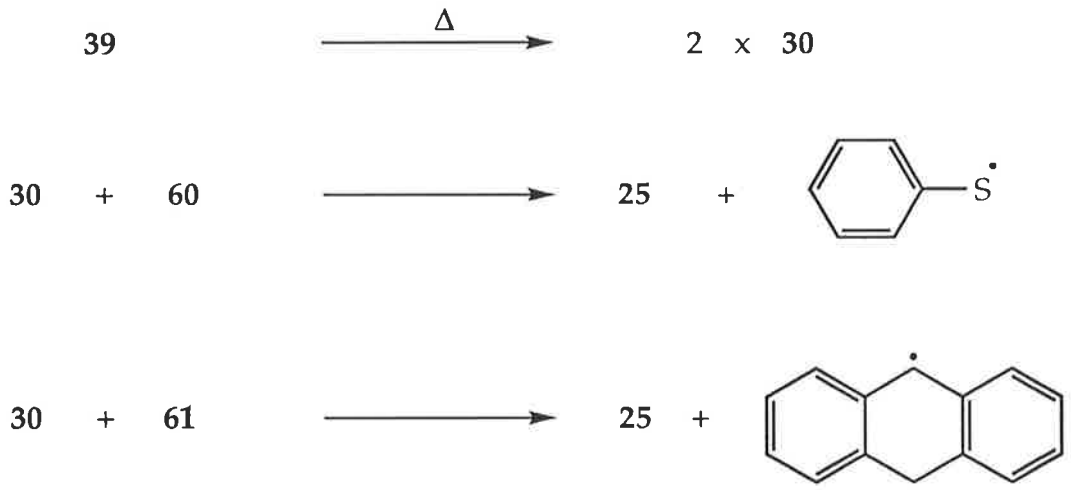

Scheme 14

with 9,10-dihydroanthracene **61** replacing the thiocresol **60**, as it had proved to be more efficient at donating hydrogen to the protected alanyl radical **31**. There was no evidence for the formation of the glycine derivative **25** by HPLC or ^{1}H NMR spectroscopic analysis, even after the reaction time was increased to 11.5 hours. Even when the *dl*-isomer of the dimer **39** was heated in 1,2,4-trichlorobenzene at 214°C for 7 days with a twenty fold molar excess of 9,10-dihydroanthracene **61**, HPLC analysis of the reaction mixture did not show any *N*-benzoylglycine methyl ester **25**, though decomposition had occurred. Thus it appears that the reactions of the diastereomers of the dimer **39** in 1,2,4-trichlorobenzene do not involve central dimer bond homolysis.

On this basis the possibility that equilibration involves keto-enol tautomerisation of the ester carbonyls (Scheme 15) was considered. If the

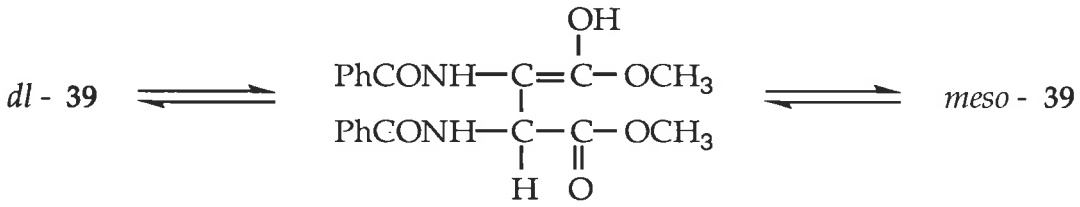

62

Scheme 15

mechanism involves keto-enol tautomerisation then equilibration of the diastereomers of the dimer **39** in the presence of an exchangeable deuterium source would give rise to the α-deuteriated dimer **64**, produced through deuterium exchange of the exchangeable hydrogens of the enol **62** (Scheme 16).

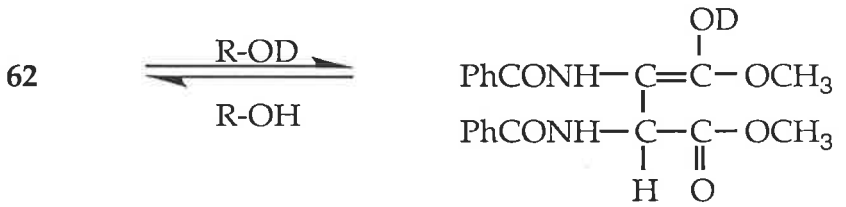

63

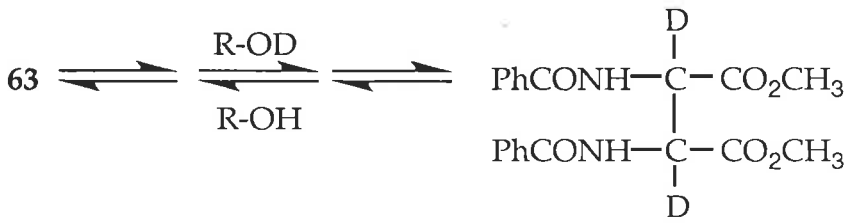

64

Scheme 16

To examine this mechanism for equilibration of the diastereomers of the dimer **39**, the *dl*-isomer of the dimer **39** was heated in 1-butanol-*d* **65** at 150°C (Scheme 17). HPLC analysis of the reaction mixture, heated for longer than four hours, showed four main components. The components were isolated by preparative HPLC and identified by ^{1}H NMR spectroscopy and mass spectrometry. The first two components to elute off the HPLC column were the diastereomers of the protected α-deuteriated glycine dimer **64** and the

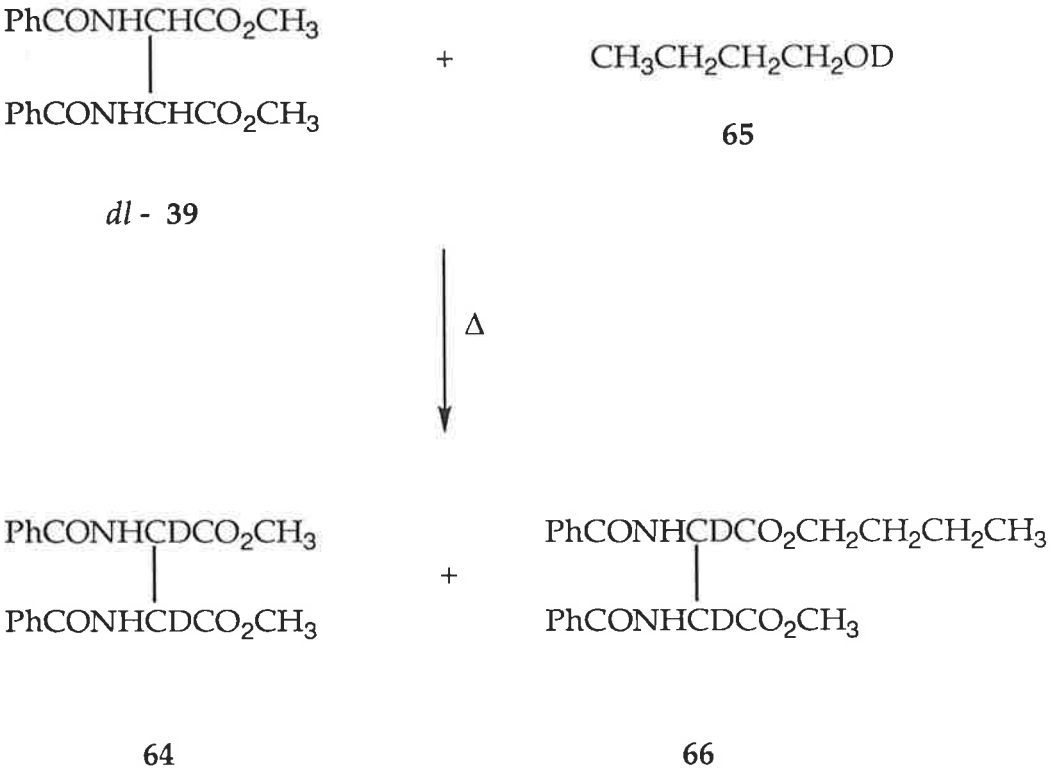

Scheme 17

other two were the diastereomers of butyl methyl 2,3-dibenzamido-2,3-dideuteriobutanedioate **66**. The ^{1}H NMR spectrum of the *dl*-isomer of the

dimer **64** showed signals for the methyl ester hydrogens at δ 3.90 and residual α-hydrogens at δ 5.3. The integration ratio of these signals was 26 : 1. The mass spectrum showed a molecular ion at m/z 386 (*c.f.* m/z 384 for the molecular ion of the dimer **39**). Similarly, the ^{1}H NMR signals for the methyl ester hydrogens and the residual α-hydrogens of the *meso*-isomer of the dimer **64**, at δ 3.84 and δ 5.3, respectively integrated in the ratio 11 : 1. Mass spectrometry showed a molecular ion at m/z 386. The diastereomers of the dimer **64** had the same retention times on the reverse phase HPLC column as the diastereomers of the dimer **39**. The ^{1}H NMR spectrum of the first diastereomer of the dimer **66** to elute from the HPLC column showed signals for the butyl ester hydrogens at δ 0.95, 1.44, 1.71 and 4.28, and for the methyl ester hydrogens at δ 3.89. Deuterium incorporation was lower than for the diastereomers of the dimer **64**, the integration ratio of the ^{1}H NMR signals for the methyl ester hydrogens and the residual α-hydrogens, at δ 5.3, was close to 4 : 1, but this still represents a greater than 50% incorporation of deuterium at the α,α'-positions. The molecular ion in the mass spectrum occurred at m/z 428. The ^{1}H NMR spectrum of the other diastereomer of the dimer **66** contained signals for the butyl ester hydrogens at δ 0.92, 1.4 and 4.26, and for the methyl ester hydrogens at δ 3.83. Unfortunately the ^{1}H NMR spectrum could not be accurately integrated neither was the mass spectrum of this sample obtainable due to a major contaminant introduced from the NMR solvent.

From the deuterium incorporation experiment results it appeared that the mechanism for equilibration of the diastereomers of the dimer **39** involves keto-enol tautomerisation rather than dimer bond homolysis. To corroborate that the diastereomers of the dimer **39** undergo keto-enol tautomerisation, the rates of equilibration of the diastereomers of the

protected α,α'-deuteriated glycine dimer **64** were examined, in 1,2,4-trichloro-benzene at 214°C, to see whether these reactions showed deuterium isotope effects. A primary deuterium isotope effect would indicate that the mechanism for equilibration involves a base-induced keto-enol tautomerisation, as deprotonation at the α-centre would be the rate determining step[51].

The synthesis of the protected α,α'-d_2-glycine dimer **64** required *N*-benzoyl-2,2-d_2-glycine methyl ester **67**. The 2,2-d_2-glycine derivative **67**

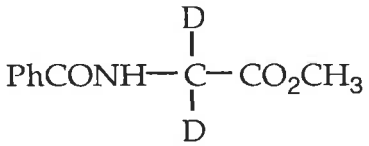

67

was prepared from 2,2-d_2-glycine[52] and had identical physical and similar spectroscopic properties to those of *N*-benzoylglycine methyl ester **25**. The ^{1}H NMR spectrum of the 2,2-d_2-glycine derivative **67** was identical to that of the glycine derivative **25** except that the integration ratio of the methyl ester hydrogens, at δ 3.81, to the α-hydrogens, at δ 4.26, was 3 : 0.3 indicating that deuterium is incorporated at the α-centre. The mass spectrum of the 2,2-d_2-glycine derivative **67** showed a molecular ion at m/z 195 (*c.f.* molecular ion of the glycine derivative **25** at m/z 193). The extent of deuterium incorporation in *N*-benzoyl-2,2-d_2-glycine methyl ester **67** was shown to be 74% d_2 and 23% d_1 by mass spectrometry.

The dimer **64** was synthesised in the same manner as for the protected glycine dimer **39**, by irradiation of a solution containing DTBP **21** and

N-benzoyl-2,2-d_2-glycine methyl ester **67** in benzene. The *dl*-isomer of the dimer **64** did not precipitate out of solution as had the *dl*-isomer of the non-deuterated dimer **39** from the product mixture of DTBP **21** and the glycine derivative **25**. The diastereomers of the dimer **64** were isolated by precipitation from an ethyl acetate solution of the residue of the evaporated reaction mixture using hexane. The diastereomers were separated by preparative TLC and isolated by precipitation from solutions of the evaporated product fractions. The diastereomers of the protected 2,2-d_2-glycine dimer **64** had identical chromatographic properties and similar melting points and spectroscopic properties to those of the diastereomers of the protected glycine dimer **39**. The ^{1}H NMR spectrum of the *dl*-isomer of the dimer **64** showed that the methyl ester hydrogens resonated at δ 3.90 and the amide hydrogens at δ 7.1. The integration ratio of the signals for the methyl ester hydrogens and the α-hydrogens, at δ 5.32, was 6 : 0.2 indicating that deuterium incorporation in the dimers **64** is slightly greater than for the 2,2-d_2-glycine derivative **67**. The mass spectrum showed a molecular ion at m/z 386, two atomic mass units more than for the analogous non-deuteriated dimer **39**. The fragmentation of the molecular ion, as shown in Scheme 10 for the protected glycine dimer **39**, gave rise to a fragment ion at m/z 194, which corresponds to the radical cation of *N*-benzoyl-2-d_1-glycine methyl ester **68**. A minor fragment ion at m/z 264 corresponded to the loss of monodeuteriated benzamide **69** from the molecular ion. A possible

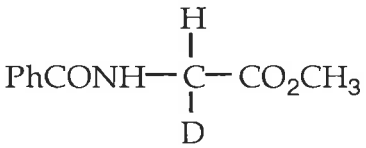

68

mechanism for this fragmentation involves the amide carbonyl removing a deuterium, followed by elimination of the monodeuteriated benzamide tautomer **69** (Scheme 18). The mechanism shown in Scheme 18 is not intended to imply either a concerted or stepwise mechanism. The ^{1}H NMR spectrum of the *meso*-isomer of the dimer **64** showed the methyl ester hydrogens and amide hydrogen signals at δ 3.84 and δ 8.0, respectively. The molecular ion was shown to occur at m/z 386 with fragment ions at m/z 264 and m/z 194.

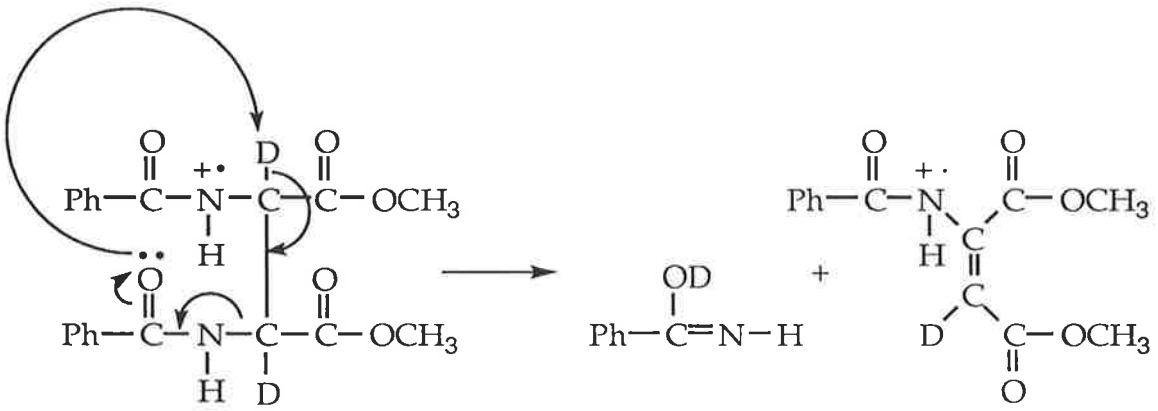

m/z 386 **69** m/z 264

Scheme 18

HPLC analysis of the reaction mixture of the protected deuteriated glycine **67** (0.13M in benzene) and DTBP **21** (4.6 mole equivalents) that had been irradiated for 23 hours showed, from the HPLC peak integrations, a ratio of 76% for the starting material **67**, 6% for a compound that had the same retention time as *N*-benzoylalanine methyl ester **26** and 9% each for the two diastereomers of the dimer **64**. The ratio of starting material to products is greater in the reaction involving the protected 2,2-d_2-glycine derivative **67**

than in the reaction of the protected glycine derivative **25**, under the same conditions. This probably reflects a deuterium isotope effect for formation of the radical **70**.

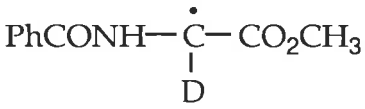

70

The reactions of the diastereomers of the protected α-deuteriated glycine dimer **64** in 1,2,4-trichlorobenzene at 214°C were conducted in the same manner as for those of the dimer **39**. The results, shown in Graph 7, represent the log of the percentage of each diastereomer in excess of the equilibrium mixture remaining with time. Equilibration was monitored until 90% of each of the diastereomers had reacted. The diastereomers of the dimer **64** were found to undergo equilibration, without decomposition, to the

Graph 7 - Reactions of the diastereomers of the dimer **64** in 1,2,4-trichlorobenzene at 214°C.

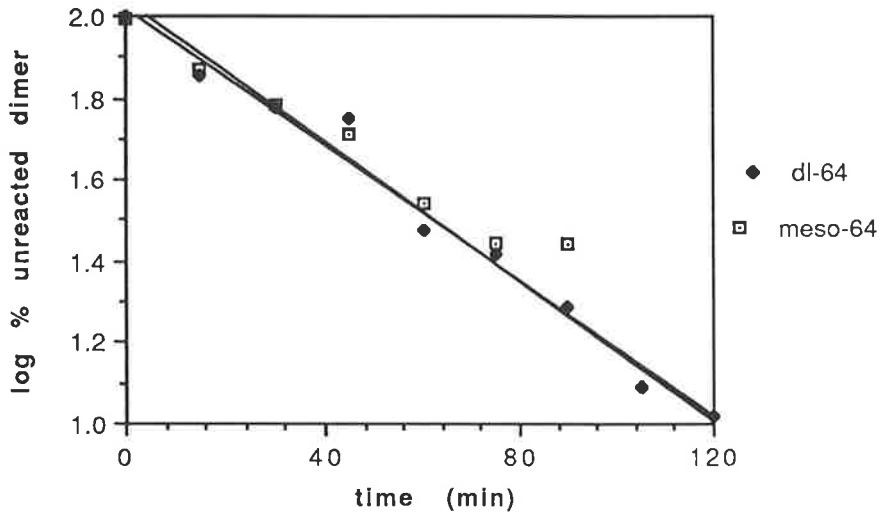

same equilibrium position as for the dimer **39**, *i.e.* 43 to 57% for the *dl*- and *meso*-isomers. From the equations for the lines of best fit, the calculated rate constants were:

$$(2.97 \pm 0.06) \times 10^{-4}\ sec^{-1}$$

and $(2.80 \pm 0.19) \times 10^{-4}\ sec^{-1}$,

for equilibration of the *dl*- and *meso*-isomers, respectively. The deuterium isotope effect for reaction of the *dl*-isomer of the dimer **64**, k_H/k_D, is 1.48 and that for the *meso*-isomer k_H/k_D is 2.35. The deuterium isotope effect for equilibration of the *meso*-isomer of the dimer **64** is greater than the maximum value for a secondary deuterium isotope effect on carbon at 25°C, which is 1.74 [53], and therefore reflects a primary deuterium isotope effect. The situation with the *dl*-isomer of the dimer **64** is less clear cut, but as the diastereomers of the dimer **64** probably equilibrate through the same mechanism, the different values for the deuterium isotope effects probably reflect a difference in the degree of proton transfer in the transition states.

The rates of equilibration of the diastereomers of the protected glycine dimer **39** appear to be unusually rapid for amino acid racemisation. To compare the rates of equilibration of the diastereomers of the protected glycine dimer **39** in 1,2,4-trichlorobenzene at 214°C with the rates of racemisation of other amino acid derivatives, the rates of racemisation of *N*-benzoyl-(2*S*)-alanine methyl ester **71** and *N*-benzoyl-(2*S*)-valine methyl ester **72** were examined under similar conditions. The amino acid derivatives **71** and **72** were chosen as the analogous racemic amino acid derivatives **26** and **27** could be resolved using chiral phase HPLC.

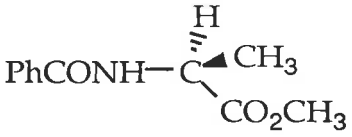

71

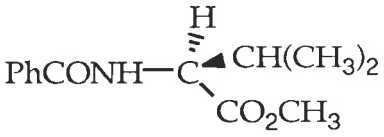

72

The *N*-benzoyl amino acid methyl esters were prepared by converting the corresponding amino acids to amino acid methyl ester hydrochlorides, by treatment of the amino acids with acidified anhydrous methanol, then reacting the hydrochlorides with base and reacting the free amino groups with benzoyl chloride. The protected (2*S*)-alanine and (2*S*)-valine derivatives **71** and **72** had similar spectroscopic properties to those of the protected alanine and valine derivatives **26** and **27**, respectively. The infrared spectrum of the (2*S*)-alanine derivative **71** is more complex than the infrared spectrum of the racemic alanine derivative **26** with two absorbances for the ester carbonyl, at 1765 and 1745 cm^{-1}, instead of the one ester absorbance, at 1750 cm^{-1}, in the infrared spectrum of the alanine derivative **26**. The melting point of the (2*S*)-alanine derivative **71**, of 57°C, is lower than the melting point, of 82°C, for the racemate **26**, while the melting point of the (2*S*)-valine derivative **72**, of 112°C, is higher than the melting point, of 90°C, for the racemic valine derivative **27**.

Crystals of the alanine derivatives **26** and **71** were grown to examine their structures by X-ray crystallographic analysis, to see whether the physical and spectroscopic differences could be accounted for. Comparison of the crystal structures of the alanine derivatives **26** and **71** (Appendix) showed that the (2*S*)-alanine derivative **71** had two molecules per unit cell, whereas the racemic alanine derivative **26** had one. The molecules in both crystal

structures were arranged by intermolecular hydrogen bonding between the amide carbonyls and the amide hydrogens. The length of the hydrogen bonds in the crystal structure of the racemic alanine derivative **26** was 2.11 Å, while in the crystal structure of the (2*S*)-alanine derivative **71** they were 2.16 and 2.23 Å. The shorter and stronger hydrogen bonds in the crystal lattice of the racemic alanine derivative **26** indicate that a greater amount of energy is required to disrupt the crystal lattice and this is reflected in the relative melting points of the amino acid derivatives **26** and **71**. Similarly, the more complex interactions between the molecules of the (2*S*)-alanine derivative **71** are apparent from the infrared spectrum when compared with the infrared spectrum of the alanine derivative **26**.

It was envisaged that the higher crystal lattice energy of the racemic alanine derivative **26** may enable solutions of *N*-benzoyl-(2*S*)-alanine methyl ester **71**, that contain some of the corresponding (2*R*)-isomer, to be enantiomerically enriched by crystallisation. A preliminary study showed that a solution of *N*-benzoyl-(2*S*)-alanine methyl ester **71** with an enantiomeric excess (*e.e.*) of 68%, determined by chiral phase HPLC analysis, was enriched to a solution with an *e.e.* of 86% after crystallisation of two crops (33%).

The (2*S*)-alanine and (2*S*)-valine derivatives **71** and **72** were heated in 1,2,4-trichlorobenzene at 214°C until measurable amounts of the racemate were detected. Heating a solution of the pure alanine derivative **71** for 4 days gave product with an *e.e.* of 82% determined through chiral phase HPLC analysis, while a solution of the pure valine derivative **72** heated for 5 days gave product with an *e.e.* of 94%. The slower rate of racemisation of the valine derivative **72**, compared with the alanine derivative **71**, reflects the greater steric interactions of the larger side chain aliphatic group when the

hybridisation changes from sp^3 to sp^2 upon deprotonation at the α-carbon. These relative rates are consistent with the findings for the rates of racemisation of alanine and valine under dilute aqueous conditions[54,55]. The rate constant for valine racemisation at pH 7.6 and 135°C is 4.1×10^{-7} sec^{-1} while the rate for alanine racemisation is three times that of valine. An amino acid that has been shown to have a greater rate of racemisation, under dilute aqueous conditions, is aspartic acid, which racemises nearly eleven times faster than valine. It was rationalised that the β-carboxyl group acts as an intramolecular base to facilitate racemisation (Scheme 19)[56,57]. The β-carboxylate anion can remove the α-proton through the formation of a five membered ring transition state. The anion on the α-carbon can then be reprotonated from either above or below the amino acid plane by the β-carboxylic acid, to reform aspartic acid with loss of chiral integrity.

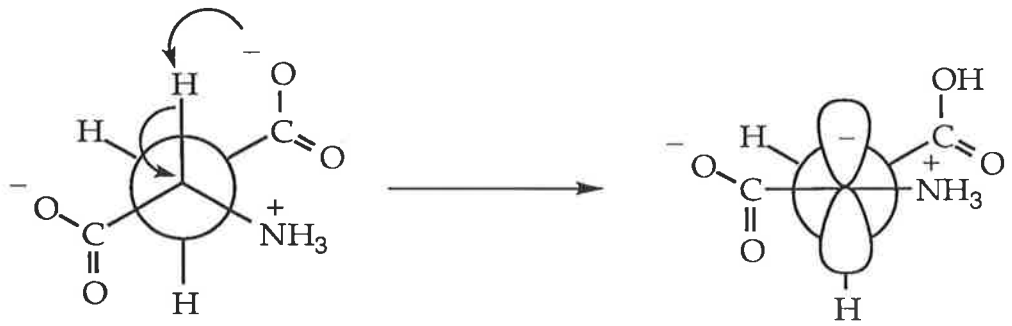

Scheme 19

As the rates of equilibration of the diastereomers of the dimer **39** are markedly faster than the rates of racemisation of the alanine and valine derivatives **71** and **72**, it seemed likely that a mechanism similar to the intramolecular assistance of the side chain β-carbonyl group in aspartic acid

racemisation would be involved in the equilibration of the diastereomers of the dimer **39**, whereby racemisation at the α-carbon of one glycine moiety would be affected by a group on the other glycine moiety. As amides are generally more basic than esters[45], this process most probably would involve the amide carbonyls acting as an intramolecular base through a six membered ring transition state. Thus a possible mechanism for the equilibration of the protected glycine dimer **39**, shown in Scheme 20, involves attack on an α-hydrogen by an amide carbonyl group.

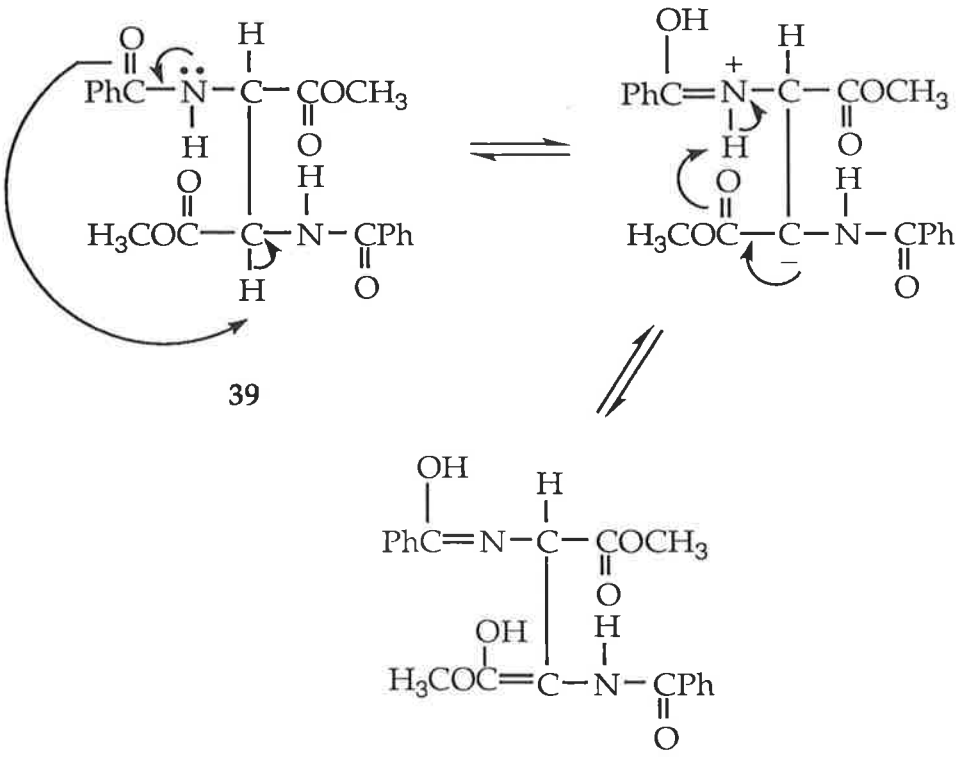

39

Scheme 20

The possibility of participation of the amide carbonyls in the equilibration was examined through studying the reactions of the diastereomers of the dimeric *N*-pentafluorobenzoylglycine derivative **75** in

1,2,4-trichlorobenzene at 214°C, by comparing the reaction rates with those of the diastereomers of the dimeric *N*-benzoylglycine derivative **39** determined under the same conditions. The nitrogen protecting group, pentafluorobenzoyl, was chosen to replace the benzoyl group as the size of the protecting group remains essentially unchanged, but the strong electron withdrawing inductive capabilities due to the electronegative fluorines reduces the basicity of the amide carbonyls. This should be reflected in decreased rates of equilibration of the diastereomers of the dimer **75**, compared with those of the diastereomers of the dimer **39**, if the mechanism involves abstraction of the α-hydrogens by the amides.

Formation of the dimeric *N*-pentafluorobenzoylglycine derivative **75** involved irradiation of a solution containing DTBP **21** and *N*-pentafluoro-benzoylglycine methyl ester **74**, which was prepared from pentafluorobenzoyl chloride **73** and the hydrochloride salt of methyl glycinate. The diastereomers

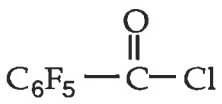

73

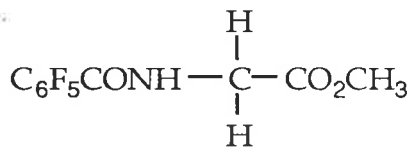

74

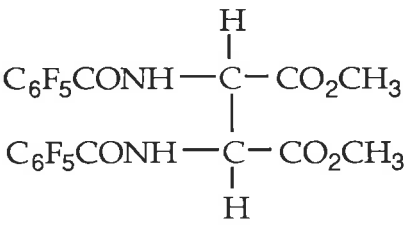

75

of the dimer **75** were isolated from the reaction mixture by chromatography, followed by fractional crystallisation of the evaporated product fractions. The stereochemistry of each diastereomer was determined by chiral phase HPLC analysis. The ^{1}H NMR spectrum of the *dl*-isomer of the dimer **75** showed the methyl ester and amide hydrogen signals at δ 3.91 and δ 6.9, respectively, and

a downfield chemical shift for the signal of the α-hydrogens, from δ 4.25 for the starting material **74** to δ 5.34. As expected, intramolecular hydrogen bonding is weaker in the *dl*-isomer of the dimer **75** than in the *dl*-isomer of the dimer **39**, based on the relative chemical shifts of the signals for the amide hydrogens at δ 6.9 and δ 7.2, respectively. A molecular ion at m/z 564 was seen in the mass spectrum of the *dl*-isomer of the dimer **75** as well as a fragment ion corresponding to the radical cation of the monomer **74** at m/z 283. The ^{1}H NMR spectrum of the *meso*-isomer of the dimer **75** showed resonances of δ 3.88, 5.40 and 7.5 for the methyl ester hydrogens, the α-hydrogens and the amide hydrogens, respectively. Again, as expected, hydrogen bonding in the *meso*-isomer of the dimer **75** is weaker than in the *meso*-isomer of the dimer **39**, as indicated by the chemical shifts of the signals for the amide hydrogens at δ 7.5 and δ 8.0, respectively. The mass spectrum of the *meso*-isomer of the dimer **75** showed a molecular ion at m/z 564 and a fragment ion at m/z 283.

HPLC analysis was carried out on a reaction mixture, from *N*-pentafluorobenzoylglycine methyl ester **74** (0.13M in benzene) and DTBP **21** (4.6 mole equivalents), that had been irradiated for 23 hours with 3500 Å lamps. The ratio of products, based on the HPLC peak integrations and given as a percentage of the total was 55% for the starting material **74**, 5% for *N*-pentafluorobenzoylalanine methyl ester **76**, 21% for the *dl*-isomer of the dimer **75** and 19% for the *meso*-isomer. The ratio of starting material to products in the reactions of DTBP **21** and the glycine derivatives **25** and **74**, carried out under the same conditions, was lower with the glycine derivative **74**. The reduced extent of reaction of the glycine derivative **74** may be attributed to a slower rate of formation of the radical **77**. The *N*-pentafluoro-benzoyl group is less able than the *N*-benzoyl group to delocalise the unpaired

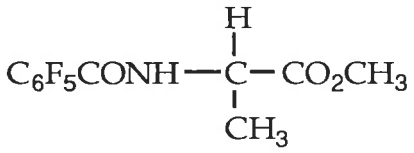

76

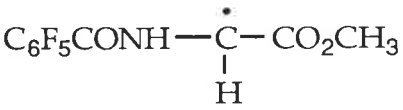

77

spin density of an adjacent carbon radical and any partial charge development during radical formation.

The reactions of the diastereomers of the protected *N*-pentafluorobenzoylglycine dimer **75**, in 1,2,4-trichlorobenzene at 214°C, were followed until 60% of the *dl*-isomer had reacted, during which time no decomposition occurred. The results are shown in Graph 8 and represent the log of the percentage of each diastereomer in excess of the equilibrium mixture remaining with time. Reverse phase HPLC analysis of samples heated for

Graph 8 - Reactions of the diastereomers of the dimer **75** in 1,2,4-trichlorobenzene at 214°C.

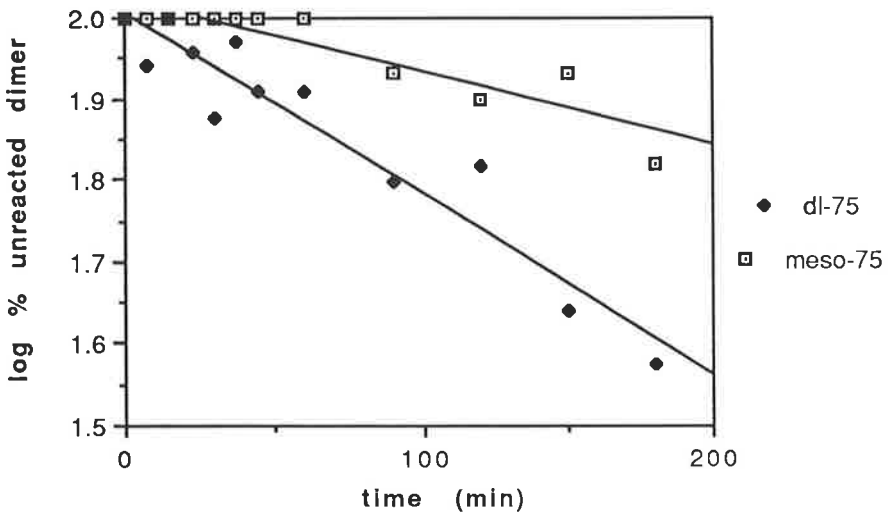

two days showed that the *dl*- and *meso*-isomers of the dimer **75** equilibrated to a 68 to 32% mixture. From the equations for the lines of best fit, the calculated rate constants were:

$$(8.79 \pm 0.81) \times 10^{-5}\ \text{sec}^{-1}$$

and $(3.72 \pm 0.60) \times 10^{-5}\ \text{sec}^{-1}$,

for equilibration of the *dl*- and *meso*-isomers, respectively. The rate of equilibration of the *dl*-isomer of the dimer **75** is 5.0 times slower than for the *dl*-isomer of the dimer **39**, while the *meso*-isomer equilibrates 17.7 times slower than does the *meso*-isomer of the dimer **39**. The relative rates of equilibration of the diastereomers of the dimers **39** and **75**, coupled with the relative basicity of the amides in those dimers, show that the mechanism for equilibration involves removal of the α-hydrogens by the amide groups as shown in Scheme 20.

The relative decreases in the rates of equilibration of the diastereomers of the dimer **75** reflect the relative extent of the deuterium isotope effects, of 1.48 and 2.35, shown for the rates of equilibration of the *dl*- and *meso*-isomers of the dimer **64**, respectively, compared with those of the corresponding diastereomers of the dimer **39**. The smaller effect of isotopic and electronic changes in the dimer **39** on the rate of equilibration of the *dl*-isomer, compared with the *meso*-isomer, indicates that the extent of proton transfer in the transition state is less for the *dl*-isomer than for the *meso*-isomer, which may be a consequence of the relative orientations of the substituents in the diastereomers of the dimer **39**.

In summary, the relative rates of equilibration of the amino acid derivatives **71** and **72** and the diastereomers of the dimers **39**, **64** and **75** in 1,2,4-trichlorobenzene at 214°C, show that the mechanism for equilibration involves deprotonation of the α-carbons by the amide substituents through a six-membered ring transition state. The rates of equilibration of the diastereomers of the dimer **39** in 1,2,4-trichlorobenzene and DMF were compared at 150°C and were found to be 100 times faster in DMF than in 1,2,4-trichlorobenzene. The enhanced reactivity in polar solvent most likely reflects stabilisation of the charged intermediates for deprotonation of the α-carbons and the disruption of intramolecular hydrogen bonding in the diastereomers of the dimer **39**.

Conclusion

In 1,2,4-trichlorobenzene at 214°C the diastereomers of the protected alanine dimer **40** undergo homolysis of their central carbon-carbon bonds, as shown through the trapping of the product alanyl radical **31** with a hydrogen source. Under the same conditions the diastereomers of the protected glycine dimer **39** appear not to undergo homolysis, indicating that the ease of radical formation through homolytic dimer dissociation is determined by steric factors in the dimer and not product radical stability.

The relative rates of decomposition of the diastereomers of the protected alanine dimer **40** in 1,2,4-trichlorobenzene at 214°C are determined by the extent of intramolecular hydrogen bonding. The *meso*-isomer with the relatively weaker hydrogen bonds undergoes homolysis of the central dimer bond faster than the racemate. The greater rate constants for reaction of the diastereomers of the protected alanine dimer **40** in DMF, than in 1,2,4-trichlorobenzene, at 150°C are consistent with the disruption of intramolecular hydrogen bonds of the dimers in polar solvent.

The reactions of the diastereomers of the dimer **39**, in 1,2,4-trichlorobenzene at 214°C, do not involve homolysis but equilibration. The mechanism for equilibration is tautomerisation, involving deprotonation of an α-carbon by a neighbouring amide carbonyl through a six-membered ring transition state. The reactivity of the diastereomers of the protected glycine dimer **39** in polar solvent was greater than in non-polar solvent, presumably due to the increased freedom of geometry associated with the disruption of hydrogen bonds and to the greater stabilisation of charged intermediates.

The rate of racemisation of amino acid residues in nature is generally very slow and has been used as an aid for dating geological material[58]. The

unusually facile interconversion of the diastereomers of the glycine dimer **39** indicates that racemisation of amino acids occurs much more easily than expected, at least under some circumstances. Indeed, where naturally occurring peptides, such as cyclosporin A[59] **78**, contain *R*-amino acid residues, formation of these may involve a mechanism similar to that for the interconversion of the diastereomers of dimethyl 2,3-dibenzamidobutane-dioate. It may be that the geometrical arrangement of the peptides is similar to that of the amino acid dimers studied in the present work.

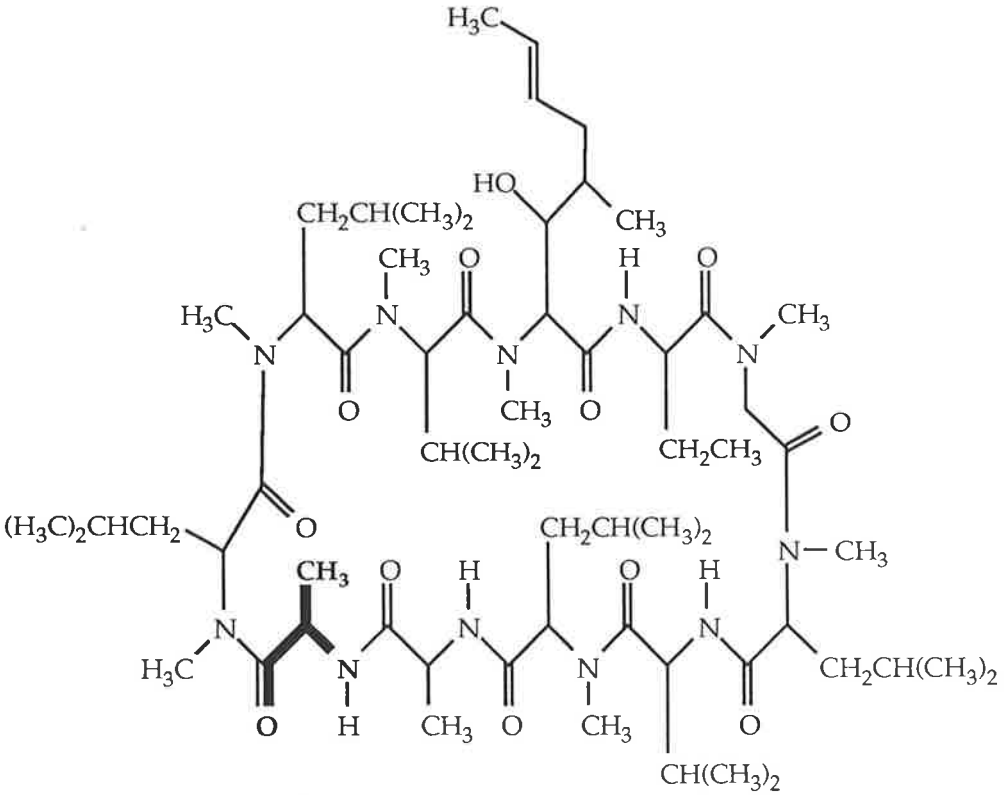

D-Ala

78

Experimental

General

Microanalyses were carried out by Chemical & Micro Analytical Services Pty. Ltd., Victoria, Australia.

Melting points were measured using a Kofler hot-stage melting point apparatus under a Reichert microscope and are uncorrected.

Infrared spectra were recorded on either a Jasco A-102 spectrophotometer or a Hitachi 270-30 infrared spectrophotometer and data processor. Samples were prepared either as nujol mulls or neat liquids, between NaCl plates. Absorptions were assigned as *s*, strong; *m*, medium; *w*, weak; *br*, broad.

^{1}H NMR spectra were recorded with either a Varian Gemini (200MHz) or a Brüker ACP300 (300MHz) spectrometer, as dilute solutions in $CDCl_3$, using TMS (δ 0.00) or chloroform (δ 7.27) as an internal reference. The multiplicity of the resonances is given as: s, singlet; d, doublet; t, triplet; dd, doublet of doublets; dq, doublet of quartets; m, multiplet; br. s, broad singlet; br. d, broad doublet.

^{13}C NMR spectra were recorded as dilute solutions in $CDCl_3$, with either a Varian Gemini (50MHz) or a Brüker ACP300 (75MHz) spectrometer and referenced with chloroform (t, δ 77.0).

Electron impact mass spectra were determined on either an AEI MS-3010 or a Vacuum Generators ZAB 2HF spectrometer. Accurate mass measurements of the molecular ions were carried out on the AEI MS-3010.

HPLC was carried out using either a Waters 501/510 solvent delivery system, Waters U6K injector and a Waters Lambda-Max 481 LC variable wavelength ultraviolet spectrophotometer or an ICI LC1110 solvent delivery system with Rheodyne injector and ICI LC1200 UV/VIS detector. Data was

collected and processed using the ICI data processing software programs DP700 or DP800. Columns used were either a Waters Nova-Pak® C_{18} Radial-Pak cartridge (8 x 100mm) (Reverse phase) or a Regis Pirkle covalent (2*S*)-phenylglycine column (4.6 x 250mm) (Chiral phase)[60]. Solvents were HPLC grade and were degassed prior to use. Samples were filtered through Millipore Millex®-HV_{13} 0.45μm disposable filters prior to injection. Co-injection of reaction mixtures with authentic samples allowed identification of products by peak enhancement.

Ultraviolet absorptions at 254 nm were measured using a Pye Unicam SP8-100 spectrophotometer.

Squat column chromatography[61] and preparative TLC were carried out using Merck silica gel 60 PF_{254} containing gypsum; flash chromatography[62] was carried out using silica gel 60 (230-400 mesh ASTM). Analytical TLC was carried out with Merck aluminium backed TLC plates (silica gel 60).

Solvents were purified and dried by standard techniques[63]; DMF was redistilled under reduced pressure just prior to use.

Bulb to bulb distillations were carried out using a Kugelrohr glass oven.

Experimental for Chapter One

N-Benzoylglycine Methyl Ester **25**

Hippuric acid (5.02g, 28mmol) was added to methanol (70ml), previously treated with thionyl chloride (3.7ml, 51mmol). The resultant solution was stirred overnight at room temperature, under a $CaCl_2$ drying tube, then evaporated to dryness, under reduced pressure, and taken up in ethyl acetate (50ml) washed with a solution of saturated aqueous $NaHCO_3$ (2 x 10ml) and water (2 x 10ml), then dried ($MgSO_4$). The ethyl acetate solution was evaporated to dryness, under reduced pressure, to give a white solid (4.03g, 74%). The solid was recrystallised from ethyl acetate-hexane to yield **25** (3.25g, 60%), 81.5 - 82°C (lit.[64] 82 - 83°C).

ν_{max} (cm^{-1}) 3300*m br* (NH), 1745*s* (C=O ester), 1640*m br* (C=O amide), 1615*m*, 1590*m*, 1560*s* (trans amide NH), 1505*m*, 1265*s br*, 1025*m*, 1010*m*, 740*m* (ArH), 715*m* (ArH).

^1H NMR (200MHz) δ 3.80, s, 3H (OCH_3); 4.26, d *J* 5Hz, 2H (CH_2); 6.8, br. d *J* 5Hz, 1H (NH); 7.40 - 7.84, m, 5H (ArH).

^{13}C NMR (50MHz) δ 41.7 (CH_2); 52.4 (OCH_3); 127.0, 128.6, 131.8, 133.6 (ArC); 167.4 (C=O amide), 170.5 (C=O ester).

m/z 193 ($M^{+\cdot}$, 12%), 161 ($(193\text{-}CH_3OH)^{+\cdot}$, 5), 134 ($(193\text{-}CO_2CH_3)^+$, 23), 105 ($C_6H_5CO^+$, 100), 77 ($C_6H_5^+$, 39), 51 ($C_4H_3^+$, 13).

Reverse phase HPLC (1,2 Dichloroethane-acetonitrile-water; 1 : 49 : 93), flow 1.5ml/min, t_R of 3.6 min.

N-Benzoylalanine Methyl Ester **26**

To an ice cooled solution of anhydrous methanol (200ml), that had been pretreated by the dropwise addition of thionyl chloride (9ml, 123mmol), was

added alanine (10.12g, 114mmol). The mixture was allowed to warm to room temperature and stir overnight under a calcium chloride drying tube. The resulting solution was evaporated to dryness, using reduced pressure, to give a crude white solid. The solid was repeatedly redissolved in methanol and evaporated to remove any residual HCl to give methyl alaninate hydrochloride (15.17g, 96%), which was used without further purification.

To a saturated aqueous solution of $NaHCO_3$ (100ml) was added the methyl alaninate hydrochloride (9.0g, 64.5mmol) followed by a solution of benzoyl chloride (7.5ml, 64.6mmol) in ethyl acetate (100ml). The resulting mixture was stirred vigorously at room temperature overnight. The organic layer was removed and washed twice with water, then dried ($MgSO_4$), before the solvent was removed, using reduced pressure, to yield a white solid (12.8g, 96%). The solid was recrystallised from ethyl acetate-hexane to yield **26** as colourless needles (11.0g, 82%), 81.5 - 82.5°C (lit.[65] 82°C).

ν_{max} (cm^{-1}) 3300*m br* (NH), 1750*s* (C=O ester), 1635*s* (C=O amide), 1600*w*, 1580*w*, 1540*s* (trans amide NH), 1495*m*, 1270*m*, 1215*s*, 1165*s*, 720*m*.

^1H NMR (300MHz) δ 1.53, d *J* 7Hz, 3H (α-CH_3); 3.80, s, 3H (OCH_3); 4.82, dq *J* 7, 7Hz, 1H (CH); 6.8, br. d *J* 7Hz, 1H (NH); 7.42 - 7.82, m, 5H (ArH).

^{13}C NMR (50MHz) δ 18.6 (α-CH_3); 48.5 (CH); 52.5 (OCH_3); 127.0, 128.6, 131.7, 133.9 (ArC); 166.8 (C=O amide); 173.7 (C=O ester).

m/z 207 ($M^{+\cdot}$, 2%), 148 ($(207\text{-}CO_2CH_3)^+$, 41), 122 ($C_6H_5CONH_3^+$, 3), 105 ($C_6H_5CO^+$, 100), 77 ($C_6H_5^+$, 45), 51 ($C_4H_3^+$, 26).

Reverse phase HPLC (1,2 Dichloroethane-acetonitrile-water; 1 : 49 : 93), flow 1.5ml/min, t_R of 4.9 min.

Chiral phase HPLC (Isopropanol-1,2 dichloroethane-hexane; 1 : 2 : 19), flow 1ml/min, t_R of 21.4, 22.5 min.

Reactions of the Protected Amino Acids **25**, **26**, **29** and **56** with DTBP **21**

Irradiation of reaction solutions contained in quartz tubes was carried out in a Rayonet Photochemical Reactor which held either 16 x 3500 Å (Woods' glass) or 16 x 3000 Å lamps. Variations of reaction conditions for photolysis of DTBP **21** in the presence of the amino acid derivatives **25** and **26** are contained in Tables 3 and 5 in Chapter One.

Reaction of *N*-Benzoylglycine Methyl Ester **25** with DTBP **21**

A solution of DTBP **21** (17.5ml, 95mmol) and *N*-benzoylglycine methyl ester **25** (4.01g, 20.8mmol) in dry benzene (110ml), was deoxygenated (x 3, N_2) then irradiated with 3500 Å lamps for 40 hours. The precipitate which had formed during the reaction was collected and identified as the *dl*-isomer of **dimethyl 2,3-dibenzamidobutanedioate (39)** (0.96g, 24%). The solid was recrystallised from benzene to yield the *dl*-isomer of the dimer **39** as a white powder (0.85g, 21%), 217 - 218.5°C (lit.[42] 206 - 207°C).

ν_{max} (cm^{-1}) 3250*m br* (NH), 1750*m* and 1740*s* (C=O ester), 1630*s* (C=O amide), 1600*w*, 1575*w*, 1540 *br* (trans amide NH), 1260*s*, 1200*m*, 1015*m*, 695*m*.

^1H NMR (300MHz) δ 3.90, s, 6H (2 x OCH_3); 5.32, d *J* 5Hz, 2H (2 x CH); 7.2, br. d *J* 5Hz, 2H (2 x NH); 7.42 - 7.81, m, 10H (ArH).

^{13}C NMR (50MHz) δ 53.4 (OCH_3); 54.5 (CH); 127.2, 128.7, 132.1, 133.2 (ArC); 167.4 (C=O amide); 170.3 (C=O ester).

m/z 384 ($M^{+\cdot}$, 3%), 204 (4), 193 ($C_6H_5CONHCH_2CO_2CH_3^{+\cdot}$, 25), 161 ((193-$CH_3OH$)$^{+\cdot}$, 10), 105 ($C_6H_5CO^+$, 100), 77 ($C_6H_5^+$, 37), 51 ($C_4H_3^+$, 11).

Reverse phase HPLC (1,2 Dichloroethane-acetonitrile-water; 1 : 49 : 93), flow 1.5ml/min, t_R of 11.1 min.

Chiral phase HPLC (Isopropanol-1,2 dichloroethane-hexane; 10.4 : 2 : 19), flow 1ml/min, t_R of 13.8, 16.7 min.

TLC (1,2 Dichloroethane-ethyl acetate; 9 : 1), R_f of 0.15.

The filtrate was evaporated to dryness, under reduced pressure, and the *meso*-isomer of **dimethyl 2,3-dibenzamidobutanedioate (39)** crystallised from an ethyl acetate-hexane solution of the residue. The solid was recrystallised from ethyl acetate-hexane to yield the *meso*-isomer of the dimer **39** as a white powder (0.46g, 11%), 184 - 186.5°C (lit.[42] 189 - 193°C /lit.[66] 181 - 182°C).

ν_{max} (cm^{-1}) 3310*s br* (NH), 1740*s br* (C=O ester), 1640*s* (C=O amide), 1600*w*, 1580*w*, 1540*s br* (trans amide NH), 1310*s*, 1270*s*, 1175*s*, 1010*m*, 720*s*, 695*m*.

^1H NMR (300MHz) δ 3.84, s, 6H (2 x OCH_3); 5.34, d *J* 6Hz, 2H (2 x CH); 7.46 - 7.92, m, 10H (ArH); 8.0, br. d *J* 6Hz, 2H (2 x NH).

^{13}C NMR (50MHz) δ 53.2 (OCH_3); 56.3 (CH); 127.4, 128.7, 132.2, 133.1 (ArC); 168.3 (C=O amide); 169.2 (C=O ester).

m/z 384 ($M^{+\cdot}$, 2%), 204 (4), 193 ($C_6H_5CONHCH_2CO_2CH_3^{+\cdot}$, 17), 161 ((193-$CH_3OH$)$^{+\cdot}$, 8), 105 ($C_6H_5CO^+$, 100), 77 ($C_6H_5^+$, 46), 51 ($C_4H_3^+$, 11).

Reverse phase HPLC (1,2 Dichloroethane-acetonitrile-water; 1 : 49 : 93), flow 1.5ml/min, t_R of 13.3 min.

Chiral phase HPLC (Isopropanol-1,2 dichloroethane-hexane; 10.4 : 2 : 19), flow 1ml/min, t_R of 12.3 min.

TLC (1,2 Dichloroethane-ethyl acetate; 9 : 1), R_f of 0.20.

TLC (Ethyl acetate-hexane; 1 : 1) analysis of the reaction mixture showed three UV active spots, R_f s of 0.70, 0.45, 0.23, amongst a large streak. The two lowest spots were due to amino acid derivatives **26** and **39**, respectively. The high R_f material was isolated by column chromatography of the reaction mixture as an off-white solid. The solid was identified as **biphenyl (51)** and recrystallised from ethanol-water to yield **51** as a white solid (0.28g, 1% based on DTPB **21**), 65 - 68°C (lit.[67] 69 - 71°C).

ν_{max} (cm^{-1}) 1600*w*, 1570*w*, 1485*m*, 735*s*, 700*s*.

^{1}H NMR (300MHz) δ 7.35 - 7.62, m (ArH).

^{13}C NMR (50MHz) δ 127.1, 127.2, 128.7, 141.2 (ArC).

m/z 155 (17%), 154 ($M^{+\cdot}$, 100), 153 (27), 152 (20).

The spectral characteristics were found to be identical to those of an authentic sample.

Reaction of *N*-Benzoylalanine Methyl Ester **26** with DTBP **21**

A solution of DTBP **21** (40ml, 218mmol) and *N*-benzoylalanine methyl ester **26** (8.03g, 38.7mmol) in *t*-butanol (200ml) was degassed (x 3, N_2) then irradiated with 3500 Å lamps for 65 hours. The yellow solution was evaporated, under reduced pressure, to dryness to give a thick yellow oil (13.98g). TLC (Ethyl acetate-hexane; 1 : 1) analysis showed two UV active spots, R_f of 0.34 and 0.23, amongst a large streak. Squat column chromatography, eluting with ethyl acetate-hexane, was carried out to separate these components. Fractional crystallisation of the higher R_f fraction, from ethyl acetate-hexane, yielded the *meso*-isomer of **dimethyl 2,3-dibenzamido-2,3-dimethylbutanedioate** (**40**) (0.20g, 3%), 178 - 179.5°C (lit.[22] 170 - 177°C).

ν_{max} (cm^{-1}) 3450*m* (NH), 1725*s* (C=O ester), 1670*s* (C=O amide), 1610*w*, 1590*w*, 1535*s br* (trans amide NH), 1500*m*, 1305*s br*, 1265*s*, 1090*m*, 720*s*, 700*w*.

^{1}H NMR (300MHz) δ 1.98, s, 6H (2 x α-CH_3); 3.80, s, 6H (2 x OCH_3); 7.43 - 7.87, m, 10H (ArH); 8.20, s, 2H (2 x NH).

^{13}C NMR (50MHz) δ 18.6 (α-CH_3); 53.3 (OCH_3); 65.9 (C); 127.2, 128.7, 131.9, 133.8 (ArC); 167.7 (C=O amide); 171.5 (C=O ester).

m/z 413 ($(M+H)^+$, 12%), 395 ($(412\text{-}OH)^+$, 9), 353 ($(412\text{-}CO_2CH_3)^+$, 3), 231 (9), 207 ($C_6H_5CONHCH(CH_3)CO_2CH_3^{+\cdot}$, 33), 175 ($(207\text{-}CH_3OH)^{+\cdot}$, 4), 105 ($C_6H_5CO^+$, 100), 77 ($C_6H_5^+$, 26), 51 ($C_4H_3^+$, 5).

Found m/z $(M+H)^+$ 413.17261. $C_{22}H_{24}N_2O_6$ + H requires m/z 413.17126.
Found: C, 64.04; H, 5.66; N, 6.77. $C_{22}H_{24}N_2O_6$ requires C, 64.07; H, 5.87; N, 6.79.
Reverse phase HPLC (1,2 Dichloroethane-acetonitrile-water; 1 : 49 : 93), flow 1.5ml/min, t_R of 34.1 min.
The configuration of the *meso*-diastereomer was determined by X-ray crystallographic analysis.

The lower R_f fraction gave an oil of **2-benzamido-2,4-dimethyl-4-hydroxy-pentanoic acid γ-lactone** (**52**) (0.79g, 10%). The oil crystallised from ethyl acetate-hexane to yield **52** as colourless needles (0.31g, 3%), 141.5 - 142.5°C.
ν_{max} (cm^{-1}) 3400*m br* (NH), 1745*s* (C=O lactone), 1650*s* (C=O amide), 1600*w*, 1575*w*, 1525*s br* (trans amide NH), 1270*s br*, 1095*s*, 720*m*, 710*m*.
^1H NMR (200MHz) δ 1.52, s, 3H (α-CH_3); 1.62, s, 3H (CH_3); 1.69, s, 3H (CH_3); 2.33, d *J* 13Hz, 1H (CH_A); 2.75, d *J* 13Hz, 1H (CH_B); 6.45, br. s, 1H (NH); 7.40 - 7.80, m, 5H (ArH).
^{13}C NMR (50MHz) δ 25.7 (CH_3); 29.4, 29.8 (2 x CH_3); 46.9 (CH_2); 58.5 (C-N); 81.7 (C-O); 127.1, 128.6, 131.1, 132.0, 133.4 (ArC); 166.7 (C=O amide); 176.8 (C=O lactone).
m/z 248 ($(M+H)^+$, 0.6%), 203 (11), 188 ($(247-C_3H_7O)^+$, 7), 160 ($(247-C_3H_7OCO)^+$, 37), 122 ($C_6H_5CONH_3^+$, 6), 105 ($C_6H_5CO^+$, 100), 77 ($C_6H_5^+$, 33), 51 ($C_4H_3^+$, 8).
Found: C, 68.23; H, 6.90; N, 5.39. $C_{14}H_{17}NO_3$ requires C, 68.00; H, 6.93; N, 5.66.
Reverse phase HPLC (1,2 Dichloroethane-acetonitrile-water; 1 : 49 : 93), flow 1.5ml/min, t_R = 6.6 min.
The structure of **52** was confirmed by X-ray crystallographic analysis.

Further elution from the squat column gave a white solid that was not UV active on the TLC plate. This material was identified as **2,5-dimethylhexane-2,5-diol (53)**. Crystallisation from hexane gave **53** as colourless platelets (0.28g, 8% based on DTBP **21**), 87 - 90°C (lit.[68] 86 - 90°C).

ν_{max} (cm^{-1}) 3275*s br* (OH), 1205*m br* (OH), 1150*s br*, 1100*m*, 910*s*.

^1H NMR (200 MHz) δ 1.24, s, 12H; 1.58, s, 4H; 1.6, br. s, 2H. Signal at δ 1.6 disappeared upon addition of D_2O.

m/z 129 ($(M^{+\cdot}-OH)^+$, 5%), 113 (33), 111 (43), 105 (10), 95 (15), 70 (46), 59 (81), 43 (100).

The spectral characteristics were found to be identical to those of an authentic sample.

Flash chromatography of the mother liquor obtained by filtration of the *meso*-isomer of the dimer **40**, eluting with 25% ethyl acetate-hexane, yielded **methyl 2-benzamido-2-methylpropanoate (50)**. Crystallisation of **50** from ethyl acetate-hexane yielded colourless needles (0.28g, 2%), 120.5 - 121.5°C (lit.[47] 122°C).

ν_{max} (cm^{-1}) 3250*m br* (NH), 1750*s* (C=O ester), 1640*s* (C=O amide), 1610*m*, 1560*s br* (trans amide NH), 1345*s*, 1290*s*, 1170*s*, 1000*w*, 940*m*, 930*m*, 710*s*.

^1H NMR (200MHz) δ 1.69, s, 6H (2 x α-CH_3); 3.79, s, 3H (OCH_3); 6.80, br. s, 1H (NH); 7.39 - 7.81, m, 5H (ArH).

m/z 222 ($(M+H)^+$, 2%), 162 ($(221-CO_2CH_3)^+$, 36), 119 (2), 105 ($C_6H_5CO^+$, 100), 77 ($C_6H_5^+$, 29).

Reverse phase HPLC (1,2 Dichloroethane-acetonitrile-water; 1 : 49 : 93), flow 1.5ml/min, t_R of 6.1 min.

Further elution yielded the *dl*-isomer of **dimethyl 2,3-dibenzamido-2,3-dimethylbutanedioate (40)**. Crystallisation of the *dl*-isomer of the dimer **40** from ethyl acetate-hexane yielded colourless cubes (0.16g, 2%), 148.5 - 151°C.

ν_{max} (cm^{-1}) 3440*m* and 3420*m* (NH), 1740*s* and 1735*s* (C=O ester), 1675*s* (C=O amide), 1610*w*, 1590*w*, 1530*s* (trans amide NH), 1500*s*, 1290*s* and 1280*s*, 1215*m*, 1125*w* and 1120*w*, 1000*w*, 730*s*, 705*s*.

^{1}H NMR (200MHz) δ 1.64, s, 6H (2 x α-CH_3); 3.92, s, 6H (2 x OCH_3); 7.44 - 7.86, m, 10H (ArH); 8.51, s, 2H (2 x NH).

^{13}C NMR (50MHz) δ 18.1 (α-CH_3); 53.3 (OCH_3); 62.7 (C); 127.1, 128.7, 132.0, 133.1 (ArC); 166.4 (C=O amide); 172.1 (C=O ester).

m/z 413 ($(M+H)^+$ 4%), 395 ($(412\text{-}OH)^+$, 2), 381 ($(412\text{-}OCH_3)^+$, 1), 353 ($(412\text{-}CO_2CH_3)^+$, 3), 231 (10), 207 ($C_6H_5CONHCH(CH_3)CO_2CH_3^{+\cdot}$, 34), 206 (16), 175 ($(207\text{-}CH_3OH)^{+\cdot}$, 6), 105 ($C_6H_5CO^+$, 100), 102 (13), 77 ($C_6H_5^+$, 27).

Found m/z $(M+H)^+$ 413.17302. $C_{22}H_{24}N_2O_6$ + H requires m/z 413.17126.

Found: C, 64.20; H, 6.13; N, 6.79. $C_{22}H_{24}N_2O_6$ requires C, 64.07; H, 5.87; N, 6.79.

Reverse phase HPLC (1,2 Dichloroethane-acetonitrile-water; 1 : 49 : 93), flow 1.5ml/min, t_R = 41.9 min.

The configuration of the *dl*-diastereomer was determined by X-ray crystallographic analysis.

Methyl Pyroglutamate **29**

A stirred solution of pyroglutamic acid (5.03g, 39mmol) in methanol (75ml) was cooled to below -10°C before thionyl chloride (2.8ml, 38mmol) was added dropwise. The resultant mixture was allowed to warm to room temperature overnight, under a calcium chloride drying tube. The methanol solution was evaporated to dryness, under reduced pressure, and the residue

was redissolved in methanol and evaporated several times to remove HCl. Bulb to bulb distillation of the residual oil gave **29** as a colourless viscous oil (5.05g, 92%), 120 - 130°C / 0.03mmHg (lit.[69] 101 - 103 / 0.15mmHg).

ν_{max} (cm^{-1}) 3275*s br* (NH), 2970, 1750*s br* (C=O ester), 1705*s br* (C=O lactam), 1450*s*, 1230*s br*, 1120*m br*, 1050*m*.

^1H NMR (300MHz) δ 2.21 - 2.53, m, 4H (2 x CH_2); 3.78, s, 3H (OCH_3); 4.27, dd *J* 5, 8Hz, 1H (CH); 6.4, br. s, 1H (NH).

^{13}C NMR (50MHz) δ 23.8 (CH_2); 28.3 (CH_2); 51.3 (OCH_3); 54.6 (CH); 172.0 (C=O ester); 177.7 (C=O lactam).

m/z 143 ($M^{+\cdot}$, 14%), 84 ($(143\text{-}CO_2CH_3)^+$, 100), 56 ($C_3H_6N^+$, 23), 41 ($C_3H_5^+$, 28), 29 (30).

TLC (Methanol), R_f of 0.64.

Reaction of Methyl Pyroglutamate **29** with DTBP **21**

Synthesis of the dimeric methyl pyroglutamate **49** was similar to the previously reported procedure[43]. The crude dimer was isolated by chromatography in 62% yield and repeated fractional crystallisation from methanol yielded the *dl*-isomer of **5,5'-bis(5-methoxycarbonyl-2-pyrrolidinone) (49)** (8%), 214 - 216°C (lit.[43] 216°C).

ν_{max} (cm^{-1}) 3250*m br* (NH), 1750*s* and 1735*s* (C=O ester), 1705*s br* (C=O lactam), 1350*m*, 1270*m br*, 1200*m*, 1170, 1160*m*, 1085*w*, 1050*w*, 995*w*, 740*m*.

^1H NMR (300MHz) δ 2.12 - 2.58, m, 8H (4 x CH_2); 3.79, s, 6H (2 x OCH_3); 6.6, s, 2H (2 x NH);

^{13}C NMR (50MHz) δ 26.7 (CH_2); 28.6 (CH_2); 53.5 (OCH_3); 68.4 (C); 174.7 (C=O ester); 177.6 (C=O lactam).

m/z 284 ($M^{+\cdot}$, 3%), 225 ($(284\text{-}CO_2CH_3)^+$, 11), 166 ($(225\text{-}CO_2CH_3)^{+\cdot}$, 4), 142 ($C_6H_8NO_3^+$, 100), 128 (5), 114 ($(142\text{-}CO)^+$, 9), 111 ($(142\text{-}OCH_3)^{+\cdot}$, 5), 82 ($(114\text{-}CH_3OH)^+$, 15), 55 ($C_3H_5N^{+\cdot}$, 13).

The physical and spectroscopic data were similar to those reported for the *dl*-isomer of the dimer **49**. Crystal structure analysis confirmed the *dl* configuration.

Crystallisation of the residue of the evaporated mother liquor obtained by filtration of the *dl*-isomer of the dimer **49**, from methanol-acetone, yielded the *meso*-isomer of **5,5'-bis(5-methoxycarbonyl-2-pyrrolidinone)** (**49**) (3%), 219 - 223°C dec. (lit.[43] 224°C).

ν_{max} (cm^{-1}) 3200 and 3090*m br* (NH), 1730*s br* (C=O ester), 1690*s br* (C=O lactam), 1375*s*, 1300*s*, 1285*s*, 1250*s br*, 1150*m*, 1045*m*, 1030*m*, 990*m*, 965*m*, 830*w*, 735*m br*.

^1H NMR (300MHz) δ 2.28 - 2.61, m, 8H (4 x CH_2); 3.79, s, 6H (2 x OCH_3); 6.9, s, 2H (2 x NH).

^{13}C NMR (50MHz) δ 26.6 (CH_2); 29.5 (CH_2); 53.3 (OCH_3); 69.0 (C); 172.6 (C=O ester); 177.6 (C=O lactam).

m/z 284 ($M^{+\cdot}$, 1%), 225 ($(284\text{-}CO_2CH_3)^+$, 11), 166 ($(225\text{-}CO_2CH_3)^{+\cdot}$, 4), 142 ($C_6H_8NO_3^+$, 100), 128 (5), 114 ($(142\text{-}CO)^+$, 10), 111 ($(142\text{-}OCH_3)^{+\cdot}$, 7), 82 ($(114\text{-}MeOH)^+$, 20), 55 ($C_3H_5N^{+\cdot}$, 19).

Crystal structure analysis showed that this diastereomer has the *meso* configuration.

N-tert-Butoxycarbonylglycine Methyl Ester **56**

The reagent, methyl glycinate hydrochloride, required for the synthesis of the glycine derivative **56** was prepared in 98% yield, from glycine

(9.48g, 126mmol) and methanol (150ml) that had been pretreated with thionyl chloride (20ml, 274mmol), by the method outlined for the synthesis of methyl alanate hydrochloride that was required for the synthesis of the alanine derivative **26**.

To a solution of acetone (25ml) and water (25ml) was added triethylamine (13.9ml, 99.7mmol) and methyl glycinate hydrochloride (5.0g, 39.8mmol) followed by BOC-ON (Aldrich)(10.76g, 43.7mmol)[70]. The resultant mixture was stirred for 5 hours at room temperature. The organic layer was separated and washed once with 10% HCl, three times with water then dried ($MgSO_4$). The solvent was evaporated to dryness, under reduced pressure, to yield a yellow oil. Bulb to bulb distillation of the oil yielded **56** as a colourless oil (4.44g, 59%), 125°C / 0.1 - 0.2mmHg.

ν_{max} (cm^{-1}) 3375*s br* (NH), 1755*s* (C=O ester), 1710*s br* (C=O carbamate), 1510*s br* (trans amide NH), 1365*s*, 1165*s br*, 1055*m*, 950*m*, 865*m*.

^1H NMR (200MHz) δ 1.41, s, 9H (3 x CH_3); 3.71, s, 3H (OCH_3); 3.87, d *J* 6Hz, 2H (CH_2); 5.1, unresolved d, 1H (NH).

^{13}C NMR (50MHz) δ 28.2 (CH_3); 42.2 (CH_2); 52.1 (OCH_3); 79.9 (C); 155.6 (C=O carbamate); 170.7 (C=O ester).

m/z 174 ($(M-CH_3)^+$, 0.2%), 134 ($(189-C_4H_7)^+$, 7), 130 ($(189-CO_2CH_3)^+$, 4), 116 ($(189-C_4H_9O)^+$, 2), 90 ($H_3NCH_2CO_2CH_3^+$, 4), 88 ($HNCH_2CO_2CH_3^+$, 4), 74 ($C_4H_9OH^{+\cdot}$, 2), 59 ($CO_2CH_3^+$, 25), 58 (35), 57 ($C_4H_9^+$, 50), 43 (100).

Reaction of *N-tert*-Butoxycarbonylglycine Methyl Ester **56** with DTBP **21**

A solution of *N-t*-butoxycarbonylglycine methyl ester **56** (1.08g, 5.7mmol) and DTBP **21** (4.6ml, 25mmol) in benzene (40ml) was deoxygenated (x 3, N_2) then irradiated with 3500 Å lamps for 48 hours. The solvent from the product mixture was removed, using reduced pressure, to give an oil (1.13g).

A portion of the oil (0.75g) was purified using flash column chromatography and yielded the crude diastereomers of the dimer **57** (0.30g, 42%) as well as some starting material **56** (82mg, 12%). The first diastereomer to elute was crystallised from hexane and yielded **dimethyl 2,3-di-*t*-butoxycarbamate-butanedioate (57a)** as a white solid (74mg, 10%), 143 - 145°C.

ν_{max} (cm^{-1}) 3350*m br* (NH), 1745*s* and 1720*s* (C=O ester), 1710*s* and 1675*s* (C=O carbamate), 1510*s br*, 1350*s*, 1160*s br*, 1070*m*, 865*w*, 720*w*.

^1H NMR (300MHz) δ 1.42, s, 18H (6 x CH_3); 3.78, s, 6H (2 x OCH_3); 4.80, d *J* 9Hz, 2H (2 x CH); 5.3, br. d *J* 9Hz, 2H (2 x NH).

^{13}C NMR (50MHz) δ 28.1 (CH_3); 53.0 (OCH_3); 55.3 (CH); 80.4 (C); 154.8 (C=O carbamate); 170.0 (C=O ester).

m/z 377 ($(M+H)^+$, 3%), 321 ($(376-C_4H_7)^+$, 6), 265 ($(321-C_4H_8)^+$, 16), 233 ($(265-CH_3OH)^+$, 5), 203 (22), 189 ($C_4H_9OCONHCH_2CO_2CH_3^{+\cdot}$, 20), 133 ($HOCONHCH_2CO_2CH_3^{+\cdot}$, 83), 88 ($NHCH_2CO_2CH_3^+$, 39), 57 ($C_4H_9^+$, 100).

Found C, 50.98; H, 7.37; N, 7.24. $C_{16}H_{28}N_2O_8$ requires C, 51.06; H, 7.50; N, 7.44.

The other diastereomer of the dimer **57** crystallised from hexane to yield **dimethyl 2,3-di-*t*-butoxycarbamatebutanedioate (57b)** as a white solid (66mg, 9%), 102.5 - 103.5°C.

ν_{max} (cm^{-1}) 3425*s* and 3350*s br* (NH), 1760*s* and 1730*s* (C=O ester), 1705*s* and 1690*s* (C=O carbamate), 1520*s br*, 1500*s*, 1320*s*, 1160*s br*, 1060*s*, 1010*s*, 900*m*, 850*m*, 760*w*.

^1H NMR (300MHz) δ 1.46, s, 18H (6 x CH_3); 3.77, s, 6H (2 x OCH_3); 4.86, d *J* 8Hz, 2H (2 x CH); 5.5, br. d *J* 8Hz, 2H (2 x NH).

^{13}C NMR (50MHz) δ 28.2 (CH_3); 52.8 (OCH_3); 55.9 (CH); 80.6 (C); 155.6 (C=O carbamate); 169.7 (C=O ester).

m/z 377 ($(M+H)^+$, 2%), 321 ($(376-C_4H_7)^+$, 3), 277 ($(321-CO_2)^+$, 3),
265 ($(321-C_4H_8)^+$, 22), 221 ($(265-CO_2)^+$, 15), 203 (10),
189 ($C_4H_9OCONHCH_2CO_2CH_3^{+\cdot}$, 3), 133 ($HOCONHCH_2CO_2CH_3^{+\cdot}$, 16),
88 ($NHCH_2CO_2CH_3^+$, 13), 57 ($C_4H_9^+$, 100).
Found C, 51.10; H, 7.33; N, 7.25. $C_{16}H_{28}N_2O_8$ requires C, 51.06; H, 7.50;
N, 7.44.

Product studies of reaction mixtures of *N*-benzoylglycine methyl ester **25** and *N*-benzoylalanine methyl ester **26** with DTBP **21**

The reaction mixtures of the glycine derivative **25** and the alanine derivative **26** with DTBP **21**, outlined in Tables 3 and 5, were analysed using reverse phase HPLC (1,2 Dichloroethane-acetonitrile-water; 1 : 49 : 93), flow 1.5ml/min, with eluents detected by absorption at 254 nm. An aliquot of the product mixture to be analysed was evaporated to dryness, under reduced pressure, taken up in the HPLC running solvent and then loaded onto the HPLC column. The ultraviolet absorptions, at 254 nm, of stock solutions (1mg in 10ml methanol) of the products shown in Tables 4 and 6, were measured and showed that the response ratio of the amino acid derivatives **25** and **26** to the protected amino acid dimers **39** and **40** was 1 : 2.

Experimental for Chapter Two

General Procedure

Stock solutions of each diastereomer of the dimer **40** were prepared in the solvent to be studied. Aliquot volumes of stock solutions were measured, with Gilson 200µl and 1,000µl Pipetmans, into 1ml ampoules which were then sealed. One ampoule containing one diastereomer of the dimer **40** was then wired to an ampoule containing the other diastereomer. The pair was then weighted with lead to ensure that they remained fully immersed in the oil bath during the reaction. The oil bath, containing silicon oil 210H, was preheated with a Camlab thermostat immersion heater to the required temperature and allowed to equilibrate before the addition of the ampoules. The order in which the ampoules were added was also the same order for their removal. The temperature of the oil bath was recorded at regular intervals throughout the study. After the allotted time had passed an ampoule pair was removed and cooled in an ice-water bath. The cooled ampoules were opened and the solvent was removed by a short path distillation carried out under high vacuum. The residue from each dried ampoule, to be analysed by reverse phase HPLC, was dissolved in a solution of the HPLC running solvent (1,2 Dichloroethane-acetonitrile-water; 1 : 49 : 93) containing benzanilide (external standard, 1mg/100ml). Each sample in the study was taken up in the same amount of solvent and stirred vigorously for one hour prior to injection onto the reverse phase HPLC column. The flow rate of the HPLC solvent through the column was 1.5ml/min, giving the external standard and the *dl*- and *meso*-isomers of the dimer **40** retention times of 15.9, 41.9 and 31.4 min, respectively. Detection of the compounds was by UV absorption at 254 nm.

Dimethyl 2,3-dibenzamido-2,3-dimethylbutanedioate **40** in 1,2,4-Trichlorobenzene

Stock solutions *dl*-isomer of the dimer **40** : 6.6mg in 25ml.

meso-isomer of the dimer **40** : 5.6mg in 25ml.

The stock solutions were filtered through 0.45µm filters.

Dimethyl 2,3-dibenzamido-2,3-dimethylbutanedioate **40** in 1,2,4-Trichlorobenzene at 214°C

Ampoules containing 500µl of stock were heated at 214.7 ± 0.5°C. Each of the dried samples was taken up in 500µl of HPLC running solvent then 100µl was loaded onto the reverse phase HPLC column.

Table 7 - Decomposition of the diastereomers of the dimer **40** in 1,2,4-trichlorobenzene at 214°C.

	time (min)						
	0	180	360	540	720	1080	1440
% *dl*-**40** / ext. std. [a]	99.8	81	66	53	34	21	15
% *dl*-**40** / dimer **40** [b]	99.8	98	97	96	96	96	96
% *meso*-**40** / ext. std. [a]	97	51	26	14			
% *meso*-**40** / dimer **40** [b]	97	88	76	66			

a: Percentage of one isomer of the dimer **40** remaining with time measured with respect to the external standard. The reproducibility of the signal for the external standard varied by ±4%. b: Percentage of one isomer of the dimer **40** in the total *dl*- and *meso*-mixture.

The data shown in Table 7 was plotted as the log of each diastereomer of the dimer **40** remaining with time (Graph 1, p 51), with the aid of the software

"Cricketgraph". The equations of the lines of best fit, calculated by the Cricketgraph program, were:

$x = 55.094 - 27.319y$ ($R^2 = 0.988$) and $x = 21.165 - 10.656y$ ($R^2 = 0.999$)

for the *dl*- and *meso*-isomers, respectively, where x represents time in minutes and y represents the log of the amount of the dimer remaining. The first half lives were calculated using the equations (y = log 50) and the errors were calculated using the correlation values given with each equation. The first half lives occur at: 8.68 ± 0.10 hrs and 3.061 ± 0.003 hrs for the *dl*- and *meso*-isomers, respectively. The rate constants calculated from the half lives, using the equation $k = - \ln 0.5 / (t_{1/2})$, are given on page 50.

Reaction of the *meso*-isomer of Dimethyl 2,3-dibenzamido-2,3-dimethyl-butanedioate **40** in the presence of Thiocresol **60** in 1,2,4-Trichlorobenzene

A mixture of the *meso*-isomer of dimethyl 2,3-dibenzamido-2,3-dimethylbutanedioate **40** (3.2mg, 7.8μmol) and thiocresol **60** (22mg, 177μmol) in 1,2,4-trichlorobenzene (1ml) was heated at reflux for 10 hrs. The solvent was removed, under reduced pressure, and the resultant residue taken up in deuteriochloroform and analysed by ^{1}H NMR spectroscopy.
^{1}H NMR spectrum (300MHz) δ 1.53, d *J* 7Hz (α-CH_3 alanine derivative **26**); 1.98, s (α-CH_3 *meso*-isomer of the dimer **40**); 2.32, s (CH_3 thiocresol **60**); 3.80, s (OCH_3 alanine derivative **26** and *meso*-isomer of the dimer **40**); 3.91, s (SH thiocresol **60**); 4.82, m (CH alanine derivative **26**); 7.09 - 7.47, m (ArH thiocresol **60**); 8.2, s (NH *meso*-isomer of the dimer **40**). The ratio of the ^{1}H NMR signals for the carbon-methyl groups of thiocresol **60**, the *meso*-isomer of the dimer **40** and the alanine derivative **26** was approximately 90 : 7 : 3. Reverse phase HPLC analysis (1,2 Dichloroethane-acetonitrile-water; 1 : 49 : 93), flow 1.5ml/min, showed a peak corresponding to

N-benzoylalanine methyl ester **26** (t_R of 4.9 min) in the reaction mixture, which was enhanced when the reaction mixture was co-injected with an authentic sample of the alanine derivative **26**.

Reaction of Dimethyl 2,3-dibenzamido-2,3-dimethylbutanedioate **40** in the presence of 9,10-Dihydroanthracene **61** in 1,2,4-Trichlorobenzene

A mixture of the *meso*-isomer of dimethyl 2,3-dibenzamido-2,3-dimethylbutanedioate **40** (2.0mg, 4.8μmol) and 9,10-dihydroanthracene **61** (18.6mg, 103μmol) in 1,2,4-trichlorobenzene (1ml) was heated at reflux for 10.5 hrs. The solvent was removed, under reduced pressure, and the residue analysed by reverse phase HPLC (1,2 Dichloroethane-acetonitrile-water; 1 : 49 : 93), flow 1.5ml/min. Comparisons of the HPLC trace integrations of the dimer **40** to benzanilide, the external standard, showed 33% of the *meso*-isomer of the dimer **40** remained at the end of the reaction. Also present in the HPLC trace were peaks corresponding to a small amount of the *dl*-isomer of the dimer **40** and *N*-benzoylalanine methyl ester **26** (27% yield, 41% corrected yield). These were identified by co-injection with authentic samples. ^{1}H NMR spectroscopic analysis of the reaction mixture also showed evidence for the formation of the alanine derivative **26**: (300MHz) δ 1.53, d *J* 8Hz (α-CH_3); 4.83, m (CH); 6.9, br. d *J* 8Hz (NH).

Similarly, a mixture of the *dl*-isomer of dimethyl 2,3-dibenzamido-2,3-dimethylbutanedioate **40** (2.0mg, 4.8μmol) and 9,10-dihydroanthracene **61** (18.6mg, 103μmol) in 1,2,4-trichlorobenzene (1ml) was heated at reflux for 10.5 hrs. There was little evidence for the production of *N*-benzoylalanine methyl ester **26** by ^{1}H NMR spectroscopic and HPLC analysis of the product mixture. Since the *dl*-isomer of the dimer **40** has a longer half life in 1,2,4-trichlorobenzene than the *meso*-isomer, the reaction was repeated with the

reaction time extended to 24 hours.

A mixture of the *dl*-isomer of dimethyl 2,3-dibenzamido-2,3-dimethyl-butanedioate **40** (4.8mg, 11.6μmol) and 9,10-dihydroanthracene **61** (43mg, 239μmol) in 1,2,4-trichlorobenzene (1ml) was heated at reflux for 24 hrs. ^{1}H NMR spectroscopic analysis of the product mixture revealed minor signals corresponding to those of *N*-benzoylalanine methyl ester **26**: (300MHz) δ 1.5, d *J* 7Hz (α-CH_3); 3.78, s (OCH_3); 4.81, m *J* 7Hz (CH). As this was a minor component in a complex reaction mixture it was not possible to accurately integrate the signals of the alanine derivative **26**. The main component identified in the ^{1}H NMR spectrum was the *dl*-isomer of the dimer **40**: δ 1.64, s (α-CH_3); 3.92, s (OCH_3). Reverse phase HPLC analysis (1,2 Dichloroethane-acetonitrile-water; 1 : 49 : 93), flow 1.5ml/min, showed that approximately 65% of the *dl*-isomer of the dimer **40** remained and that *N*-benzoylalanine methyl ester **26** was produced in a yield of 12% (corrected yield of 35%).

Dimethyl 2,3-dibenzamido-2,3-dimethylbutanedioate **40** in *N*,*N*-Dimethylformamide (DMF)

Stock solutions *dl*-isomer of the dimer **40** : 1.0mg in 25ml.

meso-isomer of the dimer **40** : 1.5mg in 25ml.

The stock solutions were filtered through 0.45μm filters.

Dimethyl 2,3-dibenzamido-2,3-dimethylbutanedioate **40** in DMF at 150°C

Ampoules containing 500μl of stock were heated at 150.8 ± 0.6°C. Each of the dried samples was taken up in 400μl of HPLC running solvent then 100μl was loaded onto the reverse phase HPLC column.

Table 8 - Decomposition of the diastereomers of the dimer **40** in DMF at 150°C.

	time (min)						
	0	15	30	60	150	180	360
% *dl*-**40** / ext. std. [a]	100	75	84	80	63	34	30
% *meso*-**40** / ext. std. [a]	97	71	61	33	60	51	17

a: Percentage of one isomer of the dimer **40** remaining with time measured with respect to the external standard. The reproducibility of the signal for the external standard varied by ±2%.

As the errors of some of the values shown in Table 8 appeared large, the study was repeated. The temperature during the study was 150.3 ± 0.6°C.

Table 9

	time (min)		
	0	60	180
% *dl*-**40** / ext. std. [a]	100	74	64
% *meso*-**40** / ext. std. [a]	100	87	54

a: Percentage of one isomer of the dimer **40** remaining with time measured with respect to the external standard.

The data shown in Tables 8 and 9 was plotted as the log of each diastereomer of the dimer **40** remaining with time (Graph 2, p 54). The equations of the lines of best fit, calculated by the Cricketgraph program, were:

$x = 1151.9 - 580.97y$ ($R^2 = 0.842$) and $x = 946.61 - 474.38y$ ($R^2 = 0.869$)

for the *dl*- and *meso*-isomers, respectively, where x represents time in

minutes and y represents the log of the amount of the dimer remaining. The first half lives were calculated using the equations (y = log 50) and the errors were calculated using the correlation values given with each equation. The first half lives occur at: 2.7 ± 0.4 hrs and 2.3 ± 0.3 hrs for the *dl*- and *meso*-isomers, respectively. The rate constants calculated from the half lives are given on page 54.

Reaction of the *meso*-isomer of Dimethyl 2,3-dibenzamido-2,3-dimethyl-butanedioate **40** in the presence of 9,10-Dihydroanthracene **61** in DMF

A mixture of *meso*-dimethyl 2,3-dibenzamido-2,3-dimethylbutane-dioate **40** (3.0mg, 7.3μmol) and 9,10-dihydroanthracene **61** (27.2mg, 151μmol) in DMF (1.5ml) was heated at reflux for 10.5 hrs. The solvent was removed, under reduced pressure, and the resulting residue was analysed by reverse phase HPLC (1,2 Dichloroethane-acetonitrile-water; 1 : 49 : 93), flow 1.5ml/min. HPLC analysis showed that approximately 3% of the dimer remained, but there was no peak corresponding to *N*-benzoylalanine methyl ester **26**. The only product identifiable by ^{1}H NMR spectroscopy was 9,10-dihydroanthracene; no signals for the diastereomers of the dimer **40** or *N*-benzoylalanine methyl ester **26** were observed.

Dimethyl 2,3-dibenzamido-2,3-dimethylbutanedioate **40** in 1,2,4-Trichlorobenzene at 150°C

Ampoules containing 500μl of stock were heated at 150.5 ± 0.7°C. Each of the dried samples was taken up in 500μl of HPLC running solvent then 100μl was loaded onto the reverse phase HPLC column.

Table 10 - Decomposition of the diastereomers of the dimer **40** in 1,2,4-trichlorobenzene at 150°C.

	time (min)							
	0	360	720	1080	1440	2160	2880	5760
% *dl*-**40** / ext. std. [a]	100	100	94	100	100	100	94	100
% *meso*-**40** / ext. std. [a]	97	103	103	97	97	97	97	97

a: Percentage of one isomer of the dimer **40** remaining with time measured with respect to the external standard. The reproducibility of the signal for the external standard varied by ±3%.

Experimental for Chapter Three

General Procedure

The general procedure for the examination of the reactions of the diastereomers of the protected glycine dimer **39** was the same as described for the reactions of the diastereomers of the dimer **40** (Chapter Two). Analysis of the heated samples was carried out using reverse phase HPLC. The samples were evaporated to dryness, under reduced pressure, then the resultant residue was dissolved in a solution of the HPLC running solvent (1,2 Dichloroethane-acetonitrile-water; 1 : 49 : 93) that contained benzanilide (external standard, 1mg/100ml). Each sample in the study was taken up in the same amount of solvent and stirred vigorously for one hour prior to injection onto the HPLC column. The flow rate of the HPLC solvent through the reverse phase column was 1.5ml/min, giving the *dl*- and *meso*-isomers of the dimer **39** and the external standard retention times of 11.1, 13.3 and 15.9 min, respectively. Detection of the compounds was by UV absorption (λ = 254 nm).

Dimethyl 2,3-dibenzamidobutanedioate **39** in 1,2,4-Trichlorobenzene

Stock solutions *dl*-isomer of the dimer **39** : 33mg in 100ml.

meso-isomer of the dimer **39** : 35mg in 100ml.

Stock solutions were filtered through 0.45µm filters.

Dimethyl 2,3-dibenzamidobutanedioate **39** in 1,2,4-Trichlorobenzene at 214°C

Ampoules containing 500µl of stock were heated at 215.0 ± 1.5°C. Each of the dried samples was taken up in 500µl of HPLC running solvent then 100µl was loaded onto the reverse phase HPLC column.

Table 11 - Reactions of the diastereomers of the dimer **39** in 1,2,4-trichlorobenzene at 214°C.

	time (min)				
	0	7.5	15	22.5	30
% *dl*-**39** / dimer **39** [a]	100	89	81	72	69
% *meso*-**39** / dimer **39** [a]	98	86	81	74	72

Table 11 cont.

	time (min)			
	37.5	45	52.5	60
% *dl*-**39** / dimer **39**	65	63	59	54
% *meso*-**39** / dimer **39**	68	64		

a: Percentage of one isomer of the dimer **39** in the total *dl*- and *meso*-mixture.

Reverse phase HPLC analysis showed that each diastereomer of the dimer **39** underwent equilibration. To determine the equilibrium position a pair of ampoules containing the diastereomers of the dimer **39** in 1,2,4-trichlorobenzene was heated for 3 hours at 214°C. The solvent was removed, under reduced pressure, and the residue was dissolved in a solution of the HPLC running solvent (1,2 Dichloroethane-acetonitrile-water; 1 : 49 : 93) containing benzanilide (external standard, 1mg/100ml). Reverse phase HPLC analysis showed that the diastereomers equilibrated to a 43 : 57% mixture for the *dl*- and *meso*-isomers, without decomposition.

The data shown in Table 11 was plotted as the log of the percentage of each diastereomer of the dimer **39** in excess of the equilibrium mixture

remaining with time (Graph 3, p 57), with the aid of the software "Cricketgraph". The equations of the lines of best fit, calculated by the Cricketgraph program, were:

$x = 182.69 - 92.121y$ ($R^2 = 0.977$) and $x = 121.39 - 61.114y$ ($R^2 = 0.984$)

for the *dl*- and *meso*-isomers, respectively, where x represents time in minutes and y represents the log of the percentage of unreacted dimer remaining. The first half lives were calculated using the equations (y = log 50) and the errors were calculated using the correlation values given with each equation. The first half lives occur at: 26.2 ± 0.6 mins and 17.6 ± 0.3 mins for the *dl*- and *meso*-isomers, respectively. The rate constants calculated from the half lives, using the equation $k = - \ln 0.5 / (t_{1/2})$, are given on page 58.

Dimethyl 2,3-dibenzamidobutanedioate **39** in *N,N*-Dimethylformamide

Stock solutions *dl*-isomer of the dimer **39** : 0.7mg in 10ml.

meso-isomer of the dimer **39** : 0.7mg in 10ml.

The stock solutions were filtered through 0.45µm filters.

dl-Isomer of Dimethyl 2,3-dibenzamidobutanedioate **39** in DMF at 214°C

Ampoules containing 250µl of stock were heated at 212.0 ± 2.0°C. Each of the dried samples was taken up in 250µl of a solution of the HPLC running solvent, then 100µl was loaded onto the reverse phase HPLC column.

Table 12 - Reaction of the *dl*-isomer of the dimer **39** in DMF at 214°C.

	time (min)					
	0	7.5	15	22.5	30	37.5
% *dl*-**39** / dimer **39** [a]	100	55	57	58	57	57
dimer **39** / ext. std. [b]	100	95	65	37	17	10

a: Percentage of the *dl*-isomer of the dimer **39** in the total *dl*- and *meso*-mixture. b: Percentage of the *dl*-isomer of the dimer **39** remaining with time measured with respect to the external standard. The reproducibility of the signal for the external standard varied by ±4%.

The heated samples were shown by reverse phase HPLC analysis to have equilibrated to a 57 : 43% mixture for the *dl*- and *meso*-isomers.

Dimethyl 2,3-dibenzamidobutanedioate **39** in DMF at 150°C

Ampoules containing 250µl of stock were heated at 150.0 ± 2.0°C. Each of the dried samples was taken up in 350µl of a solution of the HPLC running solvent, then 100µl was loaded onto the reverse phase HPLC column.

Table 13 - Reactions of the diastereomers of the dimer **39** in DMF at 150°C.

	time (min)				
	0	7.5	15	22.5	30
% *dl*-**39** / dimer **39** [a]	99	85	72	75	70
dimer **39** / ext. std. [b]	100	77	77	63	72
% *meso*-**39** / dimer **39** [a]	94	87	66	62	63
dimer **39** / ext. std. [b]	100	88	93	90	83

Table 13 cont.

	time (min)			
	37.5	45	52.5	60
% *dl*-**39** / dimer **39**	77	68	65	
dimer **39** / ext. std.	61	64	70	
% *meso*-**39** / dimer **39**	59	54	52	52
dimer **39** / ext. std.	86	90	93	88

a: Percentage of one isomer of the dimer **39** in the total *dl*- and *meso*-mixture. b: Percentage of one isomer of the dimer **39** remaining with time measured with respect to the external standard. The reproducibility of the signal for the external standard varied by ±11% for the samples at t=0 to t=30min. Thereafter it varied by ±2%.

The equilibrium mixture was established from a sample heated for 150 minutes, using reverse phase HPLC analysis, to be 60 : 40% for the *dl*- and *meso*-isomers. The data shown in Table 13 was plotted as the log of the percentage of each diastereomer of the dimer **39** in excess of the equilibrium mixture remaining with time (Graph 4, p 59). The equations of the lines of best fit, calculated by the Cricketgraph program, were:

$x = 113.52 - 56.911y$ ($R^2 = 0.767$) and $x = 164.20 - 85.887y$ ($R^2 = 0.933$)

for the *dl*- and *meso*-isomers, respectively, where x represents time in minutes and y represents the log of the amount of unreacted dimer remaining. The first half lives were calculated using the equations ($y = \log 50$) and the errors were calculated using the correlation values given with each equation. The first half lives occur at: 16.8 ± 3.9 mins and 18.3 ± 1.2 mins for

the *dl*- and *meso*-isomers, respectively. The rate constants calculated from the half lives, using the equation $k = - \ln 0.5 / (t_{1/2})$, are given on page 60.

Dimethyl 2,3-dibenzamidobutanedioate **39** in 1,2,4-Trichlorobenzene at 150°C

Ampoules containing 250µl of stock were heated at 150.3 ± 0.7°C. Each of the dried samples was taken up in 500µl of a solution of the HPLC running solvent, then 100µl was loaded onto the reverse phase HPLC column.

Table 14 - Reactions of the diastereomers of the dimer **39** in 1,2,4-trichlorobenzene at 150°C.

	time (min)					
	0	60	180	360	540	720
% *dl*-**39** / dimer **39** [a]	98	96	91	90	90	94
% dimer **39** / ext. std. [b]	100	89	104	91	100	100
% *meso*-**39** / dimer **39** [a]	95	95	94	92	91	93
dimer **39** / ext. std. [b]	100	97	100	100	107	111

Table 14 cont.

	time (min)				
	1080	1440	1800	2160	2520
% *dl*-**39** / dimer **39**	80	83	75		
% dimer **39** / ext. std.	98	79	93		
% *meso*-**39** / dimer **39**	86	91	81	80	79
% dimer **39** / ext. std.	107	97	79	100	107

a: Percentage of one isomer of the dimer **39** in the total *dl*- and *meso*-mixture. b: Percentage of one isomer of the dimer **39** remaining with time measured with respect to the external standard. The reproducibility of the signal for the external standard varied by ±3%.

The equilibrium position of the diastereomers of the dimer **39** in 1,2,4-trichlorobenzene at 150°C could not be established as decomposition made determination of the relative concentrations of the diastereomers difficult. The data shown in Table 14 was plotted as the log of the percentage of each diastereomer of the dimer **39** in excess of the equilibrium mixture, determined at 214°C, remaining with time (Graph 5, p 60). The equations of the lines of best fit, calculated by the Cricketgraph program, were:

$x = 242.91 - 121.99y$ ($R^2 = 0.838$) and $x = 296.13 - 150.74y$ ($R^2 = 0.965$)

for the *dl*- and *meso*-isomers, respectively, where x represents time in minutes and y represents the log of the amount of unreacted dimer remaining. The first half lives were calculated using the equations (y = log 50) and the errors were calculated using the correlation values given with each equation. The first half lives occur at: 35.7 ± 5.8 hrs and 40.0 ± 1.4 hrs for the

dl- and *meso*-isomers, respectively. The rate constants calculated from the half lives, using the equation $k = - \ln 0.5 / (t_{1/2})$, are given on page 61.

dl-Isomer of Dimethyl 2,3-dibenzamidobutanedioate **39** in Chlorobenzene

Stock solution *dl*-isomer of the dimer **39** : 1.1mg in 25ml.

The stock solution was filtered through 0.45µm filters.

dl-Isomer of Dimethyl 2,3-dibenzamidobutanedioate **39** in Chlorobenzene at 214°C

Ampoules containing 500µl of stock were heated at 214.0 ± 1.8°C. Each of the dried samples was taken up in 750µl of a solution of the HPLC running solvent, then 100µl was loaded onto the reverse phase HPLC column.

Table 15 - Reaction of the *dl*-isomer of the dimer **39** in chlorobenzene at 214°C.

	time (min)				
	0	7.5	15	22.5	30
% *dl*-**39** / dimer **39** [a]	100	93	86	79	73
dimer **39** / ext. std. [b]	100	46	103	105	101

Table 15 cont.

	time (min)				
	37.5	45	52.5	60	90
% *dl*-**39** / dimer **39**	68	64	60	57	51
dimer **39** / ext. std.	103	104	104	101	101

a: Percentage of the *dl*-isomer of the dimer **39** in the total *dl*- and *meso*-mixture. b: Percentage of the *dl*-isomer of the dimer **39** remaining with time measured with respect to the external standard. The reproducibility of the signal for the external standard varied by ±2%.

The equilibrium mixture was established from a sample heated for 3 hours using reverse phase HPLC analysis. The *dl*-isomer of the dimer **39** equilibrated to a 44 : 56% mixture for the *dl*- and *meso*-isomers. The data shown in Table 15 was plotted as the log of the percentage of the *dl*-isomer of the dimer **39** in excess of the equilibrium mixture remaining with time (Graph 6, p 62). The equation of the line of best fit for the *dl*-isomer, calculated by the Cricketgraph program, was:

$$x = 203.24 - 100.98y \ (R^2 = 0.997),$$

where x represents time in minutes and y represents the log of the amount of unreacted dimer remaining. The first half life was calculated using the equation (y = log 50) and the error was calculated using the correlation value given with the equation. The first half life for the *dl*-isomer occurs at: 31.7 ± 0.1 mins. The rate constant calculated from the half life, using the equation $k = - \ln 0.5 / (t_{1/2})$, is given on page 62.

Reaction of the *dl*-isomer of Dimethyl 2,3-dibenzamidobutanedioate **39** in the presence of Thiocresol **60**

A mixture of the *dl*-isomer of dimethyl 2,3-dibenzamidobutanedioate **39**

(4.0mg, 10.4μmol) and thiocresol **60** (24mg, 193μmol) in 1,2,4-trichlorobenzene (1ml) was heated at reflux for 4 hrs. The solvent was removed, under reduced pressure, and the resultant residue taken up in deuteriochloroform and analysed by ^{1}H NMR spectroscopy.
^{1}H NMR (300MHz) δ 2.32, s (CH_3 thiocresol **60**); 3.84, s (OCH_3 *meso*-isomer of the dimer **39**) and 3.90, s, 6H (OCH_3 *dl*-isomer of the dimer **39**); 5.35, m, 2H (α-CH both diastereomers); 7.09 - 7.92, m (ArH thiocresol **60**); 8.0, br. d (NH *meso*-isomer of the dimer **39**). Ratio of *dl-* : *meso-* isomer of the dimer **39** was 2 : 3 from the integration of the methyl ester signals in the ^{1}H NMR spectrum. There was no evidence for the formation of *N*-benzoylglycine methyl ester **25**.

Reaction of the *dl*-isomer of Dimethyl 2,3-dibenzamidobutanedioate **39** in the presence of 9,10-Dihydroanthracene **61**

A mixture of the *dl*-isomer of dimethyl 2,3-dibenzamidobutanedioate **39** (5.3mg, 13.8μmol) and 9,10-dihydroanthracene **61** (24mg, 133μmol) in 1,2,4-trichlorobenzene (1ml) was heated at reflux for 4 hrs. The solvent was removed, under reduced pressure, and the resultant residue taken up in deuteriochloroform and analysed by ^{1}H NMR spectroscopy.
^{1}H NMR (300MHz) δ 3.83, s (OCH_3 *meso*-isomer of the dimer **39**); 3.89, s (OCH_3 *dl*-isomer of the dimer **39**); 3.94, s (CH_2 9,10-dihydroanthracene **61**); 5.32, m (α-CH both diastereomers of the dimer **39**); 7.17 - 7.31, m (ArH 9,10-dihydroanthracene **61**) major; 7.43 - 7.92, m (ArH); 8.0, br. d (NH *meso*-isomer of the dimer **39**). Ratio of *dl-* : *meso-* isomer of the dimer **39** was 1 : 1 from the integration of the methyl ester signals in the ^{1}H NMR spectrum. There was no evidence for the formation of the glycine derivative **25**.

The above reaction was repeated except that the heating of the reaction was continued for 7 days.

^{1}H NMR (300MHz) δ 3.83, s (OCH_3 *meso*-isomer of the dimer **39**); 3.89, s (OCH_3 *dl*-isomer of the dimer **39**); 5.33, m (α-CH both diastereomers); 7.43 - 8.41, m (ArH). Ratio of *dl-* : *meso-* isomer of the dimer **39** was 2 : 3 from the integration of the methyl ester signals in the ^{1}H NMR spectrum. There was no evidence for the formation of *N*-benzoylglycine methyl ester **25**. Reverse phase HPLC analysis (1,2 Dichloroethane-acetonitrile-water; 1 : 49 : 93), flow 1.5ml/min, of the reaction mixture showed that after 7 days 58% of the diastereomers of the dimer **39** remained and that the *dl*-isomer had equilibrated to a ratio of 44 : 56 for the *dl-* and *meso*-isomers of the dimer **39**.

1-Butanol-*d* **65**

1-Butanol (10ml, 109mmol) was stirred vigorously over D_2O (30ml, 1658mmol) for three hours. The aqueous layer was removed and D_2O (0.5ml, 99.96% atom D, 28mmol) was added to the organic layer. The mixture was stirred for half an hour before the aqueous layer was removed. The organic layer was distilled. The first fraction was the azeotrope, 90°C (lit.[71] 92.7°C). The second fraction was colourless 1-butanol-*d* **65** (2ml, 20%), 110 - 115°C (lit.[72] 117 - 118°C).

^{1}H NMR (300MHz) δ 0.85, t *J* 7Hz, 3H (CH_3); 1.30, m, 2H (CH_2); 1.46, m, 2H (CH_2); 3.50, t *J* 7Hz, 2H (OCH_2).

m/z 75 ($M^{+\cdot}$, 35%), 74 ($(75\text{-}H)^+$, 63), 73 ($(75\text{-}D)^+$, 100).

c.f. *n*-BuOH m/z 74 ($M^{+\cdot}$ 51%), 73 ($(74\text{-}H)^+$, 100).

Reaction of the *dl*-isomer of Dimethyl 2,3-dibenzamidobutanedioate **39** in 1-Butanol-*d* **65** at 150°C

Ampoules containing the *dl*-isomer of dimethyl 2,3-dibenzamido-butanedioate **39** (approx. 0.8mg) and 1-BuOD **65** (250µl) were sealed then heated at 150°C in an oil bath. Samples were removed after 4, 12, 24 and 48 hours of heating. The solvent was removed, under reduced pressure, and the residue analysed by ^{1}H NMR spectroscopy and reverse phase HPLC (1,2 Dichloroethane-acetonitrile-water; 1 : 49 : 93), flow 1.5ml/min. Analysis of the HPLC traces showed four main products with retention times of 11.2, 13.4, 45.6 and 62.7 minutes. The components were isolated using reverse phase HPLC.

The component with the retention time of 11.2 minutes on the reverse phase HPLC column was identified as the *dl*-isomer of **dimethyl 2,3-dibenzamido-2,3-dideuteriobutanedioate (64)** by spectroscopic analysis.

^{1}H NMR (300MHz) δ 3.90, s (OCH_3); 5.33, d *J* 6Hz (residual α-CH); 7.1, br. s (NH); 7.43 - 7.82, m (ArH). Integration of the ^{1}H NMR spectrum showed a ratio of 1 : 26 for the α-CH and OCH_3 signals, indicating deuterium incorporation on the α-carbon.

m/z 386 ($M^{+\cdot}$, 4%), 368 ($(386-H_2O)^{+\cdot}$, 9), 236 (12),
194 ($C_6H_5CONHCHDCO_2CH_3^{+\cdot}$, 55), 193 ($(194-H)^+$, 16),
162 ($(194-CH_3OH)^{+\cdot}$, 15), 105 ($C_6H_5CO^+$, 100).

The component with the retention time of 13.4 minutes on the reverse phase HPLC column was identified as the *meso*-isomer of **dimethyl 2,3-dibenzamido-2,3-dideuteriobutanedioate (64)** by spectroscopic analysis.

^{1}H NMR (300MHz) δ 3.84, s (OCH_3); 5.35, d *J* 6Hz (residual α-CH); 7.47 - 7.93, m (ArH); 8.0, br. s (NH). Integration ratio of α-CH to OCH_3 signals was 1 : 11.

m/z 386 ($M^{+\cdot}$, 14%), 368 ((386-H_2O)$^{+\cdot}$, 17), 264 ((386-C_6H_5CONHD)$^{+\cdot}$, 17), 256 (22), 236 (24), 194 (($C_6H_5CONHCHDCO_2CH_3$)$^{+\cdot}$, 100), 193 ((194-H)$^+$, 71), 162 ((194-CH_3OH)$^{+\cdot}$, 79).

The component with the retention time of 45.6 minutes on the reverse phase HPLC column was identified as one diastereomer of **butyl methyl 2,3-dibenzamido-2,3-dideuteriobutanedioate (66)** by spectroscopic analysis.

^{1}H nmr (300MHz) δ 0.95, t *J* 7Hz (CH_3CCCO); 1.44, m (CCH_2CCO); 1.71, m ($CCCH_2CO$); 3.89, s (OCH_3); 4.28, m ($CCCCH_2O$); 5.32, m (residual α-CH); 7.1, br. s (NH); 7.42 - 7.80, m (ArH). The integration ratio of the α-CH to OCH_2 to OCH_3 signals was 0.8 : 2 : 3.

m/z 428 ($M^{+\cdot}$, 3%), 410 ((428-H_2O)$^{+\cdot}$, 3), 368 (6), 341 (6), 236 (8), 194 (($C_6H_5CONHCHDCO_2CH_3$)$^{+\cdot}$, 13), 162 ((194-CH_3OH)$^{+\cdot}$, 10), 137 (27), 105 ($C_6H_5CO^+$, 100).

The final component collected from the HPLC column, with a retention time of 62.7 minutes, was identified as the other diastereomer of **butyl methyl 2,3-dibenzamido-2,3-dideuteriobutanedioate (66)** by ^{1}H NMR analysis.

^{1}H NMR (300MHz) δ 0.92, t *J* 7Hz (CH_3CCCO); 1.4, m (CCH_2CCO); 3.83, s (OCH_3); 4.26, m ($CCCCH_2O$); 5.31, m (residual α-CH). Other NMR signals were swamped by a contaminant in the solvent.

The ratios of the components, by integration of the peak areas in the HPLC traces, with the retention times of 11.2, 13.4, 45.6 and 62.7 minutes on the reverse phase HPLC column, given as a percentage of the total peak area, were found to be:

t = 12 hours - 36 : 23 : 20 : 21.

t = 24 hours - 28 : 22 : 28 : 22.

t = 48 hours - 16 : 13 : 37 : 34.

N-Benzoyl-2,2-d_2-glycine Methyl Ester **67**

A mixture of glycine (1.02g, 13.6mmol), acetic anhydride (88ml, 933mmol) and D_2O (10ml, 553mmol) was heated at reflux for 10 minutes. A further portion of D_2O (10.8ml, 597mmol) was added and the solution was allowed to cool. The solvent was removed, under reduced pressure, and the residue was taken up in 6M HCl (50ml) and the resultant solution was heated at reflux for 90 minutes. The solvent was removed and the resultant residue was taken up in ethanol (50ml). The ethanol solution was treated with aniline (5ml, 55mmol) and allowed to stand overnight. The precipitated product was collected and washed with ethanol to give pale yellow 2,2-d_2-glycine (1.05g, 100%). The crude material was derivatised without further purification.

The 2,2-d_2-glycine was converted to methyl 2,2-d_2-glycinate hydrochloride, in 86% yield, using the method outlined for the conversion of glycine to methyl glycinate hydrochloride, prepared for use in the synthesis of the glycine derivative **56**.

To a solution of methyl 2,2-d_2-glycinate hydrochloride (1.47g, 11.5mmol) in water (40ml) was added $NaHCO_3$ (1.91g, 22.7mmol) then a solution of benzoyl chloride (1.3ml, 11.2mmol) in ethyl acetate (130ml). The resultant mixture was stirred at room temperature overnight. The organic layer was separated and washed with 10% NaOH (3 x 20ml), water (3 x 20ml) then dried ($MgSO_4$). The solvent was removed under reduced pressure to yield give a pale yellow solid (1.85g, 85%). The solid was recrystallised from ethyl acetate-hexane to yield **67** (1.65g, 76%), 82 - 82.5°C.

ν_{max} (cm^{-1}) 3290*m br* (NH), 1740*s* (C=O ester), 1640*m br* (C=O amide), 1610*m*, 1585*m*, 1550*s br* (trans NH), 1275*s br*, 1015*w*, 1000*m*, 920*w*, 725*m*, 705*m*.

^{1}H NMR (300MHz) δ 3.81, s, 3H (OCH_3); 4.25, m, 0.3H (residual CH); 6.7, br. s, 1H (NH); 7.42 - 7.84, m, 5H (ArH).

^{13}C NMR (50MHz) δ 42, small m (CD_2); 52.3 (OCH_3); 127.0, 128.5, 131.7, 133.6 (ArC); 167.5 (C=O amide); 170.4 (C=O ester).

m/z 195 ($M^{+\cdot}$, 14%), 162 ((195-CH_3OD)$^{+\cdot}$, 9), 136 ((195-CO_2CH_3)$^+$, 26), 105 ($C_6H_5CO^+$, 100), 77 ($C_6H_5^+$, 30), 51 ($C_4H_3^+$, 6).

Found d_2 74%, d_1 23%, H_2 3%.

Reverse phase HPLC (1,2 Dichloroethane-acetonitrile-water; 1 : 49 : 93), flow 1.5ml/min, t_R of 3.6 min.

Reaction of *N*-Benzoyl-2,2-*d*$_2$-glycine Methyl Ester **67** with DTBP **21**

A solution of DTBP **21** (6ml, 33mmol) and *N*-benzoyl-2,2-*d*$_2$-glycine methyl ester **67** (0.36g, 1.8mmol) in dry benzene (10ml) was deoxygenated (x 3, N_2) then irradiated with 3500 Å lamps in a Rayonet Photochemical Reactor for 41 hours. The reaction solution was concentrated to half of the original volume, under reduced pressure, and allowed to stand overnight. The solid which precipitated from the reaction mixture was collected and identified as the *dl*-isomer of the dimer **64** (8mg, 2%). The mother liquor was evaporated to dryness, under reduced pressure, and chromatography of the residue was carried out to yield the starting material **67** (124mg, 34%) and a mixture of the two diastereomers of the dimer **64** (74mg, 21%) as an oil. Preparative TLC (Ethyl acetate-1,2 dichloroethane; 1 : 9) on the oil, followed by crystallisation of the product fractions with ethyl acetate-hexane yielded the *dl*-isomer of **dimethyl 2,3-dibenzamido-2,3-dideuteriobutanedioate (64)** (7.8mg, 4% (total)), 217 - 218.5°C.

ν_{max} (cm^{-1}) 3250*m br* (NH), 1750*m* and 1735*s* (C=O ester), 1630*s* (C=O amide), 1600*w*, 1580*w*, 1535*s br* (trans NH), 1260*m br*, 1210*w*, 1035*m*, 695*m*.

^{1}H NMR (200MHz) δ 3.90, s, 6H (2 x OCH_3); 5.32, d *J* 6Hz, 0.2H (residual α-CH); 7.1, br. s, 2H (2 x NH); 7.43 - 7.82, m, 10H (ArH).

^{13}C NMR (75MHz) δ 53.4 (OCH_3); 127.2, 128.7, 132.1, 133.1 (ArC); 167.4 (C=O amide); 170.3 (C=O ester).

m/z 386 ($M^{+\cdot}$, 1%), 355 ($(386\text{-}OCH_3)^+$, 0.4), 327 ($(386\text{-}CO_2CH_3)^+$, 0.4), 264 ($(386\text{-}C_6H_5CONHD)^{+\cdot}$, 1), 194 ($C_6H_5CONHCHDCO_2CH_3^{+\cdot}$, 20), 162 ($(194\text{-}CH_3OH)^{+\cdot}$, 7), 105 ($C_6H_5CO^+$, 100), 77 ($C_6H_5^+$, 36), 51 ($C_4H_3^+$, 9).

Found m/z 386.14513. $C_{20}H_{18}D_2N_2O_6$ requires m/z 386.14469.

Found C, 62.17; H, 5.01; N, 7.17. $C_{20}H_{18}D_2N_2O_6$ requires C, 62.17; H, 4.70; N, 7.25.

Reverse phase HPLC (1,2 Dichloroethane-acetonitrile-water; 1 : 49 : 93), flow 1.5ml/min, t_R of 11.2 min.

Chiral phase HPLC (Isopropanol-1,2 dichloroethane-hexane; 10.4 : 2 : 19), flow 1ml/min, t_R 13.5, 16.2 min.

and the *meso*-isomer of **dimethyl 2,3-dibenzamido-2,3-dideuteriobutane-dioate (64)** (4.5mg, 1%), 178.5 - 181.5°C.

^{1}H NMR (200MHz) δ 3.84, s, 6H (2 x OCH_3); 7.48 - 793, m, 10H (ArH); 8.0, br. s, 2H (2 x NH).

^{13}C NMR (75Mz) δ 53.2 (OCH_3); 127.4, 128.7, 132.2, 132.9 (ArC); 168.3 (C=O amide); 169.1 (C=O ester).

m/z 386 ($M^{+\cdot}$, 2%), 355 ($(386\text{-}OCH_3)^+$, 0.4), 327 ($(386\text{-}CO_2CH_3)^+$, 0.7), 264 ($(386\text{-}C_6H_5CONHD)^{+\cdot}$, 1), 194 ($C_6H_5CONHCHDCO_2CH_3^{+\cdot}$, 23), 162 ($(194\text{-}CH_3OH)^{+\cdot}$, 8), 105 ($C_6H_5CO^+$, 100), 77 ($C_6H_5^+$, 36), 51 ($C_4H_3^+$, 8).

Found m/z 386.14365. $C_{20}H_{18}D_2N_2O_6$ requires m/z 386.14469.

Reverse phase HPLC (1,2 Dichloroethane-acetonitrile-water; 1 : 49 : 93), flow 1.5ml/min, t_R of 13.4 min.

Chiral phase HPLC (Isopropanol-1,2 dichloroethane-hexane; 10.4 : 2 : 19), flow 1ml/min, t_R 12.1 min.

Reverse phase HPLC analysis (1,2 Dichloroethane-acetonitrile-water; 1 : 49 : 93), flow 1.5ml/min, of an aliquot of the reaction mixture taken after 23 hours of irradiation, showed the product ratios to be 76 : 6 : 9 : 9% for the starting material **67**, a compound with the same retention time as for the alanine derivative **26** and the *dl*- and *meso*-isomers of the dimer **64**.

Dimethyl 2,3-dibenzamido-2,3-dideuteriobutanedioate **64** in 1,2,4-Trichlorobenzene

Stock solutions *dl*-isomer of the dimer **64** : 2.3mg in 25ml.

meso-isomer of the dimer **64** : 1.6mg in 25ml.

Stock solutions were filtered through 0.45μm filters.

Dimethyl 2,3-dibenzamido-2,3-dideuteriobutanedioate **64** in 1,2,4-Trichlorobenzene at 214°C

Ampoules containing 500μl of stock were heated at 214.5 ± 0.7°C. Each of the dried samples was taken up in 500μl of a solution of the HPLC running solvent, then 100μl was loaded onto the reverse phase HPLC column.

Table 16 - Reactions of the diastereomers of the dimer **64** in 1,2,4-trichlorobenzene at 214°C.

	time (min)				
	0	15	30	45	60
% *dl*-**64** / dimer **64** [a]	100	84	77	75	60
dimer **64** / ext. std. [b]	100	102	109	105	107
% *meso*-**64** / dimer **64** [a]	99	89	83	79	72
dimer **64** / ext. std. [b]	100	100	98	100	95

Table 16 cont.

	time (min)			
	75	90	105	120
% *dl*-**64** / dimer **64**	58	54	50	49
dimer **64** / ext. std.	107	105	109	109
% *meso*-**64** / dimer **64**	69	69		
dimer **64** / ext. std.	94	94		

a: Percentage of one isomer of the dimer **64** in the total *dl*- and *meso*-mixture. b: Percentage of one isomer of the dimer **64** remaining with time measured with respect to the external standard. The reproducibility of the signal for the external standard varied by ±6%.

The equilibrium mixture was established from a sample heated for 4 hours, using reverse phase HPLC analysis, to be 43 : 57% for the *dl*- and

meso-isomers. The data shown in Table 16 was plotted as the log of each diastereomer of the dimer **64**, in excess of the equilibrium mixture, remaining with time (Graph 7, p 70). The equations of the lines of best fit, calculated by the Cricketgraph program, were:

$x = 238.18 - 117.29y$ ($R^2 = 0.981$) and $x = 225.22 - 108.31y$ ($R^2 = 0.933$)

for the *dl*- and *meso*-isomers, respectively, where x represents time in minutes and y represents the log of the amount of unreacted dimer remaining. The first half lives were calculated using the equations (y = log 50) and the errors were calculated using the correlation values given with each equation. The first half lives occur at: 38.9 ± 0.7 mins and 41.2 ± 2.8 mins for the *dl*- and *meso*-isomers, respectively. The rate constants calculated from the half lives, using the equation $k = - \ln 0.5 / (t_{1/2})$, are shown on page 71.

<u>*N*-Benzoyl-(2*S*)-alanine Methyl Ester **71**</u>

N-Benzoyl-(2*S*)-alanine methyl ester **71** was prepared from methyl (2*S*)-alaninate hydrochloride (1.68g, 12mmol), $NaHCO_3$ (2.01g, 23.9mmol) and benzoyl chloride (1.3ml, 11.1mmol) by the method used for the preparation of *N*-benzoyl-2,2-d_2-glycine methyl ester **67** from 2,2-d_2-glycine. The crude product was crystallised from ethyl acetate-hexane to yield **71** as colourless crystals (2.01g, 87%), 56 - 57.5°C (lit.[73] 56.5 - 57.5°C).

ν_{max} (cm^{-1}) 3325*m br* (NH), 1765*s* and 1745*s* (C=O ester), 1645*s br* (C=O amide), 1610*w*, 1858*w*, 1545*s br* (trans NH), 1210*s*, 1170*s br*, 715*s*, 700*m*.

^1H NMR (300MHz) δ 1.53, d *J* 7Hz, 3H (α-CH_3); 3.80, s, 3H (OCH_3); 4.82, dq *J* 7, 7Hz, 1H (CH); 6.8, br. d *J* 7Hz, 1H (NH); 7.42 - 7.83, m, 5H (ArH).

m/z 207 ($M^{+\cdot}$, 8%), 148 ((207-CO_2CH_3)$^+$, 86), 105 ($C_6H_5CO^+$, 100), 77 ($C_6H_5^+$, 16).

Chiral phase HPLC (Isopropanol-dichloroethane-hexane; 1 : 2 : 19),

flow 1ml/min, t_R = 22.5min.

N-Benzoylvaline Methyl Ester **27**

N-Benzoylvaline methyl ester **27** was prepared from *N*-benzoylvaline (0.58g, 2.6mmol) and thionyl chloride (1ml, 14mmol) by the method used for the preparation of *N*-benzoylglycine methyl ester **25**. The crude product crystallised from the reaction solution to yield **27** as a colourless powder (0.61g, 100%), 89.5 - 90.5°C (lit.[74] 86°C).

ν_{max} (cm^{-1}) 3350*s* (NH), 1740*s* (C=O ester), 1660*s* (C=O amide), 1610*w*, 1585*w*, 1535*s br* (trans NH), 1210*s*, 1160*m*, 995*w*, 755*m*, 720*w*, 715*m*, 690*w*.

^{1}H NMR (200MHz) δ 0.99, d *J* 7Hz and 1.01, d *J* 7Hz, 6H (2 x CCH_3); 2.28, m, 1H (β-CH); 3.78, s, 3H (OCH_3); 4.79, dd *J* 5,9Hz, 1H (α-CH); 6.6, br. d *J* 9Hz, 1H (NH); 7.40 - 7.84, m, 5H (ArH).

m/z 235 ($M^{+\cdot}$, 1%), 193 ($C_6H_5CONHCH_2CO_2CH_3^{+\cdot}$, 5), 176 ($(235\text{-}CO_2CH_3)^+$, 38), 161 ($(193\text{-}MeOH)^{+\cdot}$, 5), 122 ($C_6H_5CONH_3^+$, 18), 105 ($C_6H_5CO^+$, 100), 77 ($C_6H_5^+$, 23), 51 ($C_4H_3^+$, 4).

Chiral phase HPLC (Isopropanol-1,2 dichloroethane-hexane; 1 : 2 : 19), flow 1ml/min, t_R = 11.9, 12.9 min.

N-Benzoyl-(2*S*)-valine Methyl Ester **72**

N-Benzoyl-(2*S*)-valine methyl ester **72** was prepared from (2*S*)-valine methyl ester hydrochloride (0.82g, 4.9mmol), $NaHCO_3$ (0.83g, 9.9mmol) and benzoyl chloride (0.5ml, 4.3mmol) by the method used for the preparation of *N*-benzoyl-2,2-d_2-glycine methyl ester **67** from 2,2-d_2-glycine. The crude product was crystallised from ethyl acetate-hexane to yield **72** as colourless crystals (0.92g, 91%), 112 - 112.5°C (lit.[75] 113 - 114°C).

ν_{max} (cm^{-1}) 3350*s* (NH), 1740*s* (C=O ester), 1640*s* (C=O amide), 1605*w*, 1580*w*,1520*s* (trans NH), 1205*m*, 1155*m*, 1000*w*, 750*w*, 735*m*, 720*w*, 695*m*.

^{1}H NMR (300MHz) δ 0.99, d *J* 7Hz and 1.02, d *J* 7Hz, 6H (2 x CCH_3); 2.29, m, 1H (β-CH); 3.78, s, 3H (OCH_3); 4.80, dd *J* 5, 9Hz, 1H (α-CH); 6.6, br. d *J* 9Hz, 1H (NH); 7.43 - 7.83, m, 5H (ArH).

m/z 235 ($M^{+\cdot}$, 1%), 193 ($C_6H_5CONHCH_2CO_2CH_3^{+\cdot}$,5), 176 ($(235\text{-}CO_2CH_3)^+$, 38), 161 ($(193\text{-}MeOH)^{+\cdot}$, 5), 122 ($C_6H_5CONH_3^+$, 18), 105 ($C_6H_5CO^+$, 100), 77 ($C_6H_5^+$, 23), 51 ($C_4H_3^+$, 4).

Chiral phase HPLC (Isopropanol-1,2 dichloroethane-hexane; 1 : 2 : 19), flow 1ml/min, t_R = 12.9 min.

N-Benzoyl-(2*S*)-alanine Methyl Ester **71** in 1,2,4-Trichlorobenzene

A solution of *N*-Benzoyl-(2*S*)-alanine methyl ester **71** (0.7mg) in 1,2,4-trichlorobenzene (1ml) was heated at reflux for 4 days. The solvent was removed, under reduced pressure, and the residue analysed by chiral phase HPLC (Isopropanol-1,2 dichloroethane-hexane; 1 : 2 : 19), flow 1ml/min. At t=0 only the protected *S*-alanine **71** was detected by UV absorption (λ = 254 nm), but after 4 days 8% of the *R*-isomer was evident. Of the initial amount of the alanine derivative **71** only 19% remained after 4 days.

N-Benzoyl-(2*S*)-valine Methyl Ester **72** in 1,2,4-Trichlorobenzene

A solution of *N*-Benzoyl-(2*S*)-valine methyl ester **72** (0.9mg) in 1,2,4-trichlorobenzene (1ml) was heated at reflux for 5 days. The solvent was removed, under reduced pressure, and the residue analysed by chiral phase HPLC (Isopropanol-1,2 dichloroethane-hexane; 1 : 2 : 19), flow 1ml/min. At t=0 only the protected *S*-valine **72** was detected, but after 5 days 3% of the

R-isomer was evident. Of the initial amount of the valine derivative **72**, 80% remained after 5 days.

Pentafluorobenzoyl Chloride **73**

A solution of pentafluorobenzoic acid (4.05g, 19mmol) in thionyl chloride (45ml, 617mmol) was heated at reflux for 17 hours. The cooled solution was evaporated to dryness, under reduced pressure, to give a yellow liquid (3.63g, 82%). The liquid was distilled to yield **73** as a colourless liquid (3.27g, 74%), 120°C (lit.[75] 158 - 159°C).

ν_{max} (cm^{-1}) 1790*s br* (C=O), 1660*m*, 1510*s br*, 1430*m*, 1335*s*, 1155*s br*, 1020 and 1000*s br*, 820*s*, 770*s*, 735*s*.

N-Pentafluorobenzoylglycine Methyl Ester **74**

To a solution of sat. aqueous $NaHCO_3$ (10ml) was added methyl glycinate hydrochloride (1.02g, 8.1mmol) then a solution of pentafluorobenzoyl chloride **73** (1.58g, 6.9mmol) in ethyl acetate (60ml). The resultant mixture was allowed to stir at room temperature overnight. The organic layer was washed twice with 10% HCl, three times with water and then dried ($MgSO_4$). The solvent was evaporated to dryness, under reduced pressure, to give a white solid (1.92g, 99%). The crude product was crystallised from ethyl acetate-hexane to yield **74** as a colourless crystalline solid (83%), 121.5 - 122.5°C.

ν_{max} (cm^{-1}) 3325*s* (NH), 1760*s* (C=O ester), 1680*s br* (C=O amide), 1580*s*, 1540*s*, 1520*s*, 1235*s*, 1100*m*, 1010*m br*, 990*s*, 785*m*.

^1H NMR (300MHz) δ 3.81, s, 3H (OCH_3); 4.25, d *J* 5Hz, 2H (CH); 6.8, unresolved d, 1H (NH).

^{13}C NMR (50MHz) δ 41.7 (CH_2); 52.6 (OCH_3); 157.6 (C=O amide); 169.4 (C=O ester). ArC did not show due to their long relaxation times.

m/z 283 ($M^{+\cdot}$, 3%), 251 ($(283\text{-}CH_3OH)^{+\cdot}$, 3), 224 ($(283\text{-}CO_2CH_3)^+$, 28), 195 ($C_6F_5CO^+$, 100), 167 ($C_6F_5^+$, 15), 117 (10).

Reverse phase HPLC (1,2 Dichloroethane-acetonitrile-water; 1 : 49 : 93), flow 1.5ml/min, t_R of 9.0 min.

Reaction of *N*-Pentafluorobenzoylglycine Methyl Ester **74** with DTBP **21**

A solution of *N*-pentafluorobenzoylglycine methyl ester **74** (1.01g, 3.6mmol) and DTBP **21** (3ml, 16.3mmol) in benzene (27ml) was deoxygenated (x 3, N_2) and irradiated with 3500 Å lamps for 109 hours. The yellow solution was evaporated to dryness, using reduced pressure, to yield an oil (1.38g). Chromatography of the oil yielded biphenyl **51** (59mg, 1% based on DTBP **21**), *N*-pentafluorobenzoylalanine methyl ester **76** (65mg, 6%), the *dl*-isomer of dimethyl 2,3-dipentafluorobenzamidobutanedioate **75** (75mg, 7%), *N*-pentafluorobenzoylglycine methyl ester **75** (150mg, 1.5%) and the *meso*-isomer of dimethyl 2,3-dipentafluorobenzamidobutanedioate **75** (35mg, 3%). The *dl*-isomer of **dimethyl 2,3-dipentafluorobenzamidobutanedioate (75)** was crystallised from ethyl acetate-hexane to yield the *dl*-isomer of **75** as a white solid (26mg, 2.5%), 219 - 221°C.

ν_{max} (cm^{-1}) 3275 and 3250*m* (NH), 1755 and 1745*m* (C=O ester), 1665*s br* (C=O amide), 1560 and 1550*m* (trans amide NH), 1500*s br*, 1225*m br*, 1100*w*, 1090*w*, 990*m br*, 965*w*, 720*w*.

^1H NMR (300MHz) δ 3.91, s, 6H (2 x OCH_3); 5.34, d *J* 7Hz, 2H (2 x CH); 6.9, br. d *J* 7Hz, 2H (2 x NH).

m/z 564 ($M^{+\cdot}$, 0.4%), 505 ($(564\text{-}CO_2CH_3)^+$, 1), 473 ($(505\text{-}CH_3OH)^+$, 5), 353 ($(564\text{-}C_6F_5CONH_2)^{+\cdot}$, 0.3), 283 ($C_6F_5CONHCH_2CO_2CH_3^{+\cdot}$, 26), 251 ($(283\text{-}CH_3OH)^{+\cdot}$, 18), 195 ($C_6F_5CO^{+\cdot}$, 100), 167 ($C_6F_5^{+\cdot}$, 15).

Found m/z 564.03921. $C_{20}H_{10}F_{10}N_2O_6$ requires m/z 564.03792.

Found C, 42.56; H, 1.74; N, 4.94. $C_{20}H_{10}F_{10}N_2O_6$ requires C, 42.57; H, 1.79; N, 4.96.

Reverse phase HPLC (1,2 Dichloroethane-acetonitrile-water; 1 : 49 : 93), flow 1.5ml/min, t_R of 94 min.

Chiral phase HPLC (Isopropanol-1,2 dichloroethane-hexane; 1 : 2 : 19), flow 1ml/min, t_R 23.6, 25.1 min.

The *meso*-isomer of **dimethyl 2,3-dipentafluorobenzamidobutanedioate** (75) was crystallised from ethyl acetate-hexane to give the *meso*-isomer of **75** as a white solid (13mg, 1%), 241 - 246°C.

ν_{max} (cm^{-1}) 3250*s* (NH), 1740*s* (C=O ester), 1660*s* (C=O amide), 1540*m* (trans amide NH), 1520*m*, 1350*m*, 1245*w br*, 1180*w*, 1090*w*, 990*w br*, 780*w*.

^1H NMR (300MHz) δ 3.88, s, 6H (2 x OCH_3); 5.40, d *J* 7Hz, 2H (2 x CH); 7.5, br. d *J* 7Hz, 2H (2 x NH).

m/z 564 ($M^{+\cdot}$, 0.5%), 505 ((564-CO_2CH_3)$^+$, 2), 473 ((505-MeOH)$^+$, 7), 353 ((564-$C_6F_5CONH_2$)$^{+\cdot}$, 0.6), 283 ($C_6F_5CONHCH_2CO_2CH_3^{+\cdot}$, 36), 282 ((283-H)$^+$, 18), 251 ((283-MeOH)$^{+\cdot}$, 24), 195 ($C_6F_5CO^{+\cdot}$, 100), 167 ($C_6F_5^{+\cdot}$, 13).

Found m/z 564.03817. $C_{20}H_{10}F_{10}N_2O_6$ requires 564.03792.

Found C, 42.79; H, 1.45; N, 4.89. $C_{20}H_{10}F_{10}N_2O_6$ requires C, 42.57; H, 1.79; N, 4.96.

Reverse phase HPLC (1,2 Dichloroethane-acetonitrile-water; 1 : 49 : 93), flow 1.5ml/min, t_R of 87 min.

Chiral phase HPLC (Isopropanol-1,2 dichloroethane-hexane; 1 : 2 : 19), flow 1ml/min, t_R 22.9 min.

Reverse phase HPLC analysis (1,2 Dichloroethane-acetonitrile-water; 1 : 49 : 93), flow 1.5ml/min, of an aliquot of the reaction mixture taken after 23 hours of irradiation, showed the product ratios to be 55 : 5 : 21 : 19% for the starting material **74**, the alanine derivative **76** and the *dl*- and *meso*-isomers of the dimer **75**.

N-Pentafluorobenzoylalanine Methyl Ester **76**

N-Pentafluorobenzoylalanine methyl ester **76** was prepared from pentafluorobenzoyl chloride (1.64g, 7.1mmol) and methyl alaninate hydrochloride (1.12g, 8mmol) using the procedure outlined for the preparation of *N*-pentafluorobenzoylglycine methyl ester **74**. The crude product (0.99g, 47%) was crystallised from ethyl acetate-hexane to yield **76** as a colourless crystalline solid (40%), 94 - 95°C.

ν_{max} (cm^{-1}) 3300*s* (NH), 1735*s* (C=O ester), 1655*s br* (C=O amide), 1515*s br*, 1500*s br*, 1380*s*, 1330*s*, 1230*s br*, 1105*s*, 990*s br*, 960*s*, 865*m*, 775*m*.

^{1}H NMR (200MHz) δ 1.53, d *J* 7Hz, 3H (α-CH_3); 3.80, s, 3H (OCH_3); 4.77, dq *J* 7, 7Hz, 1H (CH); 6.8, br. d *J* 7Hz, 1H (NH).

^{13}C NMR (50MHz) δ 18.3 (α-CH_3); 48.9 (CH); 52.8 (OCH_3); 156.8 (C=O amide); 172.6 (C=O ester). ArC do not show due to long relaxation times.

m/z 297 ($M^{+\cdot}$, 3%), 266 ($(297\text{-}OCH_3)^+$, 3), 238 ($(297\text{-}CO_2CH_3)^+$, 99), 195 ($C_6F_5CO^+$, 100), 167 ($C_6F_5^+$, 29), 148 ($(167\text{-}F)^{+\cdot}$, 4), 117 ($(167\text{-}CF_2)^+$, 13).

Reverse phase HPLC (1,2 Dichloroethane-acetonitrile-water; 1 : 49 : 93), flow 1.5ml/min, t_R of 12.5 min.

Dimethyl 2,3-dipentafluorobenzamidobutanedioate **75** in 1,2,4-Trichlorobenzene

Stock solutions *dl*-isomer of the dimer **75** : 2.2mg in 25ml.

meso-isomer of the dimer **75** : 2.5mg in 25ml.

Stock solutions were filtered through 0.45μm filters.

Dimethyl 2,3-dipentafluorobenzamidobutanedioate **75** in 1,2,4-Trichlorobenzene at 214°C

Ampoules containing 500μl of stock were heated at 213.8 ± 0.8°C. Each of the dried samples was taken up in 400μl of a solution of HPLC running solvent (Isopropanol-water; 7 : 13) that contained benzanilide (0.1mg/100ml), then 100μl was loaded onto the reverse phase HPLC column. The flow rate of the HPLC solvent through the reverse phase column was 1.0ml/min, giving the external standard and the *dl*- and *meso*-isomers of the dimer **75** retention times of 7.0, 26.4 and 20.3 min, respectively. Detection of the compounds was by UV absorption (λ = 254 nm).

Table 17 - Reactions of the diastereomers of the dimer **75** in 1,2,4-trichlorobenzene at 214°C.

	time (min)					
	0	7.5	15	22.5	30	37.5
% *dl*-**75** / dimer **75** [a]	100	96	100	97	92	98
dimer **75** / ext. std. [b]	100	-	116	-	-	108
% *meso*-**75** / dimer **75** [a]	100	100	100	100	100	100
dimer **75** / ext. std. [b]	100	51	59	-	-	56

Table 17 cont.

	time (min)					
	45	60	90	120	150	180
% *dl*-**75** / dimer **75**	94	94	88	89	82	80
dimer **75** / ext. std.	92	97	113	136	126	-
% *meso*-**75** / dimer **75**	100	100	90	86	90	77
dimer **75** / ext. std.	-	51	-	75	83	86

a: Percentage of one isomer of the dimer **75** in the total *dl*- and *meso*-mixture.
b: Percentage of one isomer of the dimer **75** remaining with time measured with respect to the external standard. The reproducibility of the signal for the external standard varied by ±1%.

The equilibrium mixture was established from a sample heated for 48 hrs, using reverse phase HPLC analysis, to be 68 : 32% for the *dl*- and *meso*-isomers. The data shown in Table 17 was plotted as the log of the percentage of each diastereomer of the dimer **75** in excess of the equilibrium mixture remaining with time (Graph 8, p 78). The equations of the lines of best fit, calculated by the Cricketgraph program, were:

$x = 825.86 - 408.70y$ ($R^2 = 0.908$) and $x = 1887.9 - 928.54y$ ($R^2 = 0.836$)

for the *dl*- and *meso*-isomers, respectively, where x represents time in minutes and y represents the log of the percentage of unreacted dimer. The first half lives were calculated using the equations (y = log 50) and the errors were calculated using the correlation values given with each equation. The first half lives occur at: 131.5 ± 12.1 mins and 310.3 ± 50.9 mins for the *dl*- and *meso*-isomers, respectively. The rate constants calculated from the half lives, using the equation $k = - \ln 0.5 / (t_{1/2})$, are shown on page 79.

References

1. Gordy W., Ard W. B., Shields H., *Proc. Natl. Acad. Sci. U.S.* **41**, 983 (1955).

2. Gordy W., Shields H., *Radiation Research* **9**, 611 (1958).

3. Henriksen T., Melø T. B., Saxebøl G., In *Free Radicals in Biology*, Ed. Pryor W. A.; Academic Press, New York Vol. **2**, p. 213 (1976).

4. Kurita Y., Gordy W., *J. Chem. Phys.* **34**, 282 (1961).

5. Miyagawa I., Kurita Y., Gordy W., *J. Chem. Phys.* **33**, 1599 (1960).

6. Katayama M., Gordy W., *J. Chem. Phys.* **35**, 117 (1961).

7. Drew R. C., Gordy W., *Radiation Research* **18**, 552 (1963).

8. Henriksen T., Sanner T., Pihl A., *Radiation Research* **18**, 147 (1963).

9. Elad D., Sperling J., *J. Chem. Soc. (C)*, 1579 (1969).

10. Elad D., Schwarzberg M., Sperling J., *J. Chem. Soc. Chem. Commun.*, 617 (1970).

11. Elad D., Sperling J., *J. Am. Chem. Soc.* **93**, 967 (1971).

12. Elad D., Sperling J., *J. Am. Chem. Soc.* **93**, 3839 (1971).

13. Elad D., Schwartzberg M., Sperling J., *J. Am. Chem. Soc.* **95**, 6418 (1973).

14. a. Viehe H. G., Merényi R., Stella L., Janousek Z., *Angew. Chem. Int. Ed. Eng.* **17**, 691 (1978). b. Viehe H. G., Merényi R., Stella L., Janousek Z., *Angew. Chem. Int. Ed. Eng.* **18**, 917 (1979). c. Viehe H. G., Janousek Z., Merényi R., Stella L., *Acc. Chem. Res.* **18**, 148 (1985).

15. Dewar M. J. S., *J. Am. Chem. Soc.* **74**, 3353 (1952).

16. a. Negoita N., Baican R., Balaban A. T., *Tetrahedron Lett.*, 1877 (1973). b. Balaban A. T., Istratoiu R., *Tetrahedron Lett.*, 1879 (1973). c. Balaban A. T., Caprois M. T., Negoita N., Baican R., *Tetrahedron* **33**, 2249 (1977).

17. a. Baldock R. W., Hudson P., Katritzky A. R., *Heterocycles* **1**, 67 (1973). b. Baldock R. W., Hudson P., Katritzky A. R., *J. Chem. Soc., Perkin Trans. I*, 1422 (1974). c. Katritzky A. R., Soti F., *J. Chem. Soc., Perkin Trans. I*, 1427 (1974).

18. For a review see "The Captodative Effect", Sustmann R., Korth H., *Adv. Phys. Org. Chem.* **26**, 131 (1990).

19. Katritzky A. R., Zerner M. C., Karelson M. M., *J. Am. Chem. Soc.* **108**, 7213 (1986).

20. Birkhofer H., Hädrich J., Beckhaus H.-D., Rüchardt C., *Angew. Chem. Int. Ed. Eng.* **26**, 573 (1987).

21. Beckhaus H.-D., Rüchardt C., *Angew. Chem. Int. Ed. Eng.* **26**, 770 (1987).

22. Burgess V. A., Easton C. J., Hay M. P., *J. Am. Chem. Soc.* **111**, 1047 (1989).

23. Adam J., Gosselain P. A., Goldfinger P., *Nature* **171**, 704 (1953).

24. Pearson R. E., Martin J. C., *J. Am. Chem. Soc.* **85**, 354 (1963).

25. Pearson R. E., Martin J. C., *J. Am. Chem. Soc.* **85**, 3142 (1963).

26. Russell G. A., In *Free Radicals*, Ed. Kochi J. K.; Wiley, New York Vol. **1**, p. 275 (1973).

27. Hay J. M., *Reactive Free Radicals*; Academic Press, New York, p.66 (1974).

28. Easton C. J., Hutton C. A., Rositano G., Tan E. W., *J. Org. Chem.* **56**, 5614 (1991).

29. Rüchardt C., *Top. Curr. Chem.* **88**, 1 (1980).

30. Rüchardt C., Beckhaus H.-D., *Angew. Chem. Int. Ed. Eng.* **24**, 529 (1985).

31. Beckhaus H.-D., Rüchardt C., *Top. Curr. Chem.* **130**, 1 (1986).

32. Koch T. H., Olesen J. A., DeNiro J., *J. Am. Chem. Soc.* **97**, 7285 (1975).

33. Egger K. W., Cooks A. T., *Helv. Chim. Acta* **56**, 1516, 1537 (1973).

34. Olson J. B., Koch T. H., *J. Am. Chem. Soc.* **108**, 756 (1986).

35. Haltiwanger R. C., Koch T. H., Olesen J. A., Kim C. S., Kim N. K., *J. Am. Chem. Soc.* **99**, 6327 (1977).

36. Peterson I., *J. Am. Chem. Soc.* **89**, 2677 (1967).

37. Bennett R. W., Wharry D. L., Koch T. H., *J. Am. Chem. Soc.* **102**, 2345 (1980).

38. Schulze R., Beckhaus H.-D., Rüchardt C., *Chem. Ber.* **126**, 1031 (1993).

39. Kleyer D. L., Haltiwanger R. C., Koch T. H., *J. Org. Chem.* **48**, 147 (1983).

40. Benson Jr. O., Demirdji S. H., Haltiwanger R. C., Koch T. H., *J. Am. Chem. Soc.* **113**, 8879 (1991).

41. Rüchardt C., Beckhaus H.-D., *Angew. Chem. Int. Ed. Engl.* **19**, 429 (1980).

42. Burgess V. A., Easton C. J., Hay M. P., Steel P. J., *Aust J. Chem.* **41**, 701 (1988).

43. Obata N., Niimura K., *J. Chem. Soc. Chem. Comm.*, 239 (1979).

44. Sykes P., *A guidebook to Mechanism In Organic Chemistry*, Fifth Edition; Longman Inc., New York, p. 321 (1981).

45. March J., *Advanced Organic Chemistry*, Third Edition; Wiley-Interscience, New York, p. 220 (1985).

46. Bartell L. S., Higginbotham H. K., *J. Chem. Phys.* **42**, 851 (1965).

47. Kharasch M. S., Zimmerman M., Zimmit W., Nudenberg W., *J. Org. Chem.* **18**, 1045 (1953).

48. Walling C., Wagner P. J., *J. Am. Chem. Soc.* **86**, 3368 (1964).

49. Avila D. V., Brown C. E., Ingold K. U., Lusztyk J., *J. Am. Chem. Soc.* **115**, 466 (1993).

50. Richards P. H., McBain J. W., *J. Am. Chem. Soc.* **70**, 1336 (1948).

51. March J., *Advanced Organic Chemistry*, Third Edition; Wiley-Interscience, New York, p. 528 (1985).

52. Birnbaum S. M., Levintow L., Kingsley R. B., Greenstein J. P., *J. Biol. Chem.* **194**, 455 (1952).

53. Nostrand V., *Isotope Effects in Chemical Reactions*, Ed. Collins, Bowman; ACS Monograph **167** (1970).

54. Bada J. L., *J. Am. Chem. Soc.* **94**, 1371 (1972).

55. Kemp D. S., In *The Peptides - Analysis, Synthesis, Biology*, Ed. Gross E., Meienhofer J.; Academic Press Inc., New York, p. 315 (1979).

56. Smith G. G., Reddy G. V., *J. Org. Chem.* **54**, 4529 (1989).

57. Gaetjens E., Morawetz H., *J. Am. Chem. Soc.* **82**, 5323 (1960).

58. Smith G. G., Williams K. M., Wonnacott D. M., *J. Org. Chem.* **43**, 1 (1978).

59. *The Merck Index of Chemicals and Drugs*, Tenth Edition, Ed. Windholz M.; Merck & Co., Inc., New Jersey, p. 396 (1983).

60. Pirkle W. H., Pochapsky T. C., *Advances in Chromatography* **27**, 73 (1987).

61. Harwood L. M., *Aldrichimica Acta* **18**, 25 (1985).

62. Still W. C., Kahn M., Mitra A., *J. Org. Chem.* **43**, 2923 (1978).

63. *Purification of Laboratory Chemicals*, Third Edition, Ed. Perrin D. D., Armarego W. L. F.; Pergamon Press Ltd., (1988).

64. Huang H. T., Niemann C. J., *J. Am. Chem. Soc.* **74**, 4634 (1952).

65. Faifermann I., Hoffmann E., *J. Org. Chem.* **29**, 748 (1964).

66. Hay M. P., Ph.D. thesis, University of Canterbury, New Zealand.

67. *The Merck Index of Chemicals and Drugs*, Tenth Edition, Ed. Windholz M.; Merck & Co., Inc., New Jersey, p. 485 (1983).

68. *Beilstein* **1**, 492.

69. Castagnoli N. Jr., Holden K., Rapoport H., *J. Org. Chem.* **29**, 883 (1964).

70. Itoh M., Hagiwara D., Kamiya T., *Tetrahedron Lett.*, 4393 (1975).

71. *CRC Handbook of Chemistry and Physics*, Ed. Weast R. C.; CRC Press, Inc., Florida **67**, D-12 (1986).

72. *The Merck Index of Chemicals and Drugs*, Tenth Edition, Ed. Windholz M.; Merck & Co., Inc., New Jersey, p. 214 (1983).

73. Hein G. E., Niemann C. J., *J. Am. Chem. Soc.* **84**, 4487 (1962).

74. Harada K., Ohhashi B. M., *Bull. Chem. Soc. Jpn.* **39**, 2287 (1966).

75. Dean B. M., Mijovic M. P. V., Walker J., *J. Chem. Soc.*, 3394 (1961).

76. *Aldrich Australian Chemical Catalog*, p. 972 (1992).

Appendix

Crystal Structure of the

meso-isomer of Dimethyl 2,3-Dibenzamidobutanedioate **39**

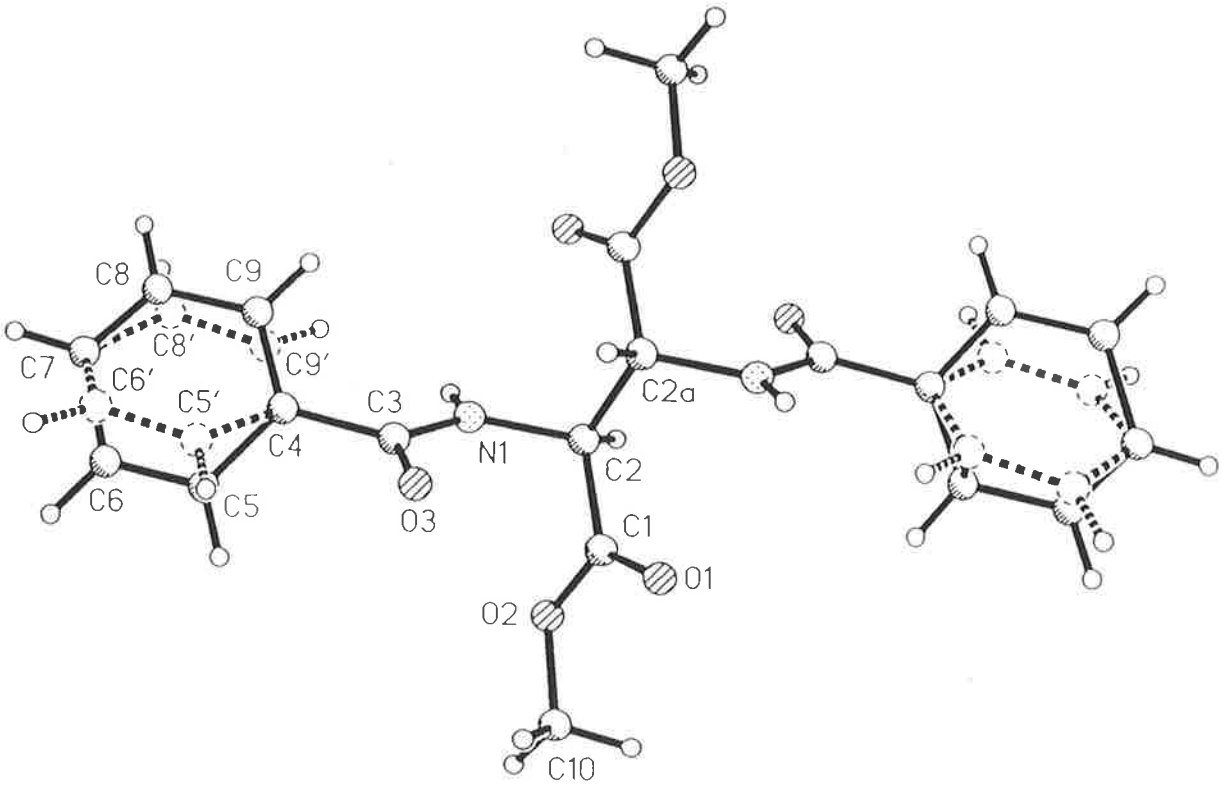

Bond Distances (Å) and Angles (°) for the

meso-isomer of Dimethyl 2,3-Dibenzamidobutanedioate **39**

O(1)-C(1)	1.199(4)	O(2)-C(1)	1.341(4)	O(2)-C(10)	1.441(4)
O(3)-C(3)	1.228(3)	N(1)-C(3)	1.328(4)	N(1)-C(2)	1.458(4)
C(1)-C(2)	1.516(4)	C(2)-C(2a)[a]	1.526(6)	C(3)-C(4)	1.495(4)
C(4)-C(9)	1.369(6)	C(4)-C(5')	1.371(6)	C(4)-C(5)	1.396(5)
C(4)-C(9')	1.399(6)	C(5)-C(6)	1.379(6)	C(6)-C(7)	1.432(6)
C(5')-C(6')	1.372(6)	C(6')-C(7)	1.345(6)	C(7)-C(8)	1.330(6)
C(7)-C(8')	1.388(7)	C(8)-C(9)	1.377(6)	C(8')-C(9')	1.389(7)

C(1)-O(2)-C(10)	115.0(3)	C(3)-N(1)-C(2)	122.3(3)
O(1)-C(1)-O(2)	123.6(3)	O(1)-C(1)-C(2)	127.3(3)
O(2)-C(1)-C(2)	109.0(3)	N(1)-C(2)-C(1)	110.9(2)
N(1)-C(2)-C(2a)[a]	111.3(3)	C(1)-C(2)-C(2a)[a]	112.2(3)
O(3)-C(3)-N(1)	121.2(3)	O(3)-C(3)-C(4)	121.2(3)
N(1)-C(3)-C(4)	117.5(3)	C(9)-C(4)-C(5)	119.5(4)
C(5')-C(4)-C(9')	118.1(5)	C(9)-C(4)-C(3)	122.8(4)
C(5')-C(4)-C(3)	119.9(3)	C(5)-C(4)-C(3)	117.7(3)
C(9')-C(4)-C(3)	121.9(4)	C(6)-C(5)-C(4)	118.7(5)
C(5)-C(6)-C(7)	119.8(5)	C(4)-C(5')-C(6')	122.8(5)
C(7)-C(6')-C(5')	118.6(5)	C(6')-C(7)-C(8')	120.5(5)
C(8)-C(7)-C(6)	120.0(5)	C(7)-C(8)-C(9)	119.7(7)
C(4)-C(9)-C(8)	122.0(6)	C(7)-C(8')-C(9')	119.8(7)
C(8')-C(9')-C(4)	119.1(7)		

[a] Generated by symmetry transformation: -x,-y,-z+1

Intermolecular Hydrogen Bonding

N(1) ···· O(3) 2.837(3) H(1) ···· O(3) 2.10(5) N(1)-H(1) ···· O(3) 151(4)

Crystal Structure of the

dl-isomer of Dimethyl 2,3-Dibenzamido-2,3-dimethylbutanedioate **40**

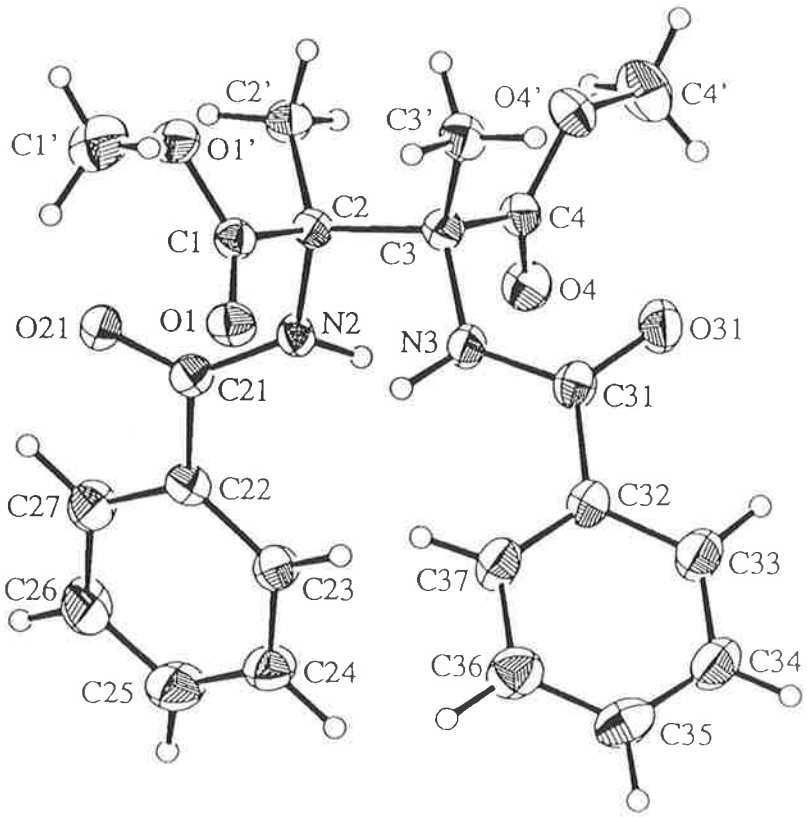

Bond Distances (Å) for the *dl*-isomer of Dimethyl 2,3-Dibenzamido-2,3-dimethylbutanedioate **40**

atom	atom	distance
O(1)	C(1)	1.200(4)
O(1')	C(1)	1.330(3)
O(1')	C(1')	1.461(5)
O(4')	C(4')	1.458(5)
O(4')	C(4)	1.318(4)
O(4)	C(4)	1.207(4)
O(21)	C(21)	1.229(4)
O(31)	C(31)	1.233(4)
N(2)	C(2)	1.460(4)
N(2)	C(21)	1.341(4)
N(2)	H(2)	0.90(3)
N(3)	C(3)	1.464(4)
N(3)	C(31)	1.347(5)
N(3)	H(3)	0.97(3)
C(1)	C(2)	1.536(4)
C(1')	H(1a)	0.91(4)
C(1')	H(1b)	1.00(5)
C(1')	H(1c)	0.95(5)
C(2')	C(2)	1.530(4)
C(2')	H(2a)	1.00(4)
C(2')	H(2b)	0.98(3)
C(2')	H(2c)	0.98(3)
C(2)	C(3)	1.579(5)
C(3')	C(3)	1.526(4)
C(3')	H(3b)	1.08(3)
C(3')	H(3c)	0.93(4)

atom	atom	distance
C(3')	H(3a)	0.95(3)
C(3)	C(4)	1.547(4)
C(4')	H(4c)	0.96(4)
C(4')	H(4a)	0.92(5)
C(4')	H(4b)	1.05(6)
C(21)	C(22)	1.488(4)
C(22)	C(23)	1.385(5)
C(22)	C(27)	1.377(5)
C(23)	C(24)	1.382(5)
C(23)	H(23)	0.95(3)
C(24)	C(25)	1.362(6)
C(24)	H(24)	1.02(4)
C(25)	C(26)	1.365(6)
C(25)	H(25)	0.93(3)
C(26)	C(27)	1.385(5)
C(26)	H(26)	0.90(4)
C(27)	H(27)	1.00(3)
C(31)	C(32)	1.492(5)
C(32)	C(33)	1.388(5)
C(32)	C(37)	1.370(5)
C(33)	C(34)	1.383(6)
C(33)	H(33)	0.99(4)
C(34)	C(35)	1.368(6)
C(34)	H(34)	0.94(3)
C(35)	C(36)	1.380(6)
C(35)	H(35)	1.02(4)
C(36)	C(37)	1.388(5)
C(36)	H(36)	0.99(4)
C(37)	H(37)	0.96(3)

Intramolecular Hydrogen Bonding

O(4) H(2) 2.11(4) O(1) H(3) 2.14(3)

Bond Angles (°) for the *dl*-isomer of Dimethyl 2,3-Dibenzamido-2,3-dimethylbutanedioate **40**

atom	atom	atom	angle
C(1)	O(1')	C(1')	115.1(3)
C(4')	O(4')	C(4)	114.8(4)
C(2)	N(2)	C(21)	122.5(3)
C(2)	N(2)	H(2)	112(2)
C(21)	N(2)	H(2)	123(2)
C(3)	N(3)	C(31)	122.0(3)
C(3)	N(3)	H(3)	117(2)
C(31)	N(3)	H(3)	120(2)
O(1)	C(1)	O(1')	124.8(3)
O(1)	C(1)	C(2)	123.4(3)
O(1')	C(1)	C(2)	111.8(3)
O(1')	C(1')	H(1a)	99(3)
O(1')	C(1')	H(1b)	109(3)
O(1')	C(1')	H(1c)	106(3)
H(1a)	C(1')	H(1b)	115(4)
H(1a)	C(1')	H(1c)	118(4)
H(1b)	C(1')	H(1c)	109(4)
C(2)	C(2')	H(2a)	112(2)
C(2)	C(2')	H(2b)	114(2)
C(2)	C(2')	H(2c)	112(2)
H(2a)	C(2')	H(2b)	106(3)
H(2a)	C(2')	H(2c)	106(3)
H(2b)	C(2')	H(2c)	107(3)
N(2)	C(2)	C(1)	106.8(3)
N(2)	C(2)	C(2')	110.7(3)
N(2)	C(2)	C(3)	107.7(3)
C(1)	C(2)	C(2')	113.3(3)
C(1)	C(2)	C(3)	106.6(3)
C(2')	C(2)	C(3)	111.3(3)
C(3)	C(3')	H(3b)	111(2)
C(3)	C(3')	H(3c)	114(2)
C(3)	C(3')	H(3a)	113(2)
H(3b)	C(3')	H(3c)	100(3)
H(3b)	C(3')	H(3a)	106(2)
H(3c)	C(3')	H(3a)	112(3)
N(3)	C(3)	C(2)	107.9(3)
N(3)	C(3)	C(3')	110.3(3)
N(3)	C(3)	C(4)	107.2(3)
C(2)	C(3)	C(3')	111.8(3)
C(2)	C(3)	C(4)	106.3(3)
C(3')	C(3)	C(4)	113.1(3)
O(4')	C(4')	H(4c)	99(3)
O(4')	C(4')	H(4a)	107(3)
O(4')	C(4')	H(4b)	108(3)
H(4c)	C(4')	H(4a)	115(4)
H(4c)	C(4')	H(4b)	114(4)
H(4a)	C(4')	H(4b)	112(4)
O(4')	C(4)	O(4)	125.1(3)
O(4')	C(4)	C(3)	111.8(3)
O(4)	C(4)	C(3)	122.9(3)
O(21)	C(21)	N(2)	122.9(3)
O(21)	C(21)	C(22)	121.5(4)
N(2)	C(21)	C(22)	116.5(3)
C(21)	C(22)	C(23)	122.2(4)
C(21)	C(22)	C(27)	119.4(3)
C(23)	C(22)	C(27)	118.3(4)
C(22)	C(23)	C(24)	120.7(4)
C(22)	C(23)	H(23)	119(2)
C(24)	C(23)	H(23)	120(2)
C(23)	C(24)	C(25)	120.2(4)
C(23)	C(24)	H(24)	119(2)
C(25)	C(24)	H(24)	120(2)
C(24)	C(25)	C(26)	119.9(4)
C(24)	C(25)	H(25)	123(2)
C(26)	C(25)	H(25)	117(2)
C(25)	C(26)	C(27)	120.4(5)
C(25)	C(26)	H(26)	122(2)
C(27)	C(26)	H(26)	118(3)
C(22)	C(27)	C(26)	120.5(4)
C(22)	C(27)	H(27)	118(2)
C(26)	C(27)	H(27)	122(2)
O(31)	C(31)	N(3)	121.2(4)
O(31)	C(31)	C(32)	121.6(4)
N(3)	C(31)	C(32)	117.1(4)
C(31)	C(32)	C(33)	118.0(4)
C(31)	C(32)	C(37)	123.4(4)
C(33)	C(32)	C(37)	118.6(4)
C(32)	C(33)	C(34)	119.8(5)
C(36)	C(35)	H(35)	120(2)
C(35)	C(36)	C(37)	119.5(5)
C(35)	C(36)	H(36)	121(3)
C(37)	C(36)	H(36)	119(3)
C(32)	C(37)	C(36)	121.6(5)
C(32)	C(37)	H(37)	122(2)
C(36)	C(37)	H(37)	116(2)
C(32)	C(33)	H(33)	115(2)
C(34)	C(33)	H(33)	126(2)
C(33)	C(34)	C(35)	121.3(5)
C(33)	C(34)	H(34)	118(3)
C(35)	C(34)	H(34)	120(2)
C(34)	C(35)	C(36)	119.3(5)
C(34)	C(35)	H(35)	121(2)

Crystal Structure of the

meso-isomer of Dimethyl 2,3-Dibenzamido-2,3-dimethylbutanedioate **40**

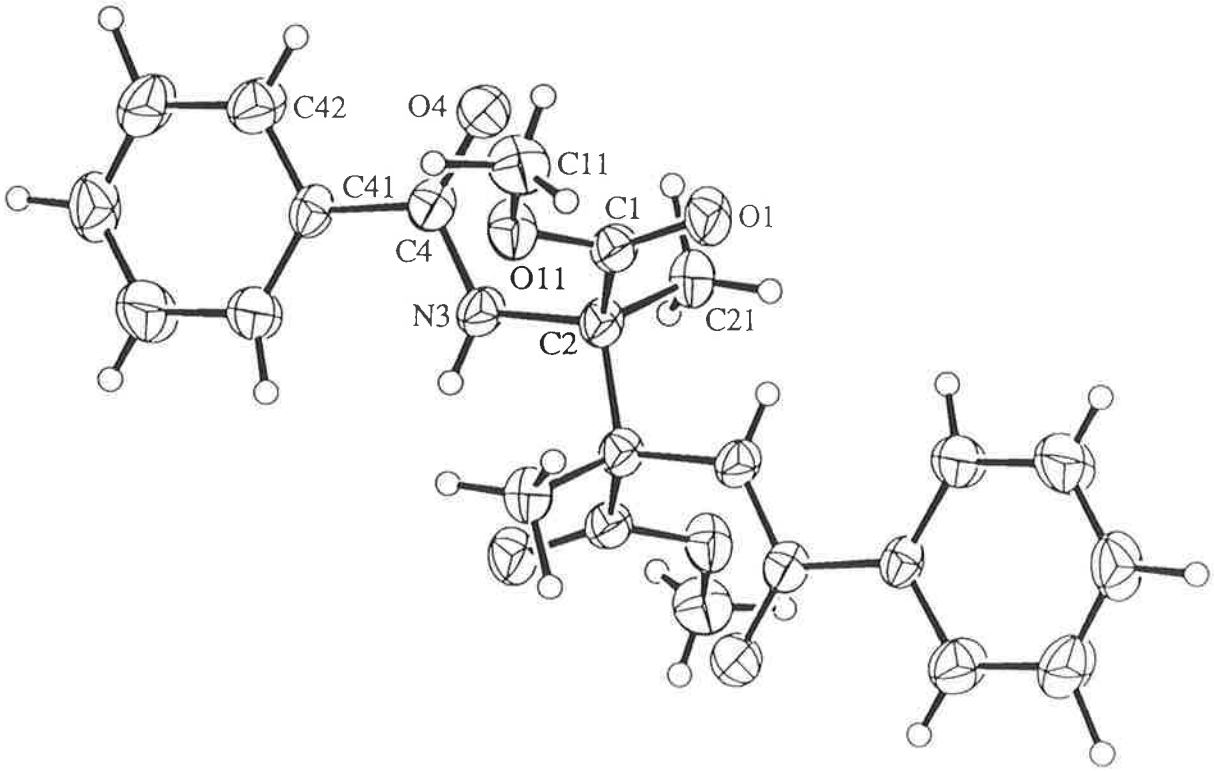

Bond Distances (Å) for the *meso*-isomer of Dimethyl 2,3-Dibenzamido-2,3-dimethylbutanedioate **40**

atom	atom	distance	ADC(*)	atom	atom	distance	ADC(*)
O(1)	C(1)	1.188(4)	1	C(21)	H(21b)	0.97(4)	1
O(4)	C(4)	1.212(4)	1	C(21)	H(21c)	0.89(4)	1
O(11)	C(1)	1.308(4)	1	C(21)	H(21a)	1.10(4)	1
O(11)	C(11)	1.435(5)	1	C(41)	C(42)	1.362(6)	1
N(3)	C(2)	1.452(4)	1	C(41)	C(46)	1.347(6)	1
N(3)	C(4)	1.341(5)	1	C(42)	C(43)	1.379(6)	1
N(3)	H(3)	0.87(4)	1	C(42)	H(42)	0.95(3)	1
C(1)	C(2)	1.517(5)	1	C(43)	C(44)	1.322(7)	1
C(2)	C(2)	1.535(7)	76703	C(43)	H(43)	1.06(5)	1
C(2)	C(21)	1.539(5)	1	C(44)	C(45)	1.332(7)	1
C(4)	C(41)	1.481(5)	1	C(44)	H(44)	0.96(4)	1
C(11)	H(11b)	0.90(5)	1	C(45)	C(46)	1.367(6)	1
C(11)	H(11c)	0.82(4)	1	C(45)	H(45)	0.89(4)	1
C(11)	H(11a)	1.06(6)	1	C(46)	H(46)	0.94(5)	1

Intramolecular Hydrogen Bonding

O(1) H(3') 2.34 O(1') H(3) 2.34

Bond Angles (°) for the *meso*-isomer of Dimethyl 2,3-Dibenzamido-2,3-dimethylbutanedioate **40**

atom	atom	atom	angle	atom	atom	atom	angle
C(1)	O(11)	C(11)	116.9(4)	C(2)	C(21)	H(21c)	104(2)
C(2)	N(3)	C(4)	122.7(4)	C(2)	C(21)	H(21a)	109(2)
C(2)	N(3)	H(3)	105(3)	H(21b)	C(21)	H(21c)	123(4)
C(4)	N(3)	H(3)	131(3)	H(21b)	C(21)	H(21a)	114(3)
O(1)	C(1)	O(11)	124.5(4)	H(21c)	C(21)	H(21a)	97(3)
O(1)	C(1)	C(2)	121.4(4)	C(4)	C(41)	C(42)	117.7(4)
O(11)	C(1)	C(2)	114.0(3)	C(4)	C(41)	C(46)	124.7(4)
N(3)	C(2)	C(1)	111.1(3)	C(42)	C(41)	C(46)	117.6(4)
N(3)	C(2)	C(2)	107.7(4)	C(41)	C(42)	C(43)	120.4(5)
N(3)	C(2)	C(21)	109.1(3)	C(41)	C(42)	H(42)	115(2)
C(1)	C(2)	C(2)	107.5(4)	C(43)	C(42)	H(42)	125(2)
C(1)	C(2)	C(21)	109.1(3)	C(42)	C(43)	C(44)	120.3(6)
C(2)	C(2)	C(21)	112.3(4)	C(42)	C(43)	H(43)	113(3)
O(4)	C(4)	N(3)	122.0(4)	C(44)	C(43)	H(43)	126(3)
O(4)	C(4)	C(41)	122.3(4)	C(43)	C(44)	C(45)	120.1(5)
N(3)	C(4)	C(41)	115.6(4)	C(43)	C(44)	H(44)	114(3)
O(11)	C(11)	H(11b)	113(3)	C(45)	C(44)	H(44)	125(3)
O(11)	C(11)	H(11c)	115(3)	C(44)	C(45)	C(46)	120.2(6)
O(11)	C(11)	H(11a)	110(3)	C(44)	C(45)	H(45)	119(3)
H(11b)	C(11)	H(11c)	106(4)	C(46)	C(45)	H(45)	120(3)
H(11b)	C(11)	H(11a)	103(4)	C(41)	C(46)	C(45)	121.2(5)
H(11c)	C(11)	H(11a)	108(4)	C(41)	C(46)	H(46)	130(3)
C(2)	C(21)	H(21b)	108(2)	C(45)	C(46)	H(46)	107(3)

Crystal Structure of

2-Benzamido-2,4-dimethyl-4-hydroxypentanoic acid γ-Lactone **52**

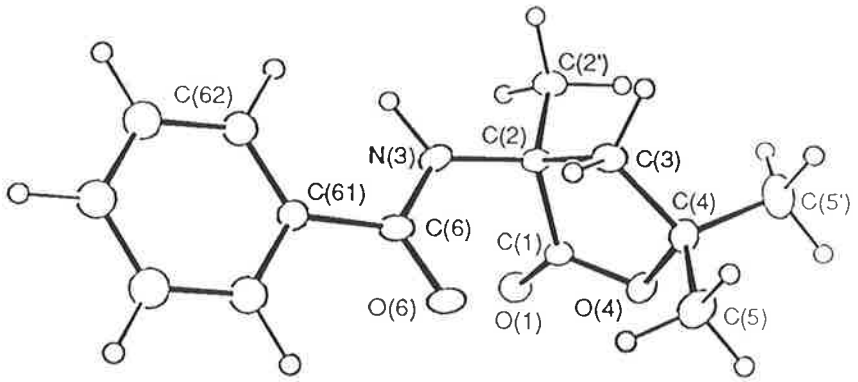

molecule a

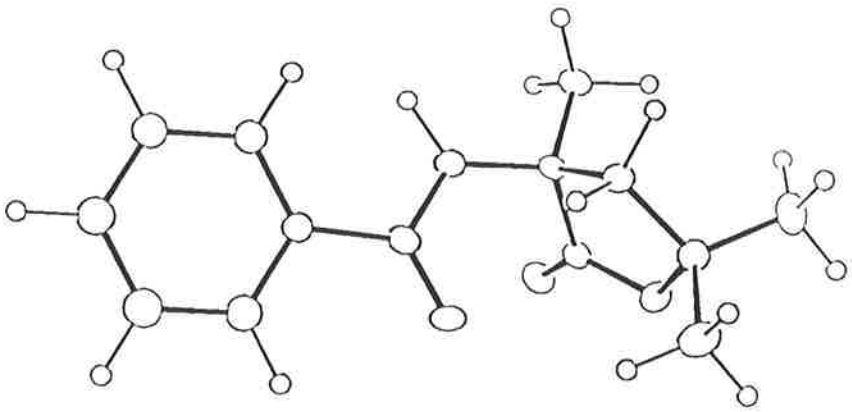

molecule b

Bond Distances (Å) and Angles (°) for

2-Benzamido-2,4-dimethyl-4-hydroxypentanoic acid γ-Lactone **52**

C(1a)	--- O(1a)	1.201(5)	C(1a)	--- O(4a)	1.321(6)
C(4a)	--- O(4a)	1.484(6)	C(6a)	--- O(6a)	1.232(6)
C(2a)	--- N(3a)	1.443(6)	C(6a)	--- N(3a)	1.344(6)
C(2a)	--- C(1a)	1.544(6)	C(2'a)	--- C(2a)	1.514(7)
C(3a)	--- C(2a)	1.537(6)	C(4a)	--- C(3a)	1.535(7)
C(5a)	--- C(4a)	1.502(8)	C(5'a)	--- C(4a)	1.507(8)
C(61a)	--- C(6a)	1.483(6)	C(63a)	--- C(62a)	1.395(-)
C(61a)	--- C(62a)	1.395(-)	C(64a)	--- C(63a)	1.395(-)
C(65a)	--- C(64a)	1.395(-)	C(66a)	--- C(65a)	1.395(-)
C(61a)	--- C(66a)	1.395(-)	C(1b)	--- O(1b)	1.202(5)
C(1b)	--- O(4b)	1.326(6)	C(4b)	--- O(4b)	1.479(5)
C(6b)	--- O(6b)	1.225(6)	C(2b)	--- N(3b)	1.446(6)
C(6b)	--- N(3b)	1.350(6)	C(2b)	--- C(1b)	1.543(7)
C(2'b)	--- C(2b)	1.537(7)	C(3b)	--- C(2b)	1.524(6)
C(4b)	--- C(3b)	1.520(7)	C(5b)	--- C(4b)	1.510(8)
C(5'b)	--- C(4b)	1.522(8)	C(61b)	--- C(6b)	1.496(6)
C(63b)	--- C(62b)	1.395(-)	C(61b)	--- C(62b)	1.395(-)
C(64b)	--- C(63b)	1.395(-)	C(65b)	--- C(64b)	1.395(-)
C(66b)	--- C(65b)	1.395(-)	C(61b)	--- C(66b)	1.395(-)

C(4a)	- O(4a)	- C(1a)	113.2(4)	C(6a)	- N(3a)	- C(2a)	121.5(4)
O(4a)	- C(1a)	- O(1a)	122.6(4)	C(2a)	- C(1a)	- O(1a)	126.2(5)
C(2a)	- C(1a)	- O(4a)	111.0(4)	C(1a)	- C(2a)	- N(3a)	111.5(4)
C(2'a)	- C(2a)	- N(3a)	108.7(4)	C(2'a)	- C(2a)	- C(1a)	107.7(4)
C(3a)	- C(2a)	- N(3a)	112.8(4)	C(3a)	- C(2a)	- C(1a)	102.6(4)
C(3a)	- C(2a)	- C(2'a)	113.4(4)	C(4a)	- C(3a)	- C(2a)	106.9(4)
C(3a)	- C(4a)	- O(4a)	104.5(4)	C(5a)	- C(4a)	- O(4a)	106.3(5)
C(5a)	- C(4a)	- C(3a)	113.0(5)	C(5'a)	- C(4a)	- O(4a)	106.8(4)
C(5'a)	- C(4a)	- C(3a)	113.1(5)	C(5'a)	- C(4a)	- C(5a)	112.4(5)
N(3a)	- C(6a)	- O(6a)	120.3(5)	C(61a)	- C(6a)	- O(6a)	121.2(5)
C(61a)	- C(6a)	- N(3a)	118.5(4)	C(61a)	- C(62a)	- C(63a)	120.0(-)
C(64a)	- C(63a)	- C(62a)	120.0(-)	C(65a)	- C(64a)	- C(63a)	120.0(-)
C(66a)	- C(65a)	- C(64a)	120.0(-)	C(61a)	- C(66a)	- C(65a)	120.0(-)
C(62a)	- C(61a)	- C(6a)	122.8(2)	C(66a)	- C(61a)	- C(6a)	117.2(2)
C(66a)	- C(61a)	- C(62a)	120.0(-)	C(4b)	- O(4b)	- C(1b)	113.1(4)
C(6b)	- N(3b)	- C(2b)	120.8(4)	O(4b)	- C(1b)	- O(1b)	123.2(5)
C(2b)	- C(1b)	- O(1b)	126.3(5)	C(2b)	- C(1b)	- O(4b)	110.2(4)
C(1b)	- C(2b)	- N(3b)	111.9(4)	C(2'b)	- C(2b)	- N(3b)	108.4(4)
C(2'b)	- C(2b)	- C(1b)	106.3(4)	C(3b)	- C(2b)	- N(3b)	113.0(4)
C(3b)	- C(2b)	- C(1b)	103.0(4)	C(3b)	- C(2b)	- C(2'b)	114.0(4)
C(4b)	- C(3b)	- C(2b)	106.9(4)	C(3b)	- C(4b)	- O(4b)	104.8(4)
C(5b)	- C(4b)	- O(4b)	106.4(4)	C(5b)	- C(4b)	- C(3b)	112.7(5)
C(5'b)	- C(4b)	- O(4b)	106.7(4)	C(5'b)	- C(4b)	- C(3b)	113.3(5)
C(5'b)	- C(4b)	- C(5b)	112.2(5)	N(3b)	- C(6b)	- O(6b)	120.8(5)
C(61b)	- C(6b)	- O(6b)	121.0(4)	C(61b)	- C(6b)	- N(3b)	118.1(4)
C(61b)	- C(62b)	- C(63b)	120.0(-)	C(64b)	- C(63b)	- C(62b)	120.0(-)
C(65b)	- C(64b)	- C(63b)	120.0(-)	C(66b)	- C(65b)	- C(64b)	120.0(-)
C(61b)	- C(66b)	- C(65b)	120.0(-)	C(62b)	- C(61b)	- C(6b)	123.0(2)
C(66b)	- C(61b)	- C(6b)	117.0(2)	C(66b)	- C(61b)	- C(62b)	120.0(-)

Crystal Structure of the

dl-isomer of 5,5'-Bis(5-methoxycarbonyl-2-pyrrolidinone) **49**

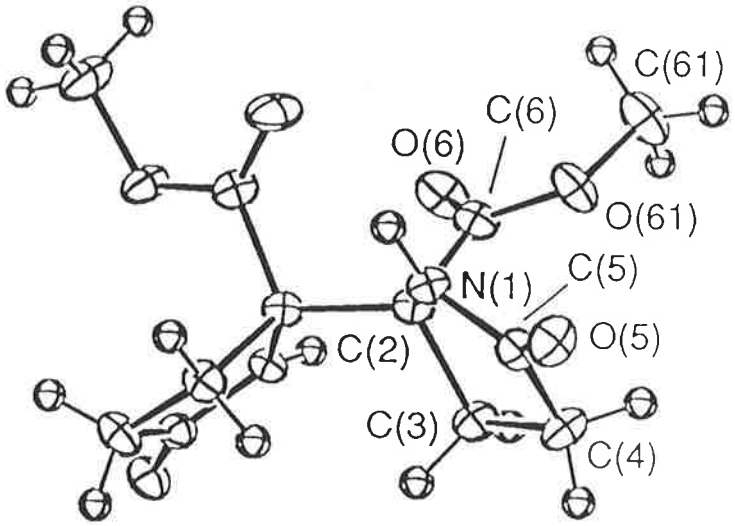

Bond Distances (Å) and Angles (°) for the *dl*-isomer of 5,5'-Bis(5-methoxycarbonyl-2-pyrrolidinone) **49**

C(5)	--- O(5)	1.230(4)	C(6)	--- O(6)	1.203(4)
C(6)	--- O(61)	1.326(4)	C(61)	--- O(61)	1.455(5)
C(2)	--- N(1)	1.459(4)	C(5)	--- N(1)	1.341(4)
H(1)	--- N(1)	0.914(36)	C(3)	--- C(2)	1.555(4)
C(6)	--- C(2)	1.531(4)	C(2)	--- C(2')	1.551(6)
C(4)	--- C(3)	1.519(5)	H(3a)	--- C(3)	0.990(37)
H(3b)	--- C(3)	0.962(35)	C(5)	--- C(4)	1.505(5)
H(4a)	--- C(4)	0.969(41)	H(4b)	--- C(4)	0.913(36)
H(61a)	--- C(61)	0.937(56)	H(61b)	--- C(61)	1.165(45)
H(61c)	--- C(61)	0.988(44)	O(s)	--- C(s)	1.27(1)
C(s)	--- C(s')	1.43(2)			

C(61)	- O(61)	- C(6)	116.2(3)	C(5)	- N(1)	- C(2)	114.2(3)
H(1)	- N(1)	- C(2)	122.5(21)	H(1)	- N(1)	- C(5)	122.9(21)
C(3)	- C(2)	- N(1)	102.0(2)	C(6)	- C(2)	- N(1)	112.7(2)
C(6)	- C(2)	- C(3)	107.9(3)	N(1)	- C(2)	- C(2')	128.6(2)
C(3)	- C(2)	- C(2')	102.7(2)	C(6)	- C(2)	- C(2')	101.4(2)
C(4)	- C(3)	- C(2)	104.2(3)				
H(3a)	- C(3)	- C(2)	108.8(20)	H(3a)	- C(3)	- C(4)	109.8(21)
H(3b)	- C(3)	- C(2)	112.1(19)	H(3b)	- C(3)	- C(4)	114.0(19)
H(3b)	- C(3)	- H(3a)	107.9(29)	C(5)	- C(4)	- C(3)	104.5(3)
H(4a)	- C(4)	- C(3)	116.2(24)	H(4a)	- C(4)	- C(5)	106.9(24)
H(4b)	- C(4)	- C(3)	114.0(21)	H(4b)	- C(4)	- C(5)	114.2(21)
H(4b)	- C(4)	- H(4a)	101.3(32)	N(1)	- C(5)	- O(5)	124.8(3)
C(4)	- C(5)	- O(5)	126.5(3)	C(4)	- C(5)	- N(1)	108.7(3)
O(61)	- C(6)	- O(6)	125.1(3)	C(2)	- C(6)	- O(6)	123.3(3)
C(2)	- C(6)	- O(61)	111.4(3)	H(61a)	- C(61)	- O(61)	105.7(31)
H(61b)	- C(61)	- O(61)	110.9(22)	H(61b)	- C(61)	- H(61a)	107.1(39)
H(61c)	- C(61)	- O(61)	108.1(27)	H(61c)	- C(61)	- H(61a)	119.7(43)
H(61c)	- C(61)	- H(61b)	105.2(34)				

Crystal Structure of the

meso-isomer of 5,5'-Bis(5-methoxycarbonyl-2-pyrrolidinone) **49**

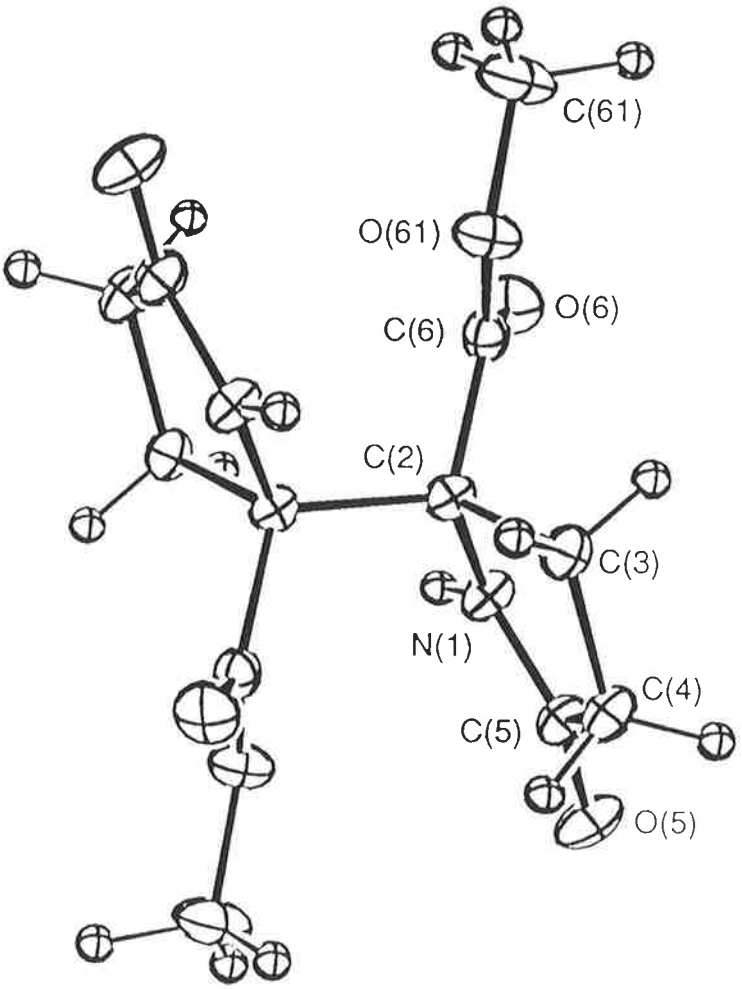

Bond Distances (Å) and Angles (°) for the *dl*-isomer of 5,5'-Bis(5-methoxycarbonyl-2-pyrrolidinone) **49**

C(5)	--- O(5)	1.231(3)	C(6)	--- O(6)	1.204(3)
C(6)	--- O(61)	1.328(3)	C(61)	--- O(61)	1.444(3)
C(2)	--- N(1)	1.440(3)	C(5)	--- N(1)	1.339(3)
H(1)	--- N(1)	0.859(26)	C(3)	--- C(2)	1.555(3)
C(6)	--- C(2)	1.534(3)	C(2)	--- C(2)'	1.585(4)
C(4)	--- C(3)	1.516(3)	H(3a)	--- C(3)	1.046(24)
H(3b)	--- C(3)	0.957(31)	C(5)	--- C(4)	1.502(3)
H(4a)	--- C(4)	0.956(29)	H(4b)	--- C(4)	0.964(31)
H(61a)	--- C(61)	0.759(29)	H(61b)	--- C(61)	0.987(40)
H(61c)	--- C(61)	1.079(39)			

C(61)	- O(61)	- C(6)	115.7(2)		C(5)	- N(1)	- C(2)	114.7(2)	
H(1)	- N(1)	- C(2)	120.0(16)		H(1)	- N(1)	- C(5)	121.8(16)	
C(3)	- C(2)	- N(1)	102.3(2)		C(6)	- C(2)	- N(1)	108.4(2)	
C(6)	- C(2)	- C(3)	111.3(2)		C(4)	- C(3)	- C(2)	104.6(2)	
H(3a)	- C(3)	- C(2)	110.2(13)		H(3a)	- C(3)	- C(4)	116.5(12)	
H(3b)	- C(3)	- C(2)	104.2(15)		H(3b)	- C(3)	- C(4)	114.9(15)	
H(3b)	- C(3)	- H(3a)	105.8(20)		C(5)	- C(4)	- C(3)	104.9(2)	
H(4a)	- C(4)	- C(3)	115.5(15)		H(4a)	- C(4)	- C(5)	108.9(15)	
H(4b)	- C(4)	- C(3)	115.8(17)		H(4b)	- C(4)	- C(5)	101.3(17)	
H(4b)	- C(4)	- H(4a)	109.2(22)		N(1)	- C(5)	- O(5)	124.9(2)	
C(4)	- C(5)	- O(5)	126.6(2)		C(4)	- C(5)	- N(1)	108.5(2)	
O(61)	- C(6)	- O(6)	124.7(2)		C(2)	- C(6)	- O(6)	123.1(2)	
C(2)	- C(6)	- O(61)	112.2(2)		H(61a)	- C(61)	- O(61)	108.1(27)	
H(61b)	- C(61)	- O(61)	111.3(21)		H(61b)	- C(61)	- H(61a)	112.8(31)	
H(61c)	- C(61)	- O(61)	112.6(20)		H(61c)	- C(61)	- H(61a)	108.0(31)	
H(61c)	- C(61)	- H(61b)	104.1(30)		C(2)'	- C(2)	- N(1)	112.0(2)	
C(2)'	- C(2)	- C(3)	109.6(2)		C(2)'	- C(2)	- C(6)	113.2(2)	

Crystal Structure of

N-Benzoylalanine Methyl Ester **26**

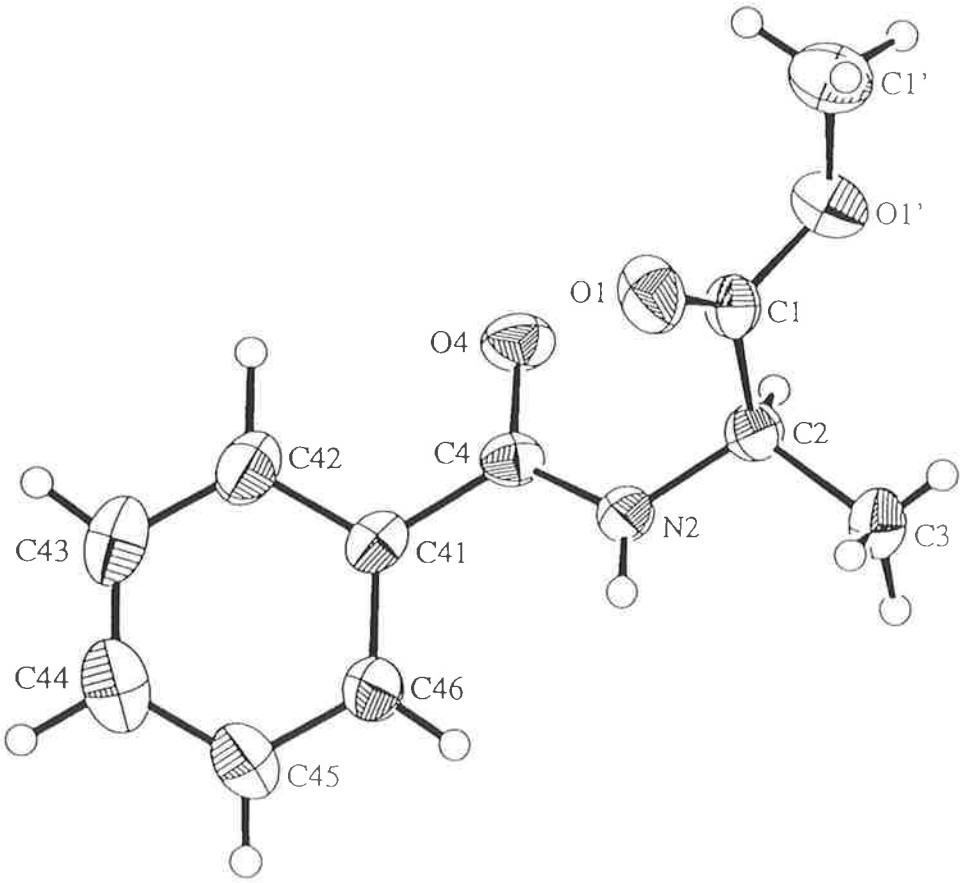

Bond Distances (Å) for *N*-Benzoylalanine Methyl Ester **26**

atom	atom	distance	atom	atom	distance
O(1)	C(1)	1.170(5)	C(3)	H(3c)	0.762
O(1')	C(1)	1.351(5)	C(3)	H(3a)	0.982
O(1')	C(1')	1.443(6)	C(4)	C(41)	1.494(5)
O(4)	C(4)	1.245(4)	C(41)	C(42)	1.382(6)
N(2)	C(2)	1.454(5)	C(41)	C(46)	1.393(5)
N(2)	C(4)	1.330(5)	C(42)	C(43)	1.407(8)
N(2)	H(2)	0.823	C(42)	H(42)	1.116
C(1)	C(2)	1.512(6)	C(43)	C(44)	1.372(8)
C(1')	H(1a)	1.051	C(43)	H(43)	0.918
C(1')	H(1b)	0.858	C(44)	C(45)	1.383(8)
C(1')	H(1c)	0.947	C(44)	H(44)	1.011
C(2)	C(3)	1.518(7)	C(45)	C(46)	1.363(6)
C(2)	H(3)	1.114	C(45)	H(45)	0.939
C(3)	H(3b)	1.055	C(46)	H(46)	0.915

Bond Angles (°) for

N-Benzoylalanine Methyl Ester **26**

atom	atom	atom	angle	atom	atom	atom	angle
C(1)	O(1')	C(1')	116.9(4)	H(3b)	C(3)	H(3a)	107.68
C(2)	N(2)	C(4)	120.6(3)	H(3c)	C(3)	H(3a)	115.74
C(2)	N(2)	H(22)	119.48	O(4)	C(4)	N(2)	119.8(3)
C(4)	N(2)	H(2)	119.85	O(4)	C(4)	C(41)	121.3(3)
O(1)	C(1)	O(1')	123.2(4)	N(2)	C(4)	C(41)	118.9(3)
O(1)	C(1)	C(2)	127.5(3)	C(4)	C(41)	C(42)	117.8(3)
O(1')	C(1)	C(2)	109.2(3)	C(4)	C(41)	C(46)	123.0(3)
O(1')	C(1')	H(1a)	85.32	C(42)	C(41)	C(46)	119.2(4)
O(1')	C(1')	H(1b)	124.74	C(41)	C(42)	C(43)	119.5(4)
O(1')	C(1')	H(1c)	111.81	C(41)	C(42)	H(42)	119.55
H(1a)	C(1')	H(1b)	124.31	C(43)	C(42)	H(42)	120.95
H(1a)	C(1')	H(1c)	103.28	C(42)	C(43)	C(44)	120.1(5)
H(1b)	C(1')	H(1c)	105.19	C(42)	C(43)	H(43)	113.48
N(2)	C(2)	C(1)	109.3(3)	C(44)	C(43)	H(43)	126.43
N(2)	C(2)	C(3)	111.0(3)	C(43)	C(44)	C(45)	120.0(5)
N(2)	C(2)	H(3)	106.99	C(43)	C(44)	H(44)	119.20
C(1)	C(2)	C(3)	110.4(4)	C(45)	C(44)	H(44)	120.09
C(1)	C(2)	H(3)	107.25	C(44)	C(45)	C(46)	120.2(4)
C(3)	C(2)	H(3)	111.81	C(44)	C(45)	H(45)	120.62
C(2)	C(3)	H(3b)	106.12	C(46)	C(45)	H(45)	118.96
C(2)	C(3)	H(3c)	108.30	C(41)	C(46)	C(45)	120.9(4)
C(2)	C(3)	H(3a)	114.33	C(41)	C(46)	H(46)	122.71
H(3b)	C(3)	H(3c)	103.70	C(45)	C(46)	H(46)	116.35

Hydrogen Bonding for

N-Benzoylalanine Methyl Ester **26**

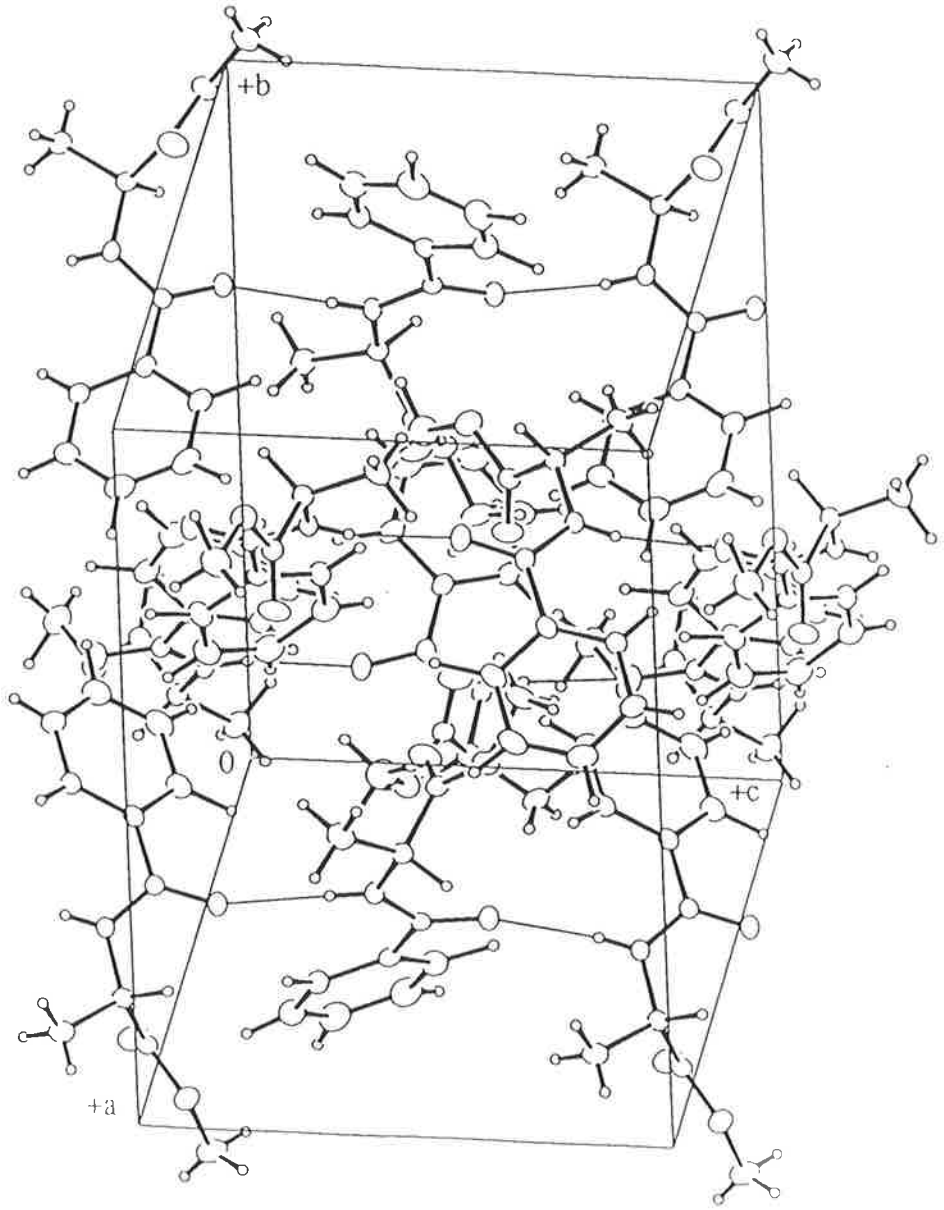

Hydrogen Bonds

A	H	B	A-H	H...B	A...B	A-H...B
N(2)	H(1)	O(4)	0.82	2.11	2.923(4)	167

Crystal Structure of

N-Benzoyl-(2*S*)-alanine Methyl Ester **71**

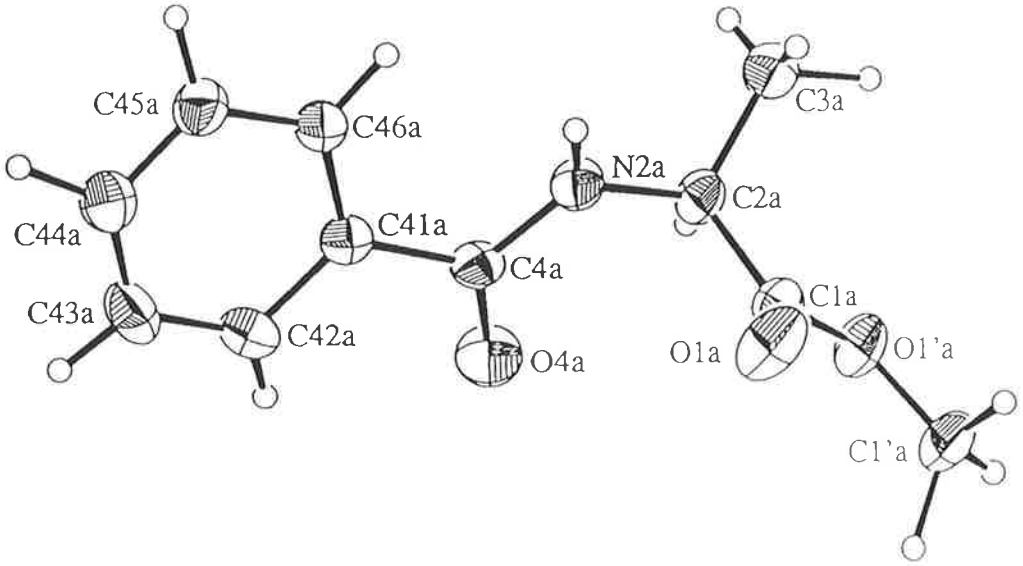

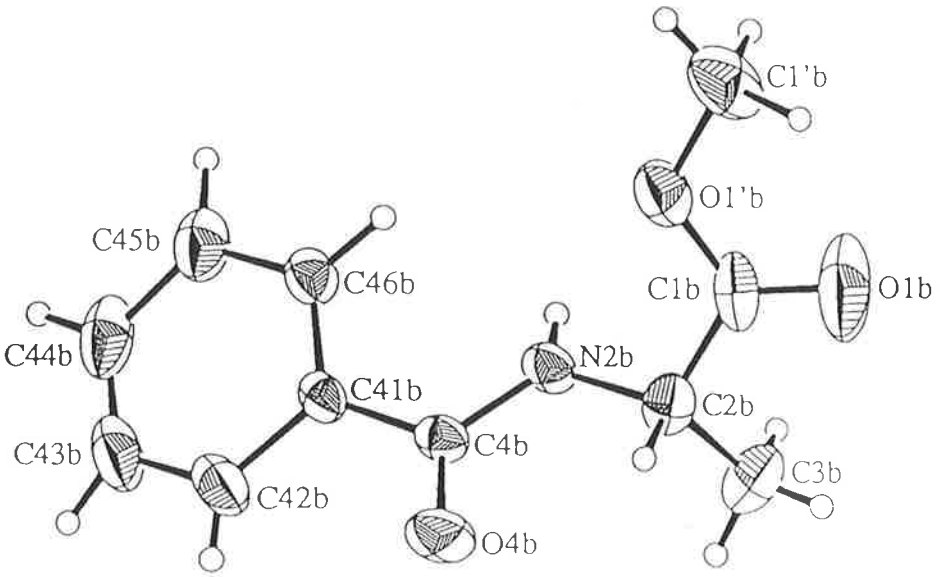

Bond Distances (Å) for
N-Benzoyl-(2*S*)-alanine Methyl Ester 71

atom	atom	distance	atom	atom	distance
O(1'b)	C(1b)	1.311(7)	C(3b)	H(3b1)	0.91(8)
O(1'b)	C(1'b)	1.439(8)	C(3b)	H(3b2)	0.96(7)
O(1'a)	C(1a)	1.318(5)	C(3b)	H(3b3)	0.84(7)
O(1'a)	C(1'a)	1.442(7)	C(3a)	H(3a1)	1.19(6)
O(1a)	C(1a)	1.184(5)	C(3a)	H(3a2)	0.94(6)
O(1b)	C(1b)	1.192(7)	C(3a)	H(3a3)	0.76(5)
O(4a)	C(4a)	1.226(5)	C(4b)	C(41b)	1.498(7)
O(4b)	C(4b)	1.229(6)	C(4a)	C(41a)	1.497(6)
N(2b)	C(2b)	1.439(7)	C(41b)	C(42b)	1.379(7)
N(2b)	C(4b)	1.319(6)	C(41b)	C(46b)	1.387(7)
N(2b)	H(2nb)	0.70(5)	C(41a)	C(42a)	1.386(7)
N(2a)	C(2a)	1.449(6)	C(41a)	C(46a)	1.384(7)
N(2a)	C(4a)	1.314(6)	C(42a)	C(43a)	1.379(8)
N(2a)	H(2na)	0.73(5)	C(42a)	H(42a)	0.85(7)
C(1a)	C(2a)	1.506(7)	C(42b)	C(43b)	1.38(1)
C(1'a)	H(1a1)	0.75(9)	C(42b)	H(42b)	0.78(9)
C(1'a)	H(1a2)	1.3(1)	C(43a)	C(44a)	1.359(9)
C(1'a)	H(1a3)	1.05(7)	C(43a)	H(43a)	0.98(6)
C(1b)	C(2b)	1.484(9)	C(43b)	C(44b)	1.34(1)
C(1'b)	H(1b1)	0.93(8)	C(43b)	H(43b)	0.9(1)
C(1'b)	H(1b2)	1.1(1)	C(44b)	C(45b)	1.39(1)
C(1'b)	H(1b3)	1.20(9)	C(44b)	H(44b)	0.91(6)
C(2a)	C(3a)	1.493(8)	C(44a)	C(45a)	1.376(8)
C(2a)	H(2a)	0.99(5)	C(44a)	H(44a)	1.07(7)
C(2b)	C(3b)	1.520(9)	C(45b)	C(46b)	1.393(8)
C(2b)	H(2b)	0.84(6)	C(45b)	H(45b)	1.02(8)
C(45a)	C(46a)	1.384(7)			
C(45a)	H(45a)	1.03(5)			
C(46a)	H(46a)	0.99(5)			
C(46b)	H(46b)	0.95(6)			

Bond Angles (°) for

N-Benzoyl-(2*S*)-alanine Methyl Ester **71**

atom	atom	atom	angle	atom	atom	atom	angle
C(1b)	O(1'b)	C(1'b)	116.1(6)	N(2a)	C(2a)	C(1a)	111.4(4)
C(1a)	O(1'a)	C(1'a)	116.9(5)	N(2a)	C(2a)	C(3a)	111.4(5)
C(2b)	N(2b)	C(4b)	122.8(5)	N(2a)	C(2a)	H(2a)	110(3)
C(2b)	N(2b)	H(2nb)	111(4)	C(1a)	C(2a)	C(3a)	111.0(5)
C(4b)	N(2b)	H(2nb)	125(4)	C(1a)	C(2a)	H(2a)	105(3)
C(2a)	N(2a)	C(4a)	122.2(4)	C(3a)	C(2a)	H(2a)	108(3)
C(2a)	N(2a)	H(2na)	114(4)	N(2b)	C(2b)	C(1b)	112.5(5)
C(4a)	N(2a)	H(2na)	124(4)	N(2b)	C(2b)	C(3b)	111.2(5)
O(1'a)	C(1a)	O(1a)	123.9(4)	N(2b)	C(2b)	H(2b)	101(4)
O(1'a)	C(1a)	C(2a)	110.3(4)	C(1b)	C(2b)	C(3b)	110.7(6)
O(1a)	C(1a)	C(2a)	125.7(4)	C(1b)	C(2b)	H(2b)	115(4)
O(1'a)	C(1'a)	H(1a1)	122(7)	C(3b)	C(2b)	H(2b)	106(4)
O(1'a)	C(1'a)	H(1a2)	122(4)	C(2b)	C(3b)	H(3b1)	113(5)
O(1'a)	C(1'a)	H(1a3)	110(3)	C(2b)	C(3b)	H(3b2)	114(4)
H(1a1)	C(1'a)	H(1a2)	94(8)	C(2b)	C(3b)	H(3b3)	120(5)
H(1a1)	C(1'a)	H(1a3)	104(7)	H(3b1)	C(3b)	H(3b2)	105(6)
H(1a2)	C(1'a)	H(1a3)	103(6)	H(3b1)	C(3b)	H(3b3)	100(7)
O(1'b)	C(1b)	O(1b)	121.1(7)	H(3b2)	C(3b)	H(3b3)	103(7)
O(1'b)	C(1b)	C(2b)	114.5(5)	C(2a)	C(3a)	H(3a1)	113(3)
O(1b)	C(1b)	C(2b)	124.3(7)	C(2a)	C(3a)	H(3a2)	112(4)
O(1'b)	C(1'b)	H(1b1)	110(6)	C(2a)	C(3a)	H(3a3)	108(5)
O(1'b)	C(1'b)	H(1b2)	99(5)	H(3a1)	C(3a)	H(3a2)	98(4)
O(1'b)	C(1'b)	H(1b3)	110(5)	H(3a1)	C(3a)	H(3a3)	113(5)
H(1b1)	C(1'b)	H(1b2)	91(8)	H(3a2)	C(3a)	H(3a3)	112(6)
H(1b1)	C(1'b)	H(1b3)	121(7)	O(4b)	C(4b)	N(2b)	121.2(5)
H(1b2)	C(1'b)	H(1b3)	124(7)	O(4b)	C(4b)	C(41b)	121.5(4)

Hydrogen Bonding for

N-Benzoyl-(2*S*)-alanine Methyl Ester **71**

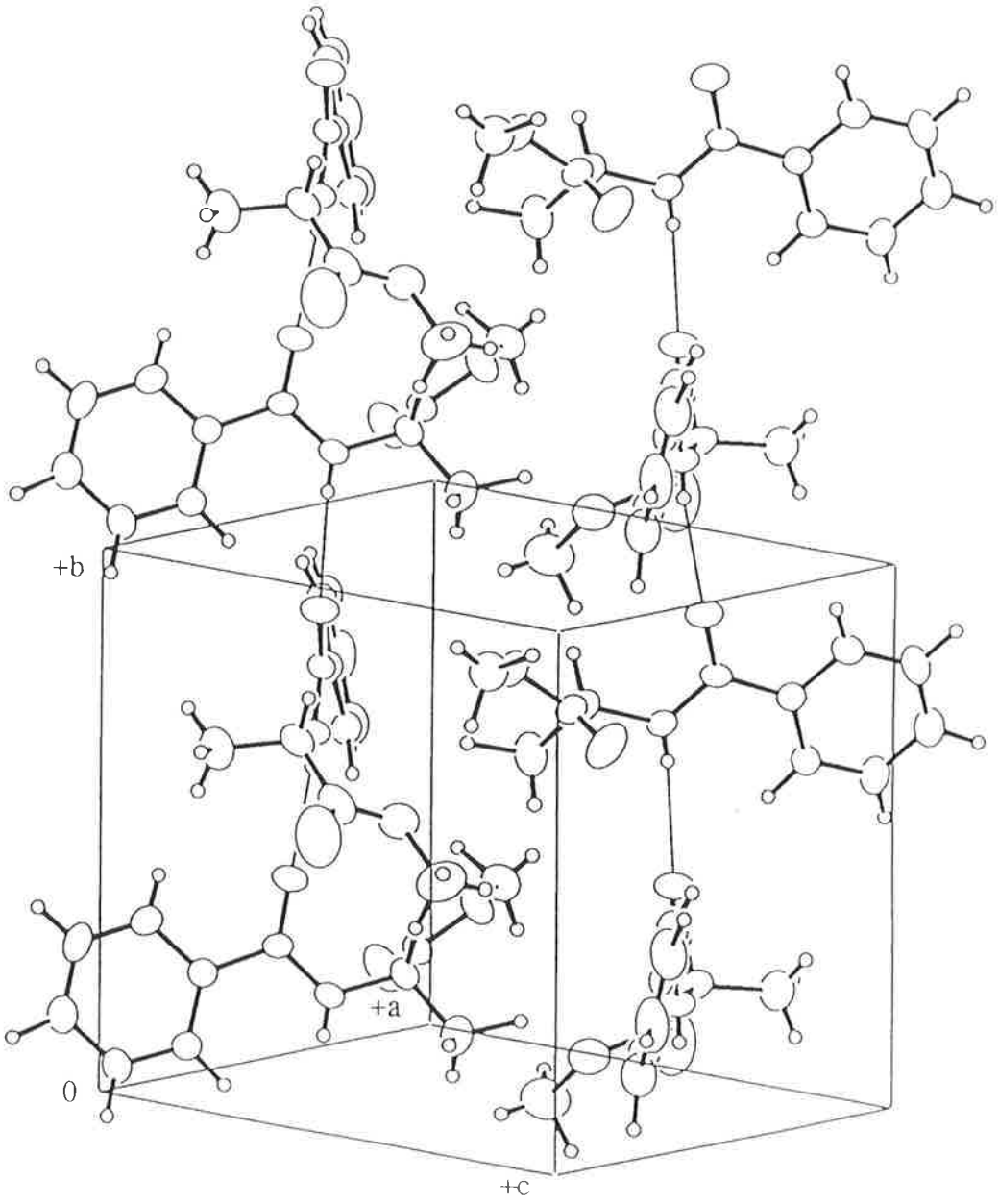

Hydrogen Bonds

A	H	B	A-H	H...B	A...B	A-H...B
N(2b)	H(2nb)	O(4a)	0.70(5)	2.16(5)	2.849(6)	168(5)
N(2a)	H(2na)	O(4b)	0.73(5)	2.23(5)	2.947(6)	166(5)